INDC-336

UNCLASSIFIED

UKNDC(70)P 19
EANDC(UK)120AL
INDC(UK)–10 G

U.K. NUCLEAR DATA PROGRESS REPORT

Mid 1968 – Mid 1969

Editor: E. R. Rae

Nuclear Physics Division,
U.K.A.E.A. Research Group,
Atomic Energy Research Establishment,
HARWELL.

April 1970.

HL70/1826

PREFACE

This document is prepared at the request of the U.K. Nuclear Data Committee. It brings together progress reports on nuclear reactor data from AERE, AWRE, NPL and other relevant U.K. sources in a single document for submission to EANDC and INDC.

As from April 1969 the Progress Report of Nuclear Physics Division AERE becomes an annual publication, and since it forms the backbone of this document, the U.K. Nuclear Data Progress Report will also be published annually in future. The present edition is in two parts. The first part contains extracts from the progress reports of Nuclear Physics Division and Chemistry Division at AERE covering roughly the period May-October 1968 together with reports from Analytical Sciences Division at AERE, Nuclear Research Division at AWRE and Radiation Sciences Division at NPL. The second part contains extracts from the progress reports of Nuclear Physics Division and Chemistry Division at AERE covering roughly the period November 1968 to April 1969.

CONTENTS

NUCLEAR PHYSICS DIVISION, A. E. R. E.

(Division Head: Dr. B. Rose)

EDITORIAL NOTE

Since the results obtained from the various machines are not easily classified according to the energy of the charged beams, individual research items are labelled with a single letter indicating on which machine the experiments were performed. These labels are as follows:

Cockcroft Walton Generator (G. Dearnaley)	A
3 MV pulsed Van de Graaff Generator IBIS (A. T. G. Ferguson)	B
5 MV Van de Graaff Generator (A. T. G. Ferguson)	C
13 MV Tandem Generator (J. M. Freeman)	D
45 MeV Electron Linac (E. R. Rae)	E
50 MeV Proton Linac: S.R.C.	F
Variable Energy Cyclotron: Chemistry Division	G
Synchrocyclotron (A. E. Taylor)	H
Nimrod Proton Synchroton: S.R.C.	I

The running analyses for the various machines operated by the division are presented as far as possible in a uniform format, but some differences exist in the way in which the scheduling is arranged, and machines such as the Electron Linac can accommodate several experiments similtaneously.

GENERAL REACTOR TECHNOLOGIES AND STUDIES

NUCLEAR DATA FOR FAST REACTORS

B. Elastic and inelastic scattering of neutrons by Pu^{239} (D. A. Boyce, P. E. Cavanagh, C. F. Coleman, G. A. Gard, A. G. Hardacre, J. C. Kerr and J. F. Turner)

An error has been found in the fitting of the observed fission neutron spectra with an $E^{1/2}e^{-E/\theta}$ distribution, so that the value of the "temperature" θ quoted earlier(1) is incorrect. Correct fitting leads to a value 1.47 ± 0.10 MeV, in better agreement with Bonner's(2) result.

Design of a neutron detector with a flat energy response for use in time of flight experiments (M. S. Coates and W. Hart (Risley))

Using the GEM 4(3) code on the Risley IBM 7090 computer further Monte Carlo calculations have been made to study the neutron sensitivity of the homogeneous ^{10}B-Vaseline detector reported earlier(4). The program tracks monoenergetic neutrons incident on the inner end of a re-entrant hole. When a neutron is absorbed its energy, spatial co-ordinates and time to absorption are recorded. A second part of the program tracks the 480 keV γ-rays produced in the $^{10}B(n,\alpha)^7Li^*,\gamma Li^7$ reaction and gives the position and energy of the γ-ray when it emerges from the surface of the sphere. In practice only γ-rays in a chosen energy range emerging from a chosen region of the sphere will be detected.

The calculations allow one to assess whether it is feasible to make a detector with an efficiency insensitive to the accuracy of the input nuclear data over the energy region of interest (~100 eV - several MeV), which responds rapidly enough to be used in time of flight experiments. So far more detailed calculations have been made only for spheres containing 1 kg of ^{10}B, with a re-entrant hole diameter of 2.5 cm and the inner end at a depth of ¼ sphere diameter (this depth was found to minimise the leakage of high energy neutrons for a given boron content). In particular we have studied a sphere of radius 12 cm, and have already shown that in this detector at least 95% of incident neutrons with $E \lesssim 1$ MeV are absorbed within a time ~0.7μs. The distribution of the number of γ-rays emerging from the sphere surface at a given incident neutron energy is symmetrical about the direction of the incident beam, but is not expected to be uniform over the surface. This is because high energy incident neutrons tend to be absorbed in the downstream, and lower energy neutrons in the upstream half of the sphere. Distributions have been obtained for the number of γ-rays with residual energies from 480-400 keV emerging from five equal segments of the sphere surface (indicated in Fig. 1a (see page 2)) as a function of incident neutron energy. The distributions are given in Fig. 1b (see page 2). The distributions are relatively flat for the three central segments but show large variations for the two capping segments. It is interesting to note that the distributions summed over all five segments vary by only 3% over the neutron energy range 100 eV - 1 MeV. A practical detector would accept γ-rays from the central region. Fig. 2 (see page 2) shows the distribution for a segment comprising half each of segments 2 and 3 in Fig. 1a. The variation is 3% in the neutron energy range 100 eV - 700 keV. To test the sensitivity of the results to the input nuclear data calculations were made with the $^{10}B(n,\alpha)$ cross section and the hydrogen scattering cross section displaced systematically by approximately two standard deviations from the best quoted values. This involved changes in the $^{10}B(n,\alpha)$ cross section of ~1% at 20 keV, 4% at 100 keV and 57% at 1 MeV and a change of ~3% in the hydrogen scattering cross section. The distribution of Fig. 2 changed relatively by 1-2%.

---

(1) Nuclear Physics Division Progress Report PR/NP 14 p. 3.

(2) Bonner T. W., Nucl. Phys. 23, 116 (1961).

(3) Hemmings P. J. UKAEA Report AHSB(S)R146 (1968).

(4) Nuclear Physics Progress Report AERE PR/NP14 (1968) p. 8.

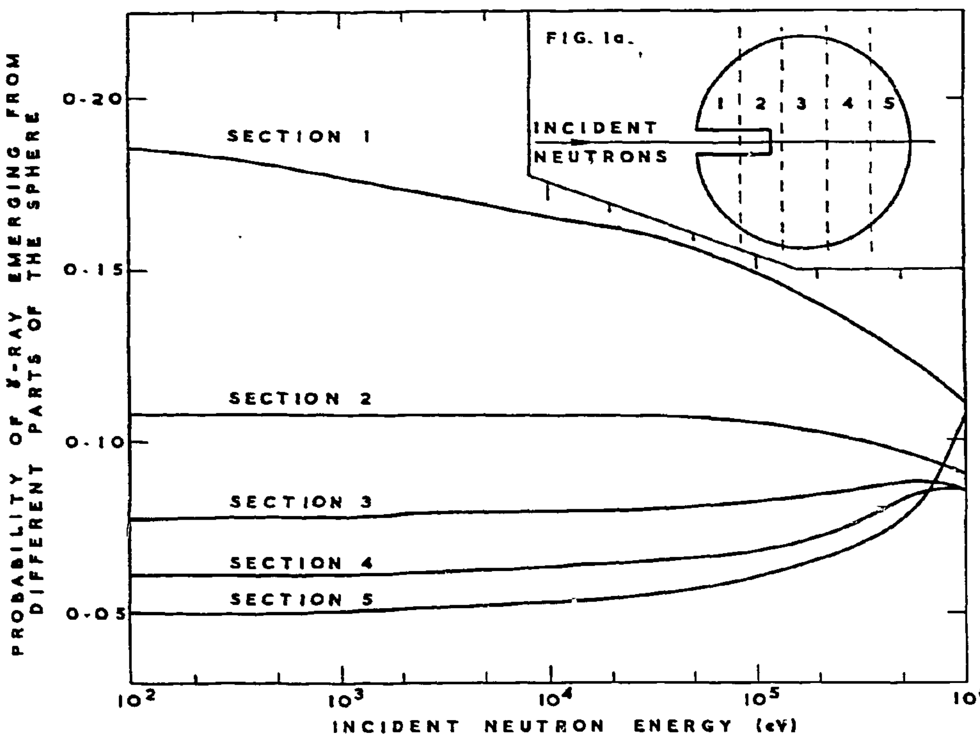

Fig. 1. (a) Five equal areas on sphere surface.

(b) Probability of emergence from specified areas of sphere surface of gamma rays with energies in the range 400 → 480 keV as a function of the energy of the incident neutrons.

It would be desirable to extend the range of flat response to higher incident neutron energies. It appears that significant improvements can only be achieved by increasing the detector size, since calculations show that the maximum energy at which at least 95% of incident neutrons are absorbed is insensitive to ^{10}B concentration. On the other hand the ^{10}B concentration strongly affects the mean delay in the counter response. To a good approximation the fraction of neutrons captured after a given time t is given by $1 - e^{-50.5\rho t}$ where ρ is the effective boron density in gm.cm^{-3} and t is in μs. For a 12 cm radius sphere containing 1 kg of ^{10}B only 1% of the incident neutrons are detected more than 0.66 μs after entry. This response is just fast enough to allow good time of flight measurements on the 300 m flight path of the neutron booster. The criterion is that the timing resolution of the detector should be sufficient to allow an accurate background determination using the black resonance technique. We intended to make a detector 12 cm radius containing 1 kg ^{10}B. Since a faster counter would be advantageous further calculations will be made to determine the γ-ray response with higher ^{10}B concentrations.

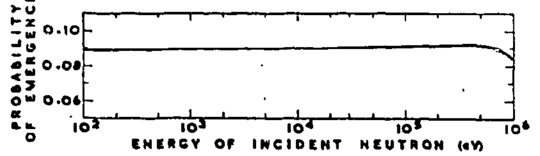

Fig. 2. Probability of emergence from segments 2-3 as a function of energy of incident neutrons.

B. Measurement of the absolute sensitivity of neutron detectors (J. M. Adams, A. T. G. Ferguson and C. D. McKenzie*)

The measurements described previously(5) of the absolute sensitivity of a Harwell long counter(6) at incident neutron energies between 50 keV and 1.3 MeV have now been completed. The data are still being analysed.

To reduce the uncertainties in the measurements several technical improvements were introduced. The initial measurements of the neutron angular distributions from the reactions $^{51}V(p,n)^{51}Cr$ (Q = -1.534 MeV) and $^{57}Fe(p,n)^{57}Co$ (Q = -1.619 MeV) exhibited pronounced 'dips' around 90° which arose because the target was inclined at 90° to the incident proton beam. This effect was eliminated by using targets inclined at 45° and 135° to the beam as shown in Fig. 3. The neutron angular distributions in the two

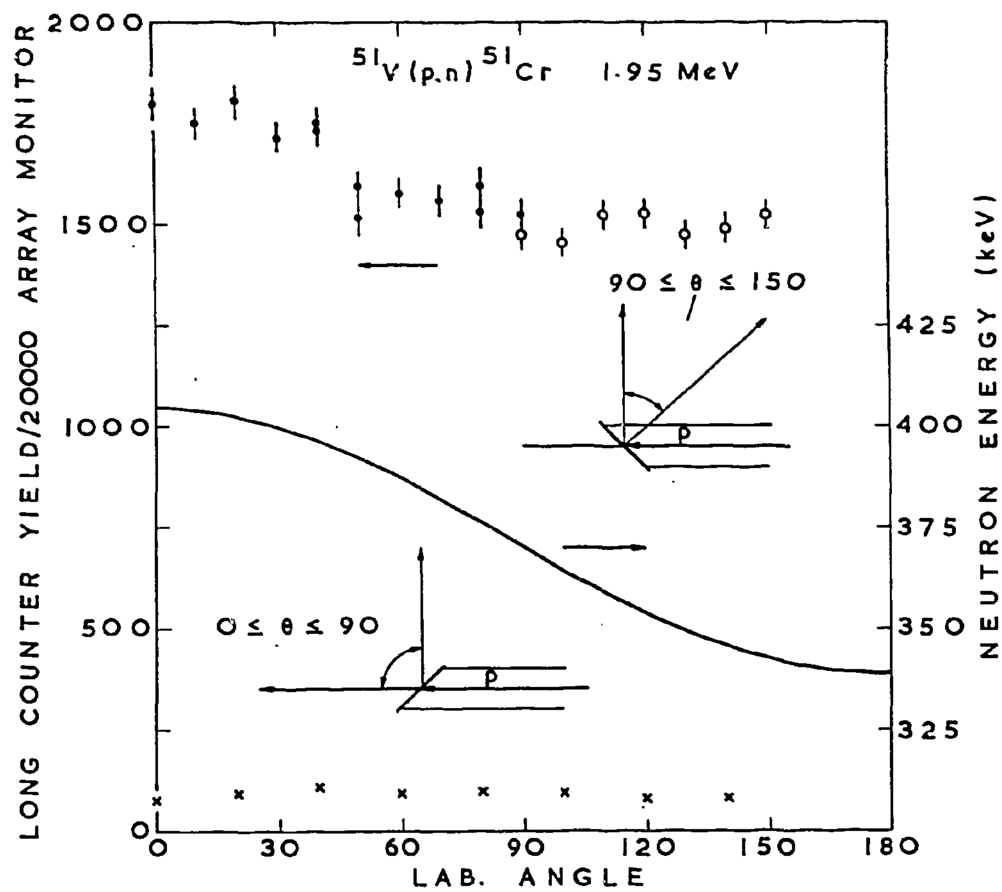

Fig. 3. Target orientation, angular dependence of neutron energy and angular dependence of long counter counts for ^{51}V target.

---

* On leave from the University of Melbourne, Australia. Since returned there.

(5) Adams J. M., Ferguson A. T. G. and McKenzie C. D. AERE PR/NP14, (1968).

(6) Allen W. D., AERE NP/R 1667.

hemispheres from the reaction $^{51}V(p,n)^{51}Cr$ can be obtained from the counting rate curve which along with the angular variation of the neutron energy is also shown in Fig. 3. The second long counter, which had previously been used to monitor the angular distribution measurements and introduced a large statistical counting error, was replaced by a 'super' long counter consisting of any array of seventeen 1 in. diam by 16 in. long BF_3 proportional counters. The background in the long counter, which had been a serious problem at lower neutron energies where the reaction yields are small[7], was greatly reduced by operating GLEEP at very low power.

We have also determined as a function of neutron energy the depth R_o inside the long counter at which effective thermalisation occurs. This redetermination was carried out with monoenergetic neutrons from the $^7Li(p,n)^7Be$ and $T(p,n)^3He$ reactions, measuring the yield as a function of distance from the target. Preliminary results indicate that the values of R_o are significantly greater than indicated by previous determinations made with neutron sources[6]. This is an important result in specifying the absolute efficiency of a long counter because it is not always either desirable or practicable to use the counter in exactly the same geometry as that employed for the calibration.

We pointed out before[5] that one of the main sources of error in the measurements arose from uncertainties in strengths of the ^{51}Cr and ^{57}Co sources used to determine the target activities. To reduce this error several ^{51}Cr sources calibrated to <0.5%[8], were obtained from NPL Teddington. The counting of the activated ^{51}V targets and of earlier ^{51}Cr sources with respect to these standard sources has now been completed and the data are being analysed. The decay of the ^{51}Cr sources obtained from NPL is now being measured, since previous determinations of the ^{51}Cr half life are not completely consistent[9].

E. Fast neutron spectra in reactor materials (A. J. H. Goddard and J. G. Williams (Imperial College) and H. Lichtblau (Birmingham University))

Theoretical and experimental studies of fast neutron spectra in spherical shells are continuing, following the work of Coates et al[10]. Here we report work concerned with natural uranium. Survey calculations have been carried out using the neutron transport theory code DTFIC, which is based on the Carlson S_n method[11]. We have studied: (1) The sensitivity of the spectra to changes in ^{238}U inelastic scattering cross-section. For a typical system at 2 MeV a 40% change in the spectrum results from a 20% change in the whole inelastic matrix; (2) the importance of a knowledge of the distribution of neutron sources within the target, using several possible source distribution models. We find that the leakage spectra from uranium shells at angles other than 0^o (the radial direction) are not changed by significant amounts as a result of plausible changes in the source model; (3) the effect of room return from the concrete walls of the target cell. This is likely to be significant only at energies below 50 keV (see Table I (page 5)).

In our experimental studies we used the $^{58}Ni(n,p)^{58}Co$ reaction to monitor the fast neutron output. Comparisons of measurements using this method with DTFIC calculations have shown that correct electron beam alignment is essential to obtain the source geometry assumed in the calculations. A beam sensing device developed by B. P. Clear of Nuclear Physics Division and described elsewhere in this report[12], has been installed to monitor the electron beam alignment during experimental runs.

We have carried out experiments to measure room return, using a uranium target displaced from its usual position so that most of the neutrons which reached the detector did so after scattering in the cell

---

(7) Johnson C. H., Galonsky A. and Inskeep C. N., ORNL-2910, p. 25.

(8) Campion P. J., Int. J. Appl. Rad. Isotops 4, 232 (1959).

(9) Lederer C. M., Hollander J. M. and Perlman I., Table of Isotopes (6th ed.) (Wiley, 1967).

(10) Coates M. S., Gayther D. B. and Goode P. D., AERE - R 5364 (1968).

(11) Carlson B. G., Los Alamos - LA 1891 (1955).

(12) Clear B. P. AERE PR/NP 15 p. 54.

wall. On the basis of this measurement the effect that the cell walls would have on a target spectrum has been calculated and is shown in Table 1 in the column headed 'Experiment'. Results based entirely on S_n calculations are shown for comparison in the column headed 'Theory' and a similar calculation for a typical shell spectrum is quoted in the final column. The larger percentages in the latter case reflect not an increase in the number of room return neutrons but a decrease in the number of neutrons in the target spectrum proper. For this spectrum experiment and theory disagree by a factor of two. This is outside statistical errors, and probably reflects an over-simplification in the calculations. The effect of room return is shown to be small over most of the energy range of interest. It is hoped that further measurements and calculations will establish reliable corrections where they are needed.

TABLE I

Percentage of spectra contributed by room return

Energy	Target spectrum		11 cm radius shell spectrum
	Experiment	Theory	Theory only
85 keV	0.5%	0.2%	1.3%
50 keV	0.9%	0.4%	1.8%
32 keV	1.2%	0.6%	3.3%
19 keV			10.0%
10 keV			25.0%

H. $\bar{\nu}$ for ^{238}Pu (D. W. Colvin)

A detailed evaluation has been made of $\bar{\nu}$ (the average number of neutrons/fission) for ^{239}Pu from thermal energies to 15 MeV. Preliminary fits to the existing data indicate that fast reactor requests for this parameter are already met at thermal energies and above 1-2 MeV if the comparison standard, ^{252}Cf, is assumed without error. However, in view of the theoretical and experimental evidence for structure below 1 MeV, consideration has been given to the design of an experiment to measure $\bar{\nu}$ as a continuous function of energy in the range from a few keV to 10 MeV using the time-of-flight facilities on the synchrocyclotron. This will avoid certain criticisms normally levelled at "spot-point" measurements carried out on electro-static generators.

H. Capture cross-section for ^{238}U (D. W. Colvin and P. H. Bowen)

First steps have been taken to set up the A.W.R.E. 80 cm liquid scintillator on the 45 MeV electron linac for feasibility tests. The counter will be used to entend measurements of the capture cross-section of ^{238}U to higher energies either on the synchrocyclotron or the linac or both.

E. The direct measurepments of alpha for ^{239}Pu over the energy range 10 eV to 30 keV (M. G. Schomberg, M. G. Sowerby and D. A. Boyce)

The work previously reported(13,14,15) has been continued and data have been obtained on a third ^{239}Pu sample of thickness 0.0044 atoms/barn, a ^{235}U sample of thickness 0.00109 atoms/barn and two

(13) Schomberg M. G., Sowerby M. G. and Evans F. W. Nuclear Physics Division Progress Report AERE - PR/NP 13 (1968).

(14) Schomberg M. G., Sowerby M. G. and Evans F. W. Fast Reactor Physics IAEA Vienna, I 289 (1968).

(15) Schomberg M. G., Sowerby M. G. and Evans F. W. Nuclear Physics Division Progress Report AERE - PR/NP 14 (1968).

lead samples. The data on the ^{235}U and lead samples are for checking that the system is operating correctly. The data from the third ^{239}Pu sample and ^{235}U sample are at present being analysed. The experiments with the lead samples show that both the fast neutron detectors and the capture gamma ray detectors are insensitive to scattered neutrons.

In the last progress report[15] it was stated that the observed efficiency of the capture gamma ray detector for fission events was higher than expected. This is thought to be mainly due to coincidences produced by two gamma rays and/or neutrons being detected in the two halves of detector. The effect is more pronounced for fission events because of the high gamma ray multiplicity and of the contribution from fission neutrons. To overcome it some changes have been made to the detector system. Two new detectors have been constructed with the thickness of the scintillator layers increased to improve the linearity of the response at lower gamma ray energies. These two detectors are arranged as shown in Fig. 4 and coincidences are taken between the following pairs of sections: AB, CD, AC and BD. The

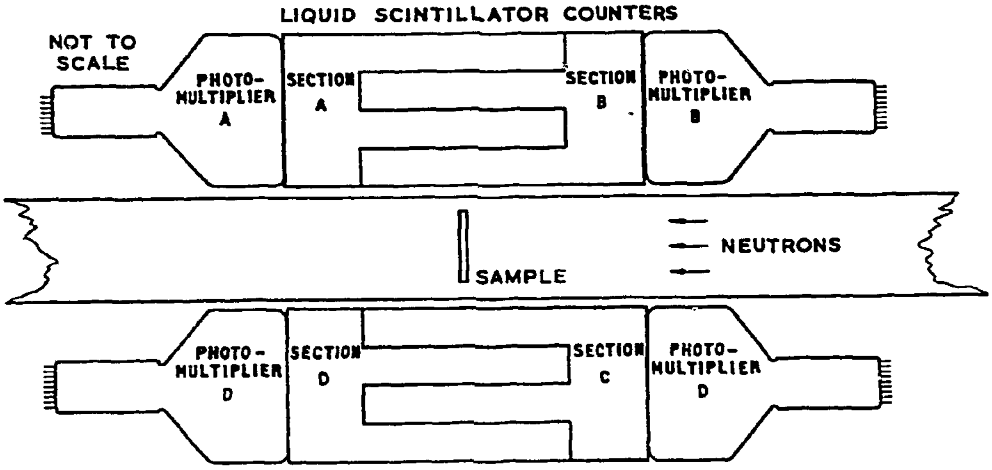

Fig. 4. Sketch showing layout of detector sections for ^{239}Pu alpha measurements.

coincidences AC and BD give a measure of the contribution from coincidences due to multiple events included in the number of AB and CD coincidences observed in each time-of-flight channel, so that this background can be subtraded off. Finally anti-coincidence techniques are used to subtract from the four coincidence outputs all events identified by the fast neutron detectors as fission events.

The re-designed detector system is now installed and is undergoing confirmatory checks to ensure that it has the desired characteristics. We now plan to make a further series of measurements of capture and fission yields from samples of ^{239}Pu with a range of different thicknesses.

Because alpha, or more specifically $\langle\sigma_{nc}\rangle/\langle\sigma_{nf}\rangle$, is one of the key quantities necessary for the efficient design of fast breeder reactors, the policy adopted with this experiment has been to publish provisional results as they become available and to reduce the uncertainty of these results as more data are obtained and the methods of analysis are improved. At the time of writing, October 1968, the provisional results of the present experiment together with other measurements and evaluations are shown in Fig. 5 (see page 7). In particular comparison can be made with the preliminary data of Gwin et al.[16] obtained at R.P.I. They discriminated between capture and fission events by observing the gamma rays produced in both types of reaction with a large liquid scintillator and using the fact that about 15% of fission events result in a pulse amplitude greater than the pulse amplitude produced by ~99% of the capture gamma ray cascades. Fairly large uncertainties are associated with both sets of data, but one can say that the results of the two experiments are in reasonable agreement. The evaluation from the

(16) Gwin R., Weston L. W., De Saussure G., Ingle R. W., Todd J. H., Gillespie F. E., Hockenbury R. W. and Block R. C. (1968) Private communication.

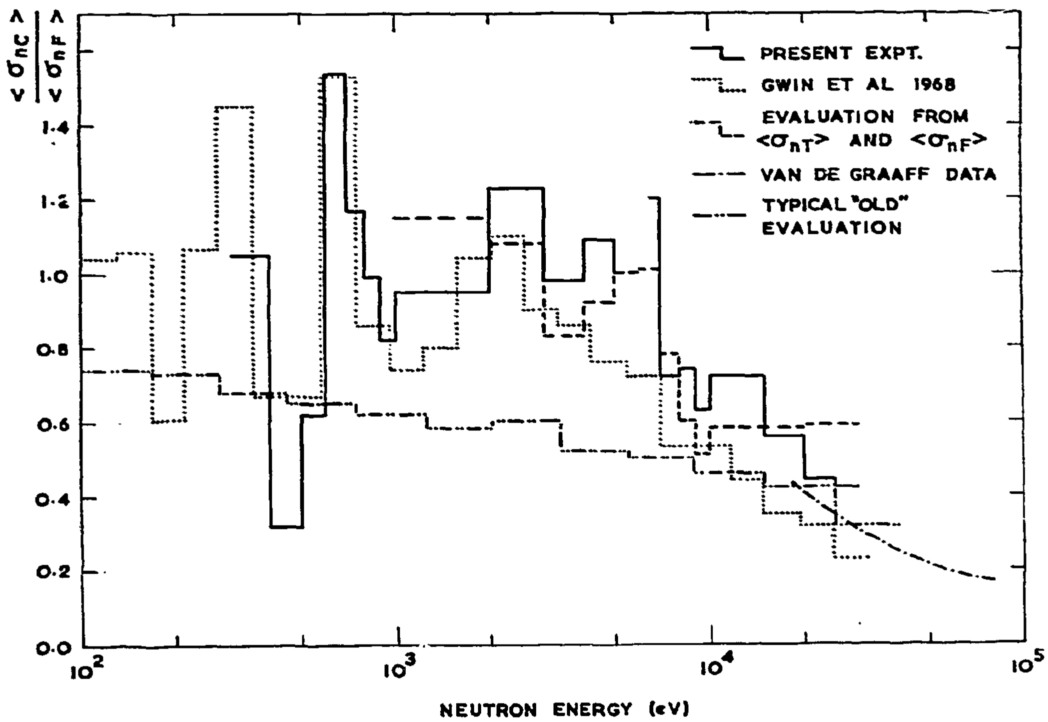

Fig. 5. Measured values of $<\sigma_{nc}>/<\sigma_{nf}>$ from various sources.

fission and total cross sections is very similar to that used in the last progress report[15] and is included to demonstrate that the results of the two direct measurements of alpha also agree with an indirect evaluation.

E. <u>Evaluation of the ^{239}Pu fission cross section in the energy range 1 keV to 100 keV (G. D. James and B. H. Patrick)</u>

Some of the input data used in this evaluation[17] depend on the $^{10}B(n,\alpha)$ cross section. These data have been revised to allow for the fact that this cross section is not strictly proportional to $1/\sqrt{E}$ but is more accurately represented below 30 keV by the equation

$$\sigma_{n,\alpha} = \frac{c}{\sqrt{E}} + a \qquad \ldots (1)$$

The constants c = 610.3 ± and a = -0.28 ± 0.12b have been deduced from the total cross section data of Diment[18] and the scattering data of Asami and Moxon[19]. A least squares analysis designed to minimise the sum of the squares of the deviations of the input data shown in Table II has been employed to deduce the recommended ^{239}Pu fission cross section which is given in column 12 of Table II. This work will be described in a forthcoming memorandum[20].

(17) James G. D. and Patrick B. H. AERE - PR/NP 14 p. 17.

(18) Diment K. M. AERE - R 5224 (1967).

(19) Asami A. and Moxon M. C., this report. p. 14.

(20) James G. D. and Patrick B. H. AERE - M 2065.

TABLE II

^{239}Pu and ^{235}U fission cross sections and ratios

E (keV)	Allen and Ferguson R	Gilboy and Knoll R	Bollinger et al. $\sigma_f(239)$	James $\sigma_f(239)$	Shunk et al. $\sigma_f(239)$	Patrick et al. $\sigma_f(239)$	White et al. $\sigma_f(239)$	Michaudon $\sigma_f(235)$	de Saussure et al. $\sigma_f(235)$	Hart evaluated $\sigma_f(235)$	Deduced Cross Sections	
											$\sigma_f(239)$	$\sigma_f(235)$
95	0.930	0.808					1.47			1.66	1.46 ± 0.06	1.67
85	0.910	0.807					1.47			1.70	1.47 ± 0.05	1.70
75	0.885	0.793					1.46			1.76	1.46 ± 0.05	1.75
65	0.867	0.771					1.46			1.82	1.47 ± 0.05	1.81
55	0.848	0.736					1.46			1.91	1.47 ± 0.06	1.90
45	0.825	0.698					1.45			2.02	1.48 ± 0.08	2.00
35	0.800	0.668								2.16	1.58 ± 0.14	2.16
25		0.639		1.62		1.53				2.36	1.57 ± 0.08	2.37
15		0.598		1.76		1.67				2.82	1.71 ± 0.04	2.82
9.5		0.554	2.28	1.85	2.14	1.99		3.27	3.04		2.06 ± 0.10	3.16
8.5		0.572	2.02	2.25	2.46	2.32		3.36	2.90		2.25 ± 0.12	3.14
7.5		0.600	1.86	2.27	2.24	2.17		3.41	3.69		2.14 ± 0.07	3.55
6.5		0.557	2.64	1.97	2.20	1.96		3.65	3.59		2.19 ± 0.13	3.62
5.5		0.548	2.74	2.41	2.71	2.17		4.13	3.77		2.50 ± 0.13	3.97
4.5			2.62	2.54	2.31	2.31		4.36	4.50		2.45 ± 0.09	4.43
3.5			3.45	2.86	2.74	2.73		4.75	5.02		2.95 ± 0.17	4.89
2.5			3.35	3.46	2.64	2.83		5.63	5.53		3.07 ± 0.20	5.58
1.5			3.91	4.40	3.43	3.64		7.42	7.42		3.85 ± 0.21	7.42

R = $\sigma_f(239)/\sigma_f(235)$

Cross sections are in barns

Results given in the last two columns are a least squares fit to the data shown in the rest of the Table.

E. Fluctuation analysis of the fission cross section of ^{239}Pu (B. H. Patrick and G. D. James)

The results of the fluctuation analysis of the fission cross section of ^{239}Pu first reported in the last progress report[21] have studied further and are now thought to be fairly well understood. The main results of the analysis are displayed in Fig. 6. In this figure every value of the serial correlation coefficient $r_k(W)$ which lies above the 1% significance level is plotted by a cross in the k-W plane. It can be seen that the highly significant values lie on parabolas corresponding to kW = 9 eV, 460 eV and 830 eV. Now the average spacing of the 0^+ levels in ^{240}Pu is 9.6 eV[22] and hence the correlation corresponding to kW = 9 eV is probably due to these levels. It is therefore reasonable to assume that the correlation corresponding to kW = 460 eV is due to levels with average spacing of 460 eV. Such levels are immediately explained by the theory of Strutinsky[23] who showed that when shell effects are taken into account, the deformed nucleus may have a second minimum in its potential energy. The 1^+ channel in the fission of $^{239}Pu + n$ lies ~200 keV below the neutron separation energy and hence we suggest that the levels built on the second minimum of the 1^+ channel, designated Class II levels by Lynn[24], have an average spacing of 460 ± 80 eV in ^{240}Pu. The error in the spacing arises from the limited number of levels in the region studied and assuming a Wigner distribution for the spacing. The correlation corresponding to kW = 830 eV is probably due to the Class II levels taken in pairs.

A paper describing the results of the correlation analysis in more detail has been accepted for publication in Physics Letters.

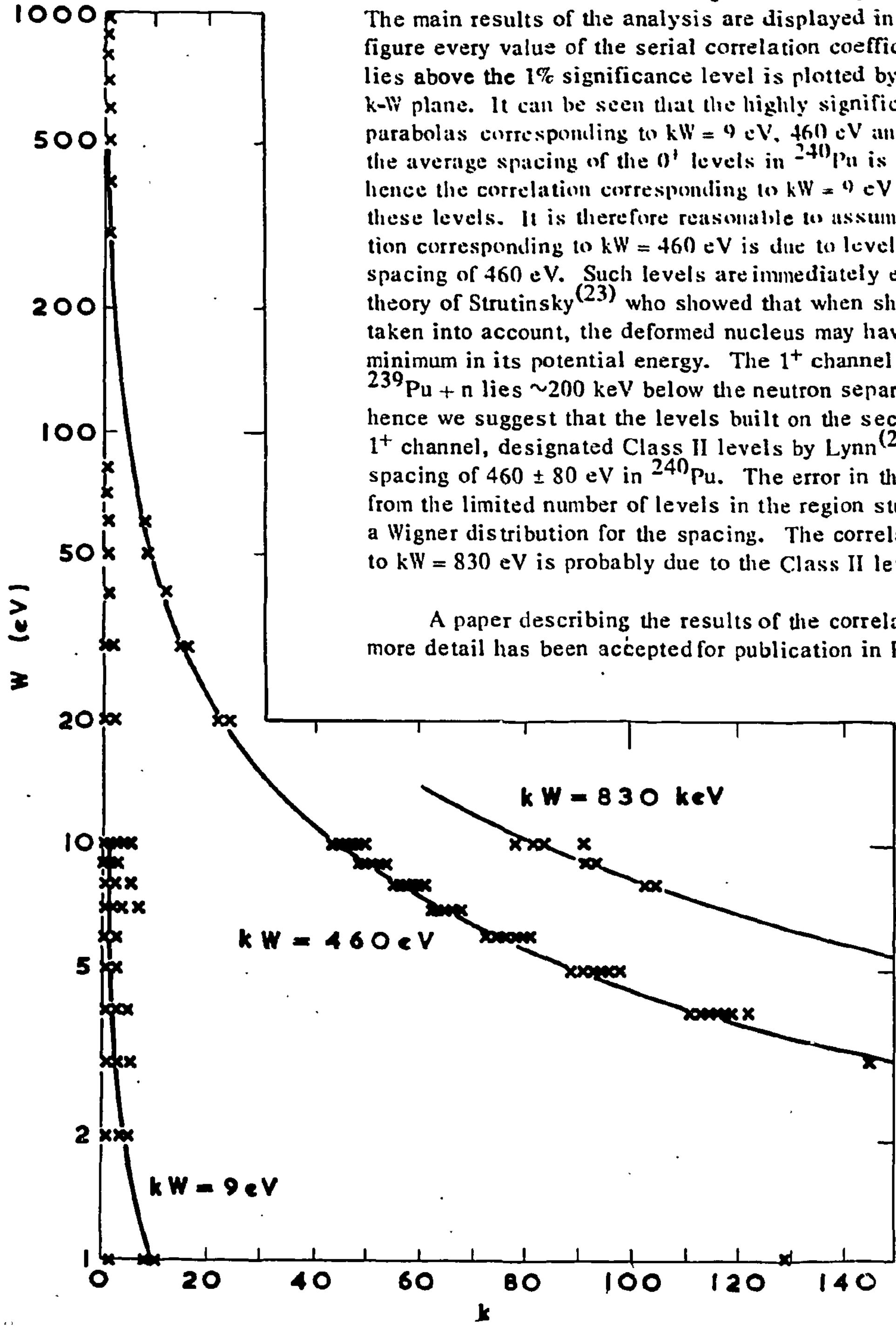

Fig. 6. Plot of k against kW for those values of $r_k(W)$ lying above the 1% significance level.

E. Search for $^{240}Pu(n,\alpha)$ reaction (N. J. Pattenden and J. E. Jolly)

Accurate measurements of neutron transmission, capture and scattering yields for ^{240}Pu performed previously on the linac gave values of resonance parameters which indicated that the three types of results were mutually inconsistent[25]. This inconsistency could be resolved if another reaction were providing an anomalously large yield. The (n,α) reaction is energetically possible, with 10.4 MeV available. An experiment was therefore carried out to see if long-range α particles could be detected at neutron resonance energies. A platinum foil coated over an area of about 3 cm^2 with 1.78 mg of ^{240}Pu was mounted about 2 cm from a surface barrier semiconductor, with 5.4 mg/cm^2 foil of Al between them (corresponding to the range of a 4.7 MeV α particle). The energy of the natural α particles from ^{240}Pu is 5.16 MeV. The discriminator threshold for the detector was set at 1.5 MeV, ensuring that natural α particles were not counted, but only those with energies greater than 6.2 MeV. The system was mounted in an evacuated chamber, and placed in a neutron beam from the linac booster at 10 m from the target.

Despite precautions there was a considerable background, some of it presumably partly due to pile-up in the detecting electronics. No effects were observed at neutron times of flight corresponding to resonances. Subsequently, runs were performed with a ^{235}U target and without the Al, the electronics bring set to count fission fragments only. The areas of the peaks in the spectrum of fission fragment yield as a function of energy were combined with the known ^{235}U resonance parameters, to fix an approximate scale to the upper limits which could be given to the α widths (Γ_α) for the ^{240}Pu resonances below 100 eV neutron energy. For the 1.06 eV resonance, the limit is $<4 \times 10^{-6}$ eV, for other resonances below 91 eV Γ_α is $<5 \times 10^{-4}$ eV and for the 92.6 eV resonance Γ_α is $<2 \times 10^{-3}$ eV.

Thus the inconsistencies in the previous measurements cannot be explained by the existence of an (n,α) reaction.

E. Total cross section measurement of ^{234}U (G. D. James, G. G. Slaughter (ORNL) and D. A. J. Endacott).

The total cross section of ^{234}U has been measured with the small sample time-of-flight spectrometer of the Harwell neutron project. The path length was 15 m, the timing channel width ⅛ μs and the electron burst width ¼μs. Transmission measurements were made with a 767 mg sample of 99.37% ^{234}U at sample thicknesses of 0.00258, 0.00619 and 0.01674 atoms per barn. These data are being analysed by the area method to deduce the resonance neutron widths. It is hoped thereby to extend the analysis of those resonances which James and Rae[26] found to have fission components.

E. Fission components in ^{242}Pu resonances (G. D. James and D. A. J. Endacott)

At least three nuclei, ^{240}Pu[27,28], ^{237}Np[29] and ^{234}U[30] are now known to have groups of

(21) A.E.R.E. report PR/NP 14, p. 18, (1968).

(22) Derrien H., Blons J., Eggermann C., Michaudon A., Paya D. and Ribon P. Proc. IAEA Conf. on Nuclear Data for Reactors, Paris (1966) Vol. II, p. 195.

(23) Strutinsky W. M. Nucl. Phys. A95, 420 (1967).

(24) Lynn J. E. Conf. on Low and Medium Energy Nuclear Physics (A.E.R.E., 1968), Report R 5744, p. 3 and "The Theory of Neutron Resonance Reactions" (Clarendon Press, Oxford, 1968) p. 463.

(25) Asghar M., Moxon M. C. and Pattenden N. J. AERE Report R - 5945 (1968) to be published.

(26) James G. D. and Rae E. R. Nucl. Phys. A118 313 (1968).

(27) Weigmann H. and Schmid H. J. Nucl. Energy 22, 317 (1968).

(28) Migneco E. and Theobald J. P. Nucl. Phys. A112, 603 (1968).

(29) Paya D., Derrien H., Fubini A., Michaudon A. and Ribon P. Nuclear Data for Reactors, Vol. II (IAEA Vienna, 1967) p. 128.

(30) James G. D. and Rae E. R., Nucl. Phys. A118, 313 (1968).

resonances in their sub-threshold fission cross sections which according to Weigmann(31) and Lynn(32) can be explained in terms of the second minimum in the fission potential barrier predicted by Strutinsky(33). A measurement over the energy range 16 eV to 35 keV of the fission cross section for ^{242}Pu shows that this nuclide also has fission components in some of its sub-fission-threshold resonances, as illustrated in Fig. 7. The separation between the two groups near 800 eV and near 30 keV is taken to be the spacing between the levels in the second potential minimum designated by Lynn(32) as Class II states. Thus D_{II} = 29 ± 15 keV corresponding to an energy difference of $3.2^{+0.6}_{-0.2}$ MeV between the first level in the second minimum and the ground state in ^{242}Pu. It has been possible to correlate the two resonances at 767 eV and 799 eV with dips in the transmission data obtained by Pattenden(34) and to deduce for these resonances the resonance parameters given in Table III.

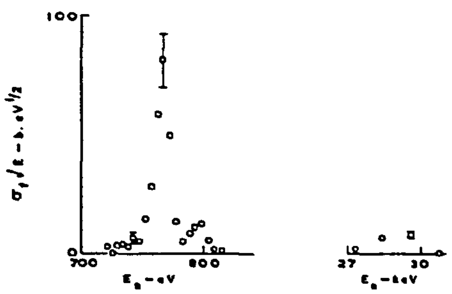

Fig. 7. ^{242}Pu fission resonances below 35 keV.

Lynn(32) has shown that under conditions of very weak coupling when the situation can be treated by perturbation theory, the observed fission widths are spread over only a few levels, and from Table III, this state of affairs appears to exist in ^{240}Pu. He shows that a level which contains a large fraction of the Class II strength, as deduced from its fission width should contain a correspondingly small fraction of the Class I strength, as deduced from its neutron width. For the two levels near 800 eV in Table III, it will be seen that at one standard deviation from the mean the proportion of Class II strength in the level at 767 eV is 84.2% from the ratio of neutron widths and 85% from the ratio of fission widths which shows that the equations of perturbation theory can be satisfied.

TABLE III

Parameters of ^{235}Pu resonances which show fission components

E_f (eV)	E_T (eV)	$\sigma_0\Gamma_f$ (b.eV)	Γ_n(a) (meV)	Γ_f(a) (meV)	Γ_γ (meV) (assumed)
767	764	47.2 ± 6.0	$89^{+49}_{-33}{}^{+24}_{-16}$	22^{-4}_{+16} ± 3	27
799	800	7.8 ± 1.4	465^{+105}_{-100} ± 50	2.5 ± 0 ± 0.44	27
29.6 keV		108 ± 27			

(a) The first errors quoted in these columns are systematic and therefore correlated, the second errors are statistical.

(31) Weigmann H. Zeits. fur Phys. 114, 7 (1968).

(32) Lynn J. E. The Theory of Neutron Resonance Reactions (Clarendon Press, Oxford, 1968) p. 463 and AERE Report R - 5891.

(33) Strutinsky V. M. Nucl. Phys. A95, 420 (1967).

(34) Pattenden N. J. Nuclear Structure with Neutrons, EANDC-50S, Vol. I, 93 (1965).

E. The total cross-section of ^{6}Li (K. M. Diment and C. A. Uttley)

In the last progress report[35] we described the results of analysing the total cross-section of ^{6}Li from 70 eV to 5 keV by fitting a curve of the form $c/\sqrt{E} + b$ to the data, and presented a preliminary analysis of the p-wave resonance at 250 keV in which it is assumed that the resonance is superimposed on an s-wave background total cross-section which is the sum of the $c/\sqrt{E}$ absorption cross-section and a potential scattering cross-section for which the value at low energies is equal to b.

The parameters of the p-wave resonance, which are determined by fitting a single level Breit-Wigner formula to the resonance, are the reduced neutron width γ_n^2, the reduced alpha width γ_α^2 and the energy eigenvalue E_λ'. These parameters depend in principle on the choice of interaction radii R_n, R_α for the entrance and exit channels respectively, but the almost constant values of χ^2 obtained show that the fits are insensitive to variations in R_n from 2.5 to 3.9 fm and in R_α from 3 to 4 fm, within which limits the channel radii are expected to lie. In fact for $R_n < 2.5$ fm the reduced neutron width γ_n^2 becomes greater than the sum rule limit $3\hbar^2/4\mu R_n^2$, where μ is the reduced neutron mass. Furthermore it is found that the p-wave absorption and scattering cross-section at energies below the resonance are also insensitive to the choice of interaction radii. Thus the presence of a minimum in the total cross-section at about 75 keV should allow the validity of the above mentioned extrapolation of the s-wave interaction to higher energies to be tested by comparing the calculated s-wave and the p-wave resonance total cross-sections with the measured data near 75 keV. This comparison is shown in Fig. 8, where the dotted curve is seen to lie systematically higher than the experimental points.

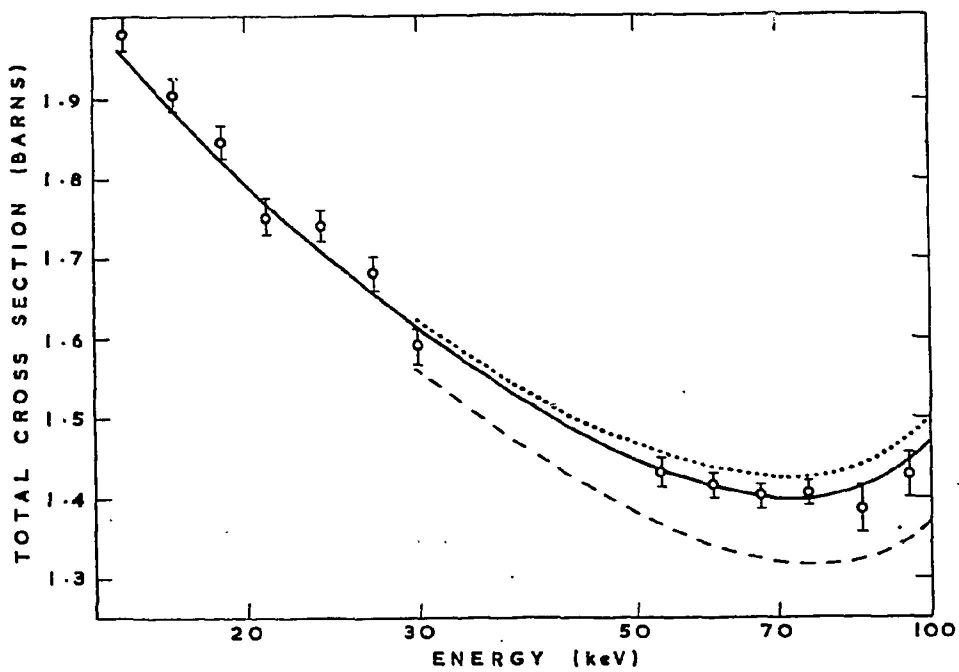

Fig. 8. Comparison of calculated and experimental cross sections for ^{6}Li near the 70 keV minimum.

(35) Diment K. M. and Uttley C. A. Nuclear Physics Division Report AERE PR/NP14 (1968).

A similar comparison can be made with the measured total cross-section near the minimum at 1 MeV and also between the calculated s- and p-wave scattering cross-section and the experimental elastic scattering data obtained by Lane et al.[36] and by Knitter and Coppola[37] at 1 MeV. In these calculations, shown as dashed curves in Fig. 9, the minimum p-wave resonance contribution was used, corresponding to an entrance channel radius of 2.5 fm. At this energy the calculated total and scattering cross-sections are both too large, indicating that the s-wave scattering at least must decrease with increasing energy faster than potential scattering.

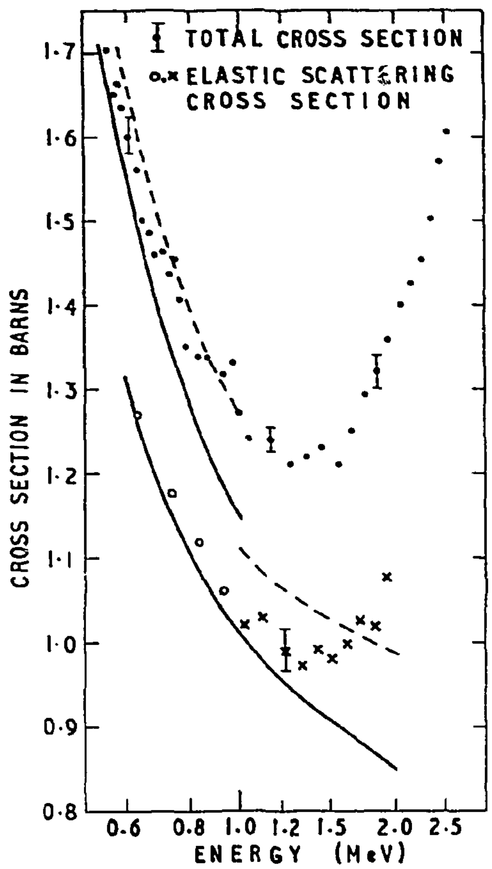

Fig. 9. Comparison of calculated total and scattering cross-sections with experimental results near 1 MeV.

The fact that the s-wave scattering cross-section varies somewhat more rapidly with energy than would be expected if the s-wave interaction were due to very distant s-states can be explained by considering the scattering lengths. The scattering lengths a_+ and a_- for the $\tfrac{3}{2}$+ and $\tfrac{1}{2}$+ s-wave spin sequences respectively are complex, because the absorption width in each channel is appreciable. If it is assumed that for each spin sequence only one resonance contributes significantly at low energies then the parameters which define the imaginary parts of the scattering lengths are those which determine the fraction of the low energy, e.g. thermal, absorption cross-section due to each spin state. It has been found[38] that 75% of the s-wave absorption cross-section is due to the $\tfrac{1}{2}$+ spin sequence. The real parts of the scattering lengths a_+, a_- can now be determined by combining the real part of the coherent scattering length (+1.8 fm) measured by Peterson et al.[39] with the measured constant $b = 0.7$ barns[35], which is close to the zero energy (free atom) scattering cross-section. Of the two possible pairs of real scattering lengths derived from this analysis, one is incompatible with the observations of Lane et al.[40] on the scattering of polarized neutrons by ^{6}Li, which show that most of the s-wave scattering cross-section takes place with channel spin $\tfrac{1}{2}$. The alternative pair makes the real parts of a_+, a_- +0.2261 fm and +4.174 fm respectively, and the large value of the latter for such a light nucleus suggests that a bound $\tfrac{1}{2}$+ state is present in ^{7}Li. The only possible location of this state is the broad level at 6.56 MeV which does not have a definitely assigned spin and parity[41]. Specifying the position of this $\tfrac{1}{2}$+ state allows one to derive both the reduced neutron width and the alpha width from the real and imaginary parts of a_- for a given choice of entrance channel radius R_n. A similar calculation can be made for the $\tfrac{3}{2}$+ state, which is much less important than the $\tfrac{1}{2}$+ state since it contributes only 25% of the absorption cross-section and a negligible fraction of the scattering cross-section. Since the real part of a_+ is small this state must be at positive energies, and it has been assumed to be the first unassigned level at 2.447 MeV (C.M.)

---

(36) Lane R. O., Langsdorf A., Monahan J. E. and Elwyn A. J. Ann. Phys. 12, 135 (1961).

(37) Knitter H. H. and Coppola M. EANDC(E)100 AL (1967).

(38) Mahaux C. and Robaye G. Nucl. Phys. 74, 161 (1965).

(39) Peterson S. W. and Smith H. G. J. Phys. Soc. Japan 17, Supplement B-11, 335 (1962).

(40) Lane R. O., Elwyn A. J. and Langsdorf A. Phys. Rev. 136, B 1710 (1964).

(41) Lauritsen T. and Ajzenberg-Selove F. Nucl. Phys. 78, 1 (1966).

The s-wave total and partial cross-section can now be calculated for different values of R_n. The value $R_n = 2.5$ fm gives a very poor fit to the total cross-section, even below 100 keV, as the dashed curve in Fig. 8 shows, because the scattering cross-section decreases too rapidly with increasing energy. An effective radius of 3.9 fm, however, produces parameters $\gamma_n^2 = 0.214$ MeV and $\Gamma_\alpha = 2.58$ MeV for the bound state, which gives a good fit, as shown by the solid curve in Fig. 8. In this case the resonance scattering is much less and potential scattering dominates. Extending the comparison to the measured data near 1 MeV we see from the solid curve in Fig. 9 that the calculated scattering cross-section joins smoothly with the measured one while the calculated total cross-section falls increasingly below the measured total cross-section as the energy rises towards 1 MeV. This is to be expected, since the states forming the maximum near 4 MeV will contribute an absorption cross-section below 1 MeV which decreases linearly with penetrability, while the resonance scattering will fall even more rapidly than the square of the penetrability because of the negative contribution from resonance - potential interference.

The s-wave absorption cross-section derived from this analysis can be expressed as (E in eV)

$$\sigma_{n,\alpha} = 149.56/\sqrt{E} + \Delta(E)$$

where $\Delta(E)$ is constant at -0.024 barns up to a few keV and decreases to -0.048 barns at 1 MeV. However the absorption cross-section still remains somewhat sensitive to the initial assumptions involved, particularly the assumed position of the $^3/_2$+ state. We suggest therefore that the $^6Li(n,\alpha)T$ cross-section up to the threshold for the $^6Li(n,dn)\alpha$ reaction at 1.7 MeV can be obtained by subtracting the scattering cross-section from the measured total cross-section.

E. Neutron scattering measurements on ^{10}B and ^6Li. (A. Asami (J.A.E.R.I. Japan) and M. C. Moxon)

The neutron scattering measurements on ^{10}B have been completed and the data have been analysed. The observed values of the scattering cross section in the energy range 0.9 to 130 keV are given in Table IV. The measurements of the scattering cross-section of ^6Li have been completed and are now being analysed.

GENERAL NUCLEAR DATA FOR REACTORS

Shape quantum numbers in sub-threshold fission (J. E. Lynn)

It has long been believed that the fission mode of motion of an excited nucleus is one that is strongly damped; i.e. the elementary fission mode, a prolate shape vibration leading to division of the nucleus, is dissolved among the compound nucleus states over a very broad energy interval. Now, however, there is evidence that the strong damping mechanism breaks down, at least for sub-threshold fission, and that this breakdown is associated with the existence of metastable shapes of the nucleus.

There are four main groups of evidence. The first starts from the discovery of spontaneous-fissioning isomers by Flerov and Polikanov in 1964. Since the original discovery, a number of these highly interesting isomeric states have been discovered, and their properties investigated, mainly by Flerov and Polikanov's group in Russia[42] and by Bjørnholm and his colleagues[43] in Copenhagen. Their half-lives are in the nanosecond to millisecond range and the principal mode of decay appears to be spontaneous fission. The energies of these states have been found in a few cases to be about 3 MeV above the ground state of the respective isotope, thus showing that their peculiar property is not the decay by spontaneous fission, but the extraordinary inhibition of gamma-decay to lower states. Analysis of the shapes of the yield curves for formation of the isomers shows that their spins are not particularly high (≈ 7).

(42) Flerov G. N., Polikanov S. M. et al., Nucl. Phys. A97, 444 (1967).

(43) Borggren J., Gangrsky Y. P., Slettin G. and Bjørnholm S. Phys. Letters 25B, 402 (1967).

TABLE IV

Total scattering cross section for ^{10}B (averaging intervals indicated).

Energy (keV)	Energy Interval (keV)	Scattering Cross Section (barns)	Total Uncertainty
0.1271E 03	0.2182E 02	0.2974E 01	0.3316E 01
0.1065E 03	0.1677E 02	0.2892E 01	0.4656E 01
0.7803E 02	0.1052E 02	0.2621E 01	0.4666E 01
0.6788E 02	0.8550E 01	0.2561E 01	0.4457E 01
0.5960E 02	0.7030E 01	0.2565E 01	0.4846E 01
0.5274E 02	0.5860E 01	0.2502E 01	0.5211E 01
0.4701E 02	0.4930E 01	0.2499E 01	0.5354E 01
0.4216E 02	0.4190E 01	0.2510E 01	0.6722E 01
0.2752E 02	0.4430E 01	0.2320E 01	0.4988E 01
0.2335E 02	0.3460E 01	0.2298E 01	0.5075E 01
0.2006E 02	0.2760E 01	0.2246E 01	0.5062E 01
0.1743E 02	0.2230E 01	0.2237E 01	0.5188E 01
0.1528E 02	0.1830E 01	0.2252E 01	0.5332E 01
0.1350E 02	0.1520E 01	0.2210E 01	0.5457E 01
0.1202E 02	0.1280E 01	0.2248E 01	0.5590E 01
0.1025E 02	0.2012E 01	0.2230E 01	0.5526E 01
0.8400E 01	0.1493E 01	0.2237E 01	0.5789E 01
0.7010E 01	0.1139E 01	0.2259E 01	0.6026E 01
0.5940E 01	0.8880E 00	0.2264E 01	0.6687E 01
0.5100E 01	0.7060E 00	0.2203E 01	0.6343E 01
0.4420E 01	0.5710E 00	0.2236E 01	0.6817E 01
0.3870E 01	0.4680E 00	0.2191E 01	0.7858E 01
0.1935E 01	0.3300E 00	0.2203E 01	0.7778E 01
0.1625E 01	0.2540E 00	0.2163E 01	0.7515E 01
0.1385E 01	0.2000E 00	0.2153E 01	0.7598E 01
0.1195E 01	0.1600E 00	0.2170E 01	0.7833E 01
0.1040E 01	0.1310E 00	0.2169E 01	0.8103E 01
0.9150E 00	0.1070E 00	0.2155E 01	0.8238E 01
0.7000E 00	0.2840E 00	0.2108E 01	0.8223E 01
0.4700E 00	0.1570E 00	0.2063E 01	0.8881E 01

The second line of research, due to Strutinsky[44], is a purely theoretical investigation into the deformation energy of nuclei. In an effort to explain the equilibrium deformations of non-magic nuclei as well as the heights and saddle-point deformations of fission barriers, Strutinsky adopted a combination of liquid-drop model, which provides the major component of the nuclear mass, and a Nilsson deformed shell-model; the latter provides a correction term to the liquid-drop energy. Minima in the shell-correction term occur where there are gaps in the single-particle level structure near the Fermi energy of the system. For spherical nuclei these minima are most pronounced at the magic numbers, but the important property of the Nilsson diagram which Strutinsky emphasises is that other gaps occur at non-zero deformations, and that for a given nucleon number such gaps recur with increasing deformation. Thus according to the calculations several minima can occur in the potential energy of deformation of a nucleus, and in particular a secondary minimum of this kind is expected to be strongly pronounced in the trans-uranic nuclei. This secondary minimum provides a possible explanation of the spontaneous fissioning isomers; such an isomer would be the lowest vibrational state of the secondary minimum. For such an isomer tunnelling towards decay by spontaneous fission would be less inhibited than usual, while gamma decay would be strongly reduced because of the small amplitude of the wave function in the normal minimum.

The Strutinsky theory also provides a possible explanation of the third phenomenon. This is the coarse structure found in neutron-induced sub-threshold fission cross-sections. Typical of these data (averaged over many resonances) are the peak at 750 keV in the cross-section of ^{230}Th, which rises[45] to 50 mb and falls to 10 mb in less than 100 keV, the peaks at 1.6 and 1.7 MeV in the cross-section of ^{232}Th, and the 15 keV wide peak[46] at 12 keV in the cross-section of ^{241}Am. Such structure cannot be explained quantitatively in terms of competition from inelastic scattering. It appears to be gross structure in the fission mode, of a kind that can be explained phenomenologically by a complex potential model having a very small damping component (of the order of tens of keV). Damping widths are believed to be strong functions of the intrinsic excitation energy available to a compound nucleus, so the small width might be explained as being due to the occurrence of the sub-threshold fission mode as a vibration in a shallow, secondary minimum.

The fourth phenomenon lends still more support to the idea of a secondary minimum in the deformation energy. This phenomenon was discovered originally in the compound nucleus ^{238}Np at Saclay[47], in ^{241}Pu at Geel[48] and a little later in ^{235}U, ^{240}Pu and ^{243}Pu at Harwell[49], when observations revealed that in the slow neutron cross-sections of these fissionable, but sub-fissile, nuclei narrow bands of resonances with large fission widths occurred among the normal resonances with very weak fission. These 'fissile bands' are spaced at intervals of the order of 50 to 1000 times that of the fine structure resonances. This kind of resonance structure indicates the influence of a new, nearly good, quantum number, in addition to the usual ones of total angular momentum and parity. The properties of the observed structure strongly suggest that this new quantum number is a shape quantum number associated with the Strutinsky deformation potential[50,51]. The second minimum in the potential energy curve provides a second class of states, of complicated 'compound nucleus' type, that are associated

(44) Strutinsky V. M. Nucl. Phys. A95, 420 (1967).

(45) Evans J. E. and Jones G. A. - private communication (1965).

(46) Seeger P. A., Hemmendinger A. and Diven B. C. Nucl. Phys. A96, 605 (1967).

(47) Fubini A., Blons J., Michaudon A. and Paya D. Phys. Rev. Letters 20, 1373 (1968).

(48) Migneco E. and Theobald J. P. Nucl. Phys. A112, 603 (1968).

(49) James G. D. and Rae E. R. Nucl. Phys. A118, 313 (1968).
Patrick B. H. and James G. D. Phys. Letters (in press)
James G. D. Nucl. Phys. (to be published) and Harwell Report AERE - R 5924.

(50) Lynn J. E. "Theory of Neutron Resonance Reactions", (Clarendon Press, Oxford 1968) p. 461.
Harwell Report AERE - R 5891 (1968).
Structure effects in nuclear fission, invited paper at Dubna International Symposium on Nuclear Structure, July 1968.

(51) Weigmann H. Zeits fur Phys. 114, 7 (1968).

with prolate shape vibrations having most of their amplitude in this minimum. The lowest, or 'ground', state of this class of states is the spontaneously fissioning isomer. For a given total energy of the compound nucleus, these states are much less dense than compound states of the other class (associated with vibrations in the deeper minimum), because the effective excitation energy for intrinsic nucleonic motion is less. At the same time they have a much greater probability of fissioning (having only one barrier, the saddle-point barrier, to tunnel through) and negligible chance of elastic neutron emission. [illegible]h intermediate maximum between the two wells causes the coupling between the two classes of [illegible] to be weak, thus accounting for the observed phenomenon that the fission width of each class II state spread into a few only of its class I neighbours.

The detailed quantitative structure in the cross-section depends on a number of factors. The spacing of the fissile bands (the class II level spacing) relative to the normal resonance spacing (the class I level spacing) is governed principally by the potential energy difference between the two minima. The application of a statistical level density law to the cross sections so far measured suggests that this difference ranges from about 1.9 MeV (in ^{241}Pu) to about 3.3 MeV (in ^{243}Pu). The widths of the fissile bands are expected to depend in a rather complex manner on the height of the intermediate maximum (which determines a 'damping' or 'spreading' width of the class II states into the denser class I states) and on the height of the saddle-point barrier which governs the 'natural' decay of the class II states by fission. These relations are complicated even more by the possible existence of gross structure in the class II fission and by statistical fluctuations of the individual coupling matrix elements and the class II fission widths; such statistical fluctuations are of the kind very familiar in normal resonance cross sections.

Some of these effects have already been studied semi-quantitatively[50] and we are now beginning more detailed theoretical studies. In particular, we are attempting numerical calculations of complicated intermediate coupling situations so that experimental data can be analysed more fully, and we are also making a quantitative study of the dependence of coupling widths on the height and 'thickness' of the intermediate barrier.

E. <u>Capture γ-ray spectra following resonance neutron capture (P. Axmann (Vienna), M. C. Moxon and P. Riehs (Vienna))</u>

In many laboratories germanium crystal diodes have been used in conjunction with time of flight techniques to examine γ-ray spectra following resonance neutron capture. However, because the efficiency of these detectors is low, high neutron fluxes are required in these measurements and only a few low energy resonances can be resolved well enough to allow the γ-ray spectra to be examined. Although large sodium iodide crystals have a much poorer γ-ray energy resolution than germanium detectors, their overall efficiency for detecting high energy γ-rays is at least an order of magnitude greater, so that they can be used with longer flight paths and hence, better neutron energy resolution. Thus they allow more resonances to be examined, and so indicate elements and neutron energy regions where germanium crystals can be usefully employed to study the spectra in finer detail.

We have used an 8 inch diameter 6 inch thick NaI crystal at the end of a 45 m flight path to examine γ spectra following neutron capture. The overall timing resolution ranged from ~23 nsec/m for $E_n < 50$ eV to ~5 nsec/m for $E_n \leqslant 1$ keV. The data were recorded in 16 bit binary form on 1 inch magnetic tape, 10 bits for the time of flight data and 6 bits for the gamma ray energy information.

The γ-ray spectrum for each individual resonance was obtained by summing each gamma ray energy channel over the time of flight channels spanning the resonance. The background for each summed gamma ray channel was calculated from the gamma spectra for time of flight channels on either side of the resonance. The resulting γ-ray spectra were then normalised to unit area, so that the gamma ray spectra of several resonances could be easily compared.

The high energy γ-ray spectra emitted following neutron capture by ^{198}Hg showed marked fluctuations over the first five resonances, and suggested that the γ spectrum for the 23 eV resonance was more typical of the isotope than the spectrum for the 98 eV resonance. The nature of these spectra suggested that this isotope should be studied with a germanium spectrometer[52]. Data for the other isotopes of Hg, for ^{197}Au and for ^{181}Ta have also been accumulated and are at present being analysed. In the case of ^{197}Au, where 55 resonances could be easily examined, the observed fluctuations in the spectra can probably be explained in terms of Porter-Thomas distributions for the partial radiation width.

E. Gamma-ray spectra from resonance neutron capture (B. W. Thomas, J. Murray, E. R. Rae and C. A. Uttley)

Much of the work carried out during the last six months has been a measurement of the resonance capture gamma-ray spectra of mercury, particularly for the reaction ^{198}Hg(n,γ)^{199}Hg[53].

Experimental data from a target of natural mercuric oxide were collected on the 10 metre flight path of the Harwell linear accelerator, using a 25 cm^3 co-axial Ge(Li) detector for the gamma rays. The raw data were handled by an on-line system based on the PDP-4 computer, which permits the storage of capture data for continuous ranges of neutron and gamma-ray energy, by associating with each capture event both time-of-flight and pulse height co-ordinates.

Analysis of the data into resonance gamma-ray spectra was carried out by selecting those events falling in the appropriate intervals in the time-of-flight spectrum. In this way gamma-ray spectra were obtained for known resonances in ^{198}Hg and ^{201}Hg, the background spectra being deduced from analysis of data between resonances.

Figure 10 shows a time-of-flight spectrum for mercury obtained by summation over pulse heights ≥800 keV, while Figure 11 shows high energy (4-7 MeV) gamma-ray spectra for five resonances in ^{198}Hg.

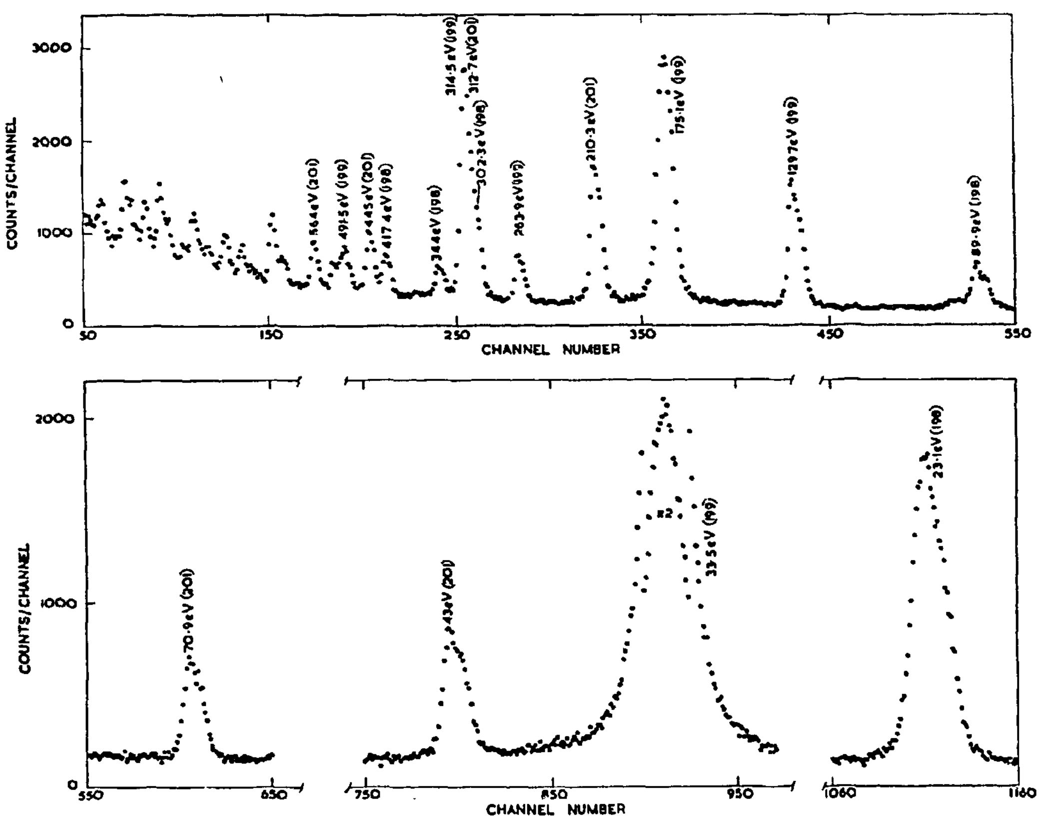

Fig. 10. Time of flight spectrum of mercury for E_γ > 800 keV.

(52) Thomas B. W., Murray J., Rae E. R. and Uttley C. A. This report p. 18.

(53) Thomas B. W., Uttley C. A. and Rae E. R. Nuclear Physics Division Progress Report AERE - PR/NP 14 p. 23, (1968).

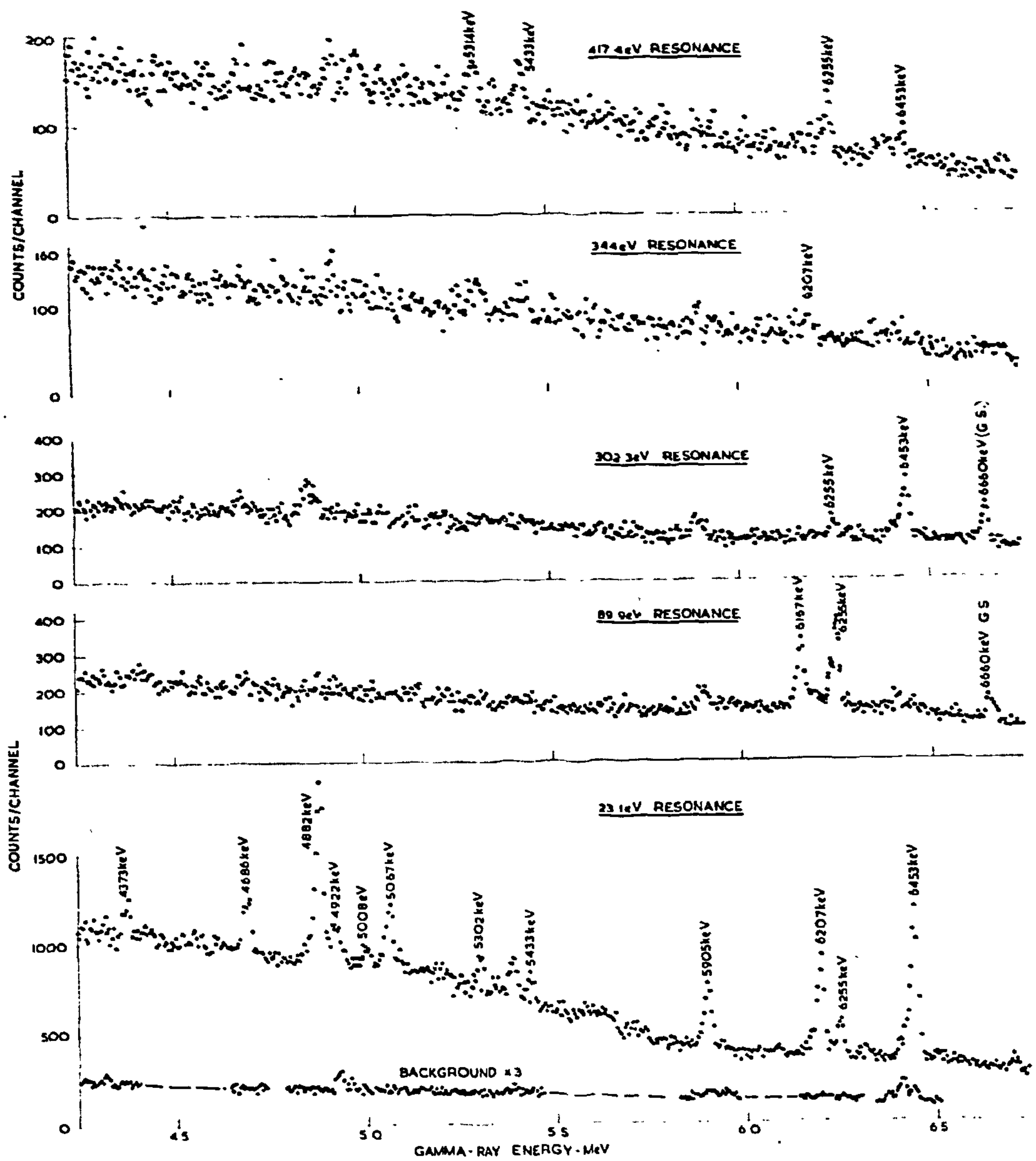

Fig. 11. Gamma rays in range 4 → 7 MeV from five slow neutron capture resonances of ^{198}Hg.

Table V (see page 20) lists estimates of the relative intensities of the gamma-rays observed. Several gamma-rays with energies below 2 MeV were distinguishable only at the relatively strong 23 eV resonance. An outstanding feature of the ^{198}Hg data is the sharp contrast in the 23 eV and 90 eV resonance spectra between 4.5 and 5.5 MeV.

An energy calibration was obtained by comparing the caputre spectrum of the 34 eV resonance in ^{199}Hg with published data on thermal neutron capture(54) and the resonance spectra were normalised using the integrated pulse height spectrum between 1.5 and 2.3 MeV.

---

(54) Schult O. W. B. et al. Phys. Rev. 164, 1548 (1967).

TABLE V

Relative intensities of gamma ray transitions in ^{199}Hg following its formation in various slow neutron capture resonances.

E_γ keV	Relative intensities of Gamma-rays(b)				
	23.1 eV res.	89.9 eV res.	301 eV res.	344 eV res.	417 eV res.
(a) 755	7.9 (0.8)				
876	1.7 (0.8)				
896	1.3 (0.8)				
1012	6.6 (0.9)				
1055	3.8 (0.9)				
1138	4.3 (1.0)				
1321	3.8 (1.1)				
1381	8.5 (1.0)				
1532	4.8 (1.2)				
1568	8.6 (1.2)				
1775	6.8 (1.0)				
4373	3.5 (0.5)	-0.6 (1.8)	2.8 (1.7)	2.9 (4.3)	-1.6 (3.0)
4686	6.7 (0.6)	2.9 (1.1)	4.2 (1.6)	4.1 (3.8)	5.6 (2.8)
4882	23.0 (0.8)	3.2 (1.6)	7.4 (1.5)	- 1.3 (3.9)	1.3 (3.3)
4922	5.3 (0.6)	1.7 (1.7)	-0.1 (1.6)	3.2 (3.4)	0.8 (2.5)
5008	3.5 (0.4)	-0.7 (1.7)	-0.2 (1.8)	2.9 (3.6)	14.7 (3.5)
5067	7.4 (0.6)	0.1 (1.8)	0.9 (1.6)	0.2 (3.8)	3.8 (2.7)
5302	3.9 (0.5)	-1.3 (1.6)	-0.1 (1.0)	5.5 (2.8)	-
5314	-	0.7 (1.4)	0.6 (1.2)	10.4 (3.1)	13.6 (3.4)
5433	3.2 (0.5)	1.3 (1.3)	2.4 (1.5)	4.5 (3.1)	12.5 (3.1)
5517	0.2 (0.4)	-0.5 (2.0)	-1.0 (1.3)	2.7 (2.8)	0.2 (4.0)
5905	7.2 (0.4)	8.1 (1.2)	4.2 (1.2)	7.2 (2.9)	-0.3 (2.5)
6167	0.2 (0.3)	33.2 (2.3)	0.2 (1.6)	1.1 (2.8)	0.8 (2.4)
6207	9.7 (0.4)	6.8 (1.7)	1.3 (1.2)	10.1 (3.1)	1.5 (2.0)
6255	4.3 (0.4)	39.8 (2.0)	8.0 (1.3)	-0.7 (2.8)	14.1 (2.2)
6453	17.2 (0.5)	1.6 (1.6)	25.5 (1.8)	0.8 (2.5)	8.4 (2.1)
6660	0.1 (0.2)	11.9 (1.5)	14.7 (1.5)	2.0 (2.2)	-0.9 (1.5)

(a) Energies are in most cases accurate to ± 3 keV.

(b) Numbers in parentheses denote statistical errors. Systematic errors due to uncertainties in the efficiency curve and the normalisation may add a further 15%.

The resolution of the mercury gamma ray spectra is poorer than expected and the lines show low energy tails characteristic of radiation damage, which would arise in this experiment because of the fast neutrons scattered into the detector from the target. The resolution was recovered by annealing at 0°C.

A second flight path at 20 metres has now been established to obtain resonance capture gamma-ray spectra with better time of flight resolution.

E. Angular distributions of fragments from ^{235}U neutron-induced fission in resonances (N. J. Pattenden, J. E. Jolly, H. Postma and K. Ravensberg (F.O.M. Netherlands) and J. C. Waldron (Chemistry))

A new experiment is being prepared to study the angular distribution of fragments omitted from ^{235}U nuclei undergoing fission induced by slow neutrons. The resonances found in slow neutron cross sections correspond to compound nucleus levels with total angular momentum $J = |I \pm \frac{1}{2}|$ (I is the target spin) and with the parity of the target nucleus. The total angular momentum and parity are almost certainly the only remaining good quantum numbers for the levels of a highly excited nucleus (the excitation energy is about 6 MeV for fissile targets). In the process of fissioning, the compound nuclei formed from the commoner fissile targets pass over the saddle point in the deformation energy surface with an "internal" excitation of about 1 MeV; at this low excitation value the number of transition states at the saddle point is very small, their wave functions are "collective" in character, and they have the projection K of the angular momentum on the cylindrical symmetry axis of the nucleus as an additional good quantum number. Furthermore, all the evidence points to the fact that K remains a good quantum number as the nucleus deforms from its saddle point shape to its scission point. If, now, the spin axes of the target nuclei are aligned, say, perpendicular to the incident neutron beam, the total angular momentum of the compound nuclei will be aligned mainly in this direction too. Consequently, when fission proceeds through a particular transition state, the value of K of the transition state determines the probable direction of the nuclear symmetry axis with respect to the beam, and this is the direction for emission of fission fragments. Thus, by measuring the angular distribution of fission products it is possible to find the probability that the fissioning nucleus passes through transition states of different K. If this information is known for a large number of compound nucleus levels it becomes possible to answer the following questions of nuclear theory in general and fission theory in particular:-

(1) The mean rate of fission through a transition state that is known to be low-lying (e.g. one with K = 0) with show whether the transition state is strongly coupled to the compound nucleus wave function (as intuitively expected) or is more weakly coupled (the case for neutron and proton single particle states).

(2) It may be possible to determine the positions of some of the higher transition states. This will provide evidence of the behaviour of nuclear collective states as a function of deformation.

It may also be possible to see if other phenomena (e.g. mass yields or ternary fission) are associated with particular transition states.

To produce anisotropic angular distributions the ^{235}U nuclei in the sample must be partially aligned. Dabbs [55] achieved alignment by cooling a crystal of rubidium uranyl nitrate, $RbUO_2(NO_3)_3$, to about 0.5°K in a ^3He cryostat. The nuclear electric quadrupole moment interacts with the crystal field to give alignment of the major nuclear axis in a plane perpendicular to the c-axis of the crystal. The degree of alignment is approximately inversely proportional to the absolute temperature. We will depart from Dabbs' technique in certain details, which should produce significantly lower sample temperatures and thus increase the experimental anisotropies. In particular we will use a ^3He-^4He dilution refrigerator[56,57] in the cryostat, instead of an ^3He evaporation refrigerator.

The experiment is an example of co-operation between laboratories in different countries viz. the Stichting voor Fundamenteel Onderzoek der Materie (Organization for Fundamental Research on Matter, abbreviated to F.O.M.) Netherlands, and A.E.R.E. A preliminary experiment was performed at the Dutch high flux reactor at Petten, using the F.O.M. facilities of a neutron beam, crystal monochromator and nuclear orientation cryostat, to show that our method would produce anisotropy effects of the right order. The cryostat was designed and made by the F.O.M. Group, and then brought to the Harwell electron linac,

---

(55) Dabbs J. W. T., Walter F. J. and Parker G. W. Proc. Physics and Chemistry of Fission Conference, 1, 39 (1965).

(56) London H., Clarke G. R. and Mendoza E. Phys. Rev. 128, 1992 (1962).

(57) Wheatley J. C., Vilches D. E. and Abel W. R. Physics 4, 1 (1968).

and reassembled on a 10 m flight path in a specially designed blockhouse. Tests have shown that the refrigerator can attain temperatures of less than about 0.06°K. The next step, which is to mount a sample and fission fragment detectors in the cryostat and to make the first run on the linac, will take place shortly.

The technique of growing crystals with a coating of enriched ^{235}U has been learned by the Preparative Group, Chemistry Division, who are now producing samples for the linac experiment.

The $^{31}P(n,n'\gamma)^{31}P$ reaction (B. H. Armitage, A. T. G. Ferguson, G. C. Neilson* and W. D. N. Pritchard+)

We have investigated the gamma-rays emitted following inelastic neutron scattering from phosphorus, using equipment described in a preceding Progress Report(58). The scattering sample consisted of red phosphorus powder contained in a thin walled polystyrene can, and formed a hollow right circular cylinder 5 cm in length, with inner and outer diameters of 1.3 and 5.2 cm respectively.

Gamma-ray spectra were taken using 5.3 MeV and 4.3 MeV neutrons, with the detector at 90° to the beam, and backgrounds were obtained from corresponding "sample out" measurements. The spectra obtained from the empty polystyrene can did not differ significantly from those obtained in the corresponding sample-out measurements.

The gamma-ray spectra produced in the $^{31}P(n,n'\gamma)^{31}P$ reaction are consistent with the level scheme shown in Fig. 12. All the transitions shown correspond to gamma-rays observed in our '5.3 MeV' spectra. The full lines represent transitions observed in both runs, the broken lines, transitions observed in the '5.3 MeV' runs only. The energy levels were determined from the measured energies of the gamma rays, and the numbers in parenthesis are intensities relative to the 1266.6 keV gamma-ray. No significant disagreement exists between the present decay scheme and that of Wolff et al.(59) derived from the $^{30}Si(p,\gamma)^{31}P$ reaction. In particular the branching ratio obtained for the decay of the 4593 keV level by Wolff et al(59) is consistent with the relative intensities of the 3326.1 keV and the 4593.4 keV gamma-rays observed here.

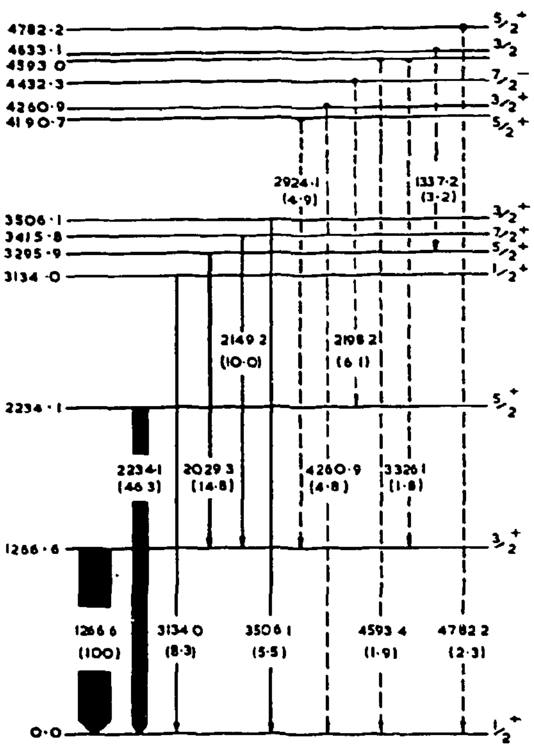

Fig. 12. Energy levels and gamma ray transitions in ^{31}P associated with the $^{31}P(n,n'\gamma)^{31}P$ reaction. The spin assignments are obtained from reference (60).

(58) Nuclear Physics Division Progress Report AERE – PR/NP 13 (1968).

(59) Wolff A. C., Mayer M. A. and Endt P. M. Nuclear Physics A107, 332 (1968).

(60) Endt P. M. and C. Van der Leun, Nuclear Physics A105, 1 (1967).

* University of Alberta

\+ On attachment from Univ. of Exeter

G. Nuclear Structure Information from the Study of Isomeric States

I Isomeric States in the region Z = 63 - 83 (T. W. Conlon)

This region continues to be of considerable interest because of the variety of nuclear phenomena which can lead to the existence of isomers. These isomers include the shell model isomers expected in the closed shell regions Z = 82, N = 126, where states of high and low spins are expected to have similar energies, isomers the dacay of which violates selection rules on the quantum number K and asymptotic quantum numbers, N, n_Z and Ω of the Unifield Model, and finally isomers associated with equilibrium nuclear shapes markedly different from those for lower lying levels. The last group are discussed further in the next section.

In the hope of studying all three types of transition a survey of this region over the time range 10^{-5} to 10^{-1} seconds is continuing. The A.E.R.E. Variable Energy Cyclotron can provide for this work pulsed proton beams with energies up to 50 MeV.

This survey has revealed many new isomers produced by the irradiation of natural targets. Table VI presents a partial summary of the information obtained to date. Only the target and the measured half-life are quoted, because the gamma-ray spectra from each isomeric state have not yet been considered in detail. Fig. 13 (see page 24) shows examples of gamma-ray spectra observed at the stated times after pulsed beam irradiation of selected targets. On the right of Fig. 13 the intensity of particular gamma-rays is shown as a function of time after irradiation.

TABLE VI

Measured lifetimes of isomeric activities observed in current observations

Z	Target	Half life in Seconds ± 20%
64	Gd	6×10^{-5}, 1.8×10^{-4}
65	Tb	4×10^{-4}
66	Dy	8×10^{-5}
67	Ho	5×10^{-4}, 1.2×10^{-3}
68	Er	5×10^{-5}
70	Yb	1.4×10^{-3}
74	W	2×10^{-3}
76	Os	8×10^{-3}
77	Ir	10×10^{-5}
82	Pb	1.1×10^{-3}

Experiments are now underway to identify – and to investigate in detail – the decay scheme of the isomeric nuclei. These experiments involve irradiation of separated isotopes of the targets of Table VI, and careful measurements of the energy of the K_α X-ray produced by internal conversion in the isomeric nucleus, of the relative intensities of the gamma-rays emitted, and in some cases, of the excitation functions for the states of interest.

II Shape Isomers (T. W. Conlon and A. J. Elwyn)

Shape hindered gamma-ray transitions or shape isomers were predicted[61] to occur in those isotopes of samarium and neighbouring elements with 88 to 90 neutrons. Such transitions have not yet been

(61) Sheline R. K., Kenefick R. A., Nealy C. L. and Udagawa T. Phys. Lett. 18 330 (1965).

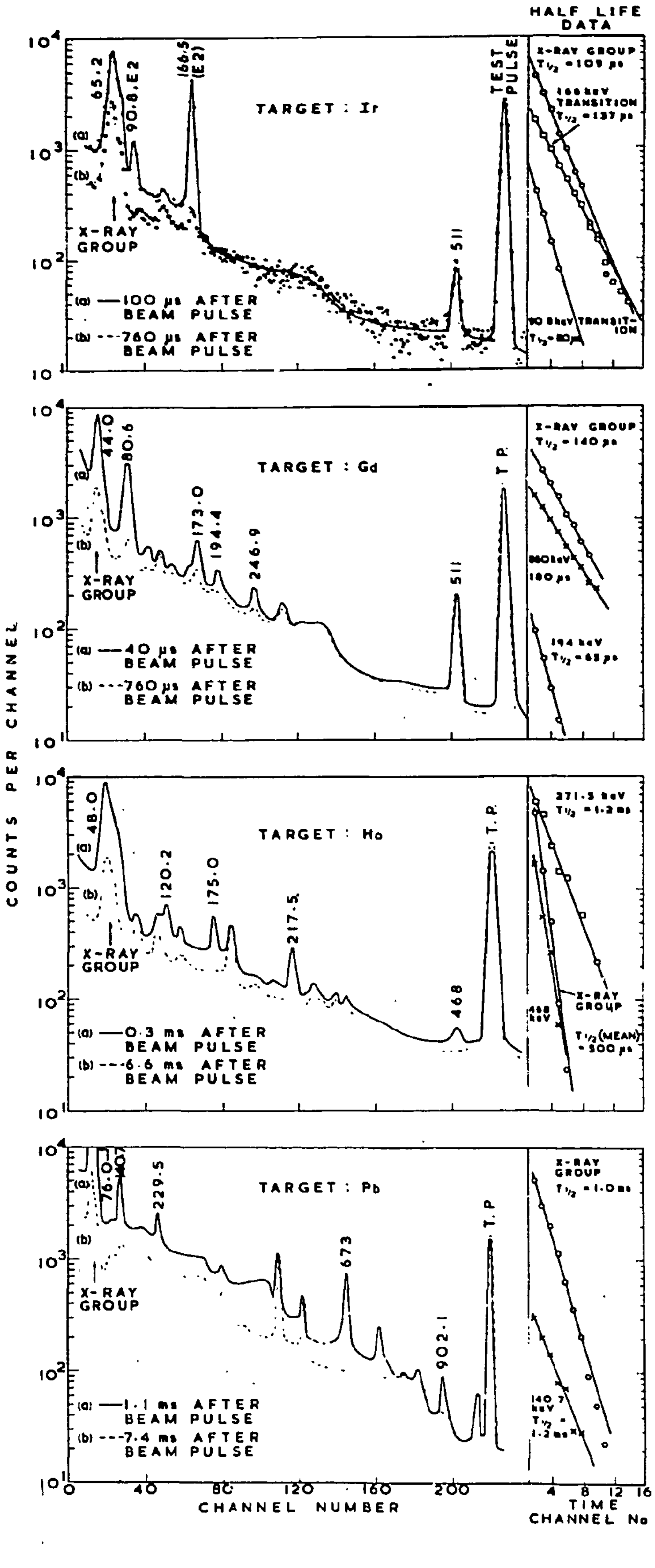

Fig. 13. Gamma ray spectra from isomeric activities induced by irradiation of Ir, Cd, Ho and Pb with 35 MeV protons.

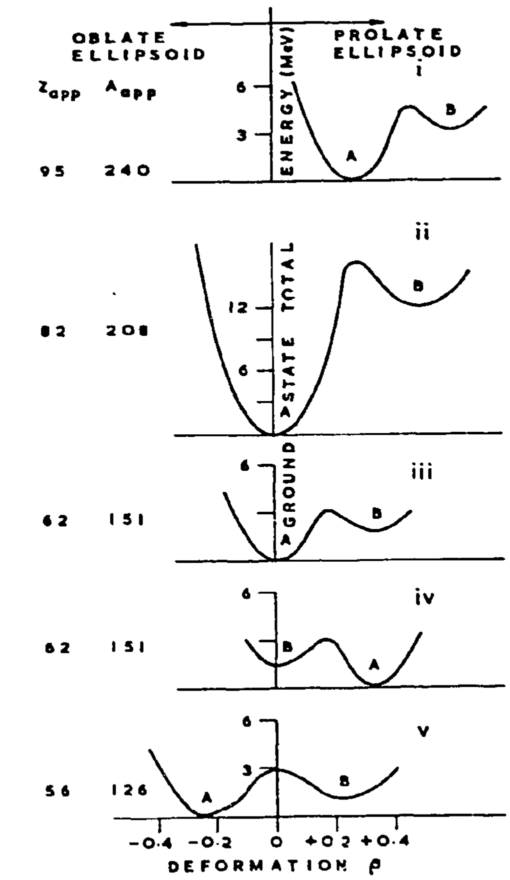

Fig. 14. Characteristic variation of nuclear binding energy with deformation β for particular combinations of N and Z.

confirmed experimentally although one possible example has been discussed[62]. Meanwhile further calculations predict that shape isomers should occur in other regions of the periodic table. The current situation is summarised schematically in Fig. 14 where the nuclear energy is plotted as a function of the deformation parameter β. The common feature in this diagram is that more than one minimum occurs in the energy profile. Shape isomerism will occur whenever a transition occurs from a state of nuclear shape depicted by B in Fig. 14 to a state of shape A.

Evidence for the energy profile shown in (i) of Figure 14 is found in the observation of fissioning isomers[63,64,65] while evidence for the profiles shown in (iii) and (iv) has been discussed by Sheline et al[61]. Recent calculations by Strutinsky[65] suggest for the Pb region the profile (ii), and finally calculations of Arseniev et al.[66] predict that the profile (v) will occur in the newly discovered region of deformation in the neighbourhood of ^{126}Ba[67]. A survey of the type already underway (Section I) is well suited to study transitions in all the cases outlined above provided that half-lives involved are greater than about 10^{-6} seconds. The calculations of Wakai et al.[68] for the case of a nucleus represented by Fig. 14 (i) yield a gamma-ray inhibition of order 10^6 to 10^8 for a change in β from 0.5 (B) to 0.25 (A). This means that all but the fastest E1 and M1 transitions would have half-lives amendable to to study by the techniques of Section I. We are extending the survey to search for the gamma-ray decay branch of the fissioning isomers. We also hope to investigate nuclei in the barium region (Fig. 14(v)) by heavy ion reactions such as $^{A}Sn(^{12}C,Xn)^{A+6-X}Ba$.

A programme to develop pulsed beams of ^{12}C ions of the required energy at the Variable Energy Cyclotron has been started.

H. Neutron time-of-flight experiments

I Asymmetry in charge particle production for 100 MeV polarized neutrons (A. Langsford and G. C. M. Sharman (Oxford)

Data from this experiment[69] (carried out in collaboration with Southampton University and the Rutherford High Energy Laboratory) are now being analysed. Progress has hitherto been hampered by the

(62) Conlon T. W. Nucl. Phys. A100 No. 3 545 (1967).

(63) Bjornholm M. G., Borgreen J., Westgaard L. and Karnaukov V. A. Nucl. Phys. A97, 444 (1967).

(64) Lynn J. E. Nucl. Phys. (to be published).

(65) Strutinsky, V. M. Nucl. Phys. A95, 420 (1967).

(66) Arseniev D. A., Malov L. A., Sohiczenski V. and Soloviev V. G. Dubna Conf. Report, p. 93 (1968).

(67) Chanda R. N. UCRL Report No. 10798.

(68) Wakai M., Harada K. and Ohnishi N. Dubna Conf. Report, p. 91 (1968).

(69) Nuclear Physics Division Progress Report AERE PR/NP 13, p. 32 (1968).

problems of reading the data from the 7-track magnetic tape on which it was recorded.

II High precision n-p total cross-section (A. Langsford and P. J. Clements (Oxford)

All our data from this experiment have now been subjected to a preliminary analysis, which, however, did not include corrections for correlations in the neutron time spectra arising from dead time effects and from after-pulsing[70] in the detectors. These correlations led to discrepancies ~ ± 0.5% in the cross-section values calculated for different transmission sample combinations in the region 1-5 MeV, where the data have highest statistical accuracy. First calculations indicate that the application of suitable corrections will significantly reduce this discrepancy. Bearing in mind the effect of these corrections, our results so far support the measurements of Engelke et al[71] rather than the somewhat smaller cross-section values measured in earlier experiments.

---

(70) Nuclear Physics Division Progress Report AERE PR/NP 12, p. 37 (1967).

(71) Engelke C. E., et al. Phys. Rev., 122, 324 (1963).

REPORTS, PUBLICATIONS AND CONFERENCE PAPERS

REPORTS

AERE – R 5891 Structure in sub-threshold fission modes. J. E. Lynn

AERE – R 5924 Fission components in ^{242}Pu resonances. G. D. James.

AERE – R 5945 The neutron resonance parameters of ^{240}Pu. M. Asghar, M. C. Moxon and N. J. Pattenden (to be published).

PUBLICATIONS

ASGHAR M., CHAFFEY C. M. and MOXON M. C. The neutron resonance parameter and average capture cross section of ^{165}Ho. Nuc. Phys. A108, 535 (1968).

COATES M. S., GAYTHER D. B., GOODE P.D. and TRIPP D. J. Time of flight measurements of the neutron spectrum in a sub-critical fast reactor assembly. J. Nucl. Energy 22, 547 (1968).

JAMES G. D. and RAE E. R. Fission components in ^{234}U resonances. Nuc. Phys. A118, 313 (1968).

LYNN J. E. The theory of neutron resonance reactions (Clarendon Press, Oxford, 1968).

IN COURSE OF PUBLICATION

COATES M. S., GAYTHER D. B., JAMES G. D. and LANGSFORD A. The fission cross-section of ^{235}U in the energy range 0.1 to 10 MeV. AERE Report.

JAMES G. D. Fission components in ^{242}Pu resonances. Nuc. Phys.

JAMES G. D. and PATRICK B. H. A correlation analysis of the slow neutron fission cross-section of ^{239}Pu. Phys. Letters.

CONFERENCE PAPERS

Invited Papers

LYNN J. E. Structure Effects in Nuclear Fission. International Symposium on Nuclear Structure, Dubna, USSR, July 1968.

Contributed Papers

UK/USSR Seminar on Nuclear Constants, Dubna, USSR, 11-14 June, 1968

ASAMI A. and MOXON M. C. Low Energy Neutron Scattering Cross-section of ^{10}B. UK/19.

ASAMI A., MOXON M. C. and STEIN W. E. A new Technique for the Partial Wave Assignment of a Slow Neutron Resonance. UK/18.

ASGHAR M., MOXON M. C. and PATTENDEN N. J. The Neutron Resonance Parameters of ^{240}Pu. UK/20.

JAMES G. D. and PATRICK B. H. Evaluation of the ^{239}Pu Fission Cross-section in the Energy Range 1 keV to 100 keV. UK/14.

JAMES G. D. and RAE E. R. Fission Components in ^{234}U Resonances. UK/15.

JAMES G. D. Multilevel Analysis of ^{239}Pu Fission Cross-section near 83 eV. UK/16.

MOXON M. C. The Average Level Spacing from Neutron Cross-section Data. UK/17.

MOXON M. C., RAE E.R., RIEHS P., STEIN W.E. and THOMAS B. W. Gamma-ray Spectra from Neutron Resonance Capture. UK/22.

PATRICK B. H., SCHOMBERG M. G., SOWERBY M. G. and JOLLY J. E. Measurements of Eta, Alpha and the Neutron Cross-sections of ^{239}Pu. UK/24.

RAE E. R. Some Notes on the Accuracy of Neutron Cross-section Measurements. UK/21.

SCHOMBERG M. G., SOWERBY M. G., BOYCE D. A. and EVANS F. W. The Direct Measurement of $\alpha(E)$ for ^{239}Pu. UK/23.

SOWERBY M. G. and PATRICK B. H. The Ratio of the $^{6}Li(n,\alpha)$ to $^{10}B(n,\alpha)$ cross-section in the Energy Range 10 eV to 70 keV. UK/25.

Theses

Some problems in neutron physics – An investigation of the p-wave neutron strength function in the mass 100 region. Thesis for the degree of Doctor of Philosophy submitted by C. M. Newstead to the University of Oxford, October 1967. Degree conferred December 1967.

The measurement of average neutron capture cross-sections in the mass region above 100. Thesis for the degree of M.Sc. submitted by M. C. Moxon to the University of London, June 1968. Pass result obtained October 1968.

A re-assessment of Harwell mass spectrometric measurements of the cross sections of plutonium isotopes for Maxwellian neutrons (M. J. Cabell)

In 1966 M. J. Cabell and M. Wilkins reported the results of an experiment in which mixtures of highly-enriched samples of ^{239}Pu, ^{240}Pu, ^{241}Pu and ^{242}Pu were irradiated, with cobalt monitors, in an almost uncontaminated Maxwellian neutron spectrum (J. Inorg. Nucl. Chem. 28, 2467 (1966)). The chief object of this experiment was to measure α (the ratio of a neutron capture to fission) for ^{241}Pu but, in addition, it yielded values of α for ^{239}Pu, for the neutron absorption cross sections of ^{239}Pu and ^{241}Pu and for the neutron capture cross sections of ^{239}Pu, ^{240}Pu and ^{241}Pu.

A major consequence of the publication of these new values was that, when included with other data, they cause a substantial change in the I.A.E.A. evaluation of the most probable values of the 2200 m/sec constants for ^{241}Pu. In view of the fact that the I.A.E.A. is currently carrying out a revised survey of the 2200 m/sec constants for the major fissile nuclides, a re-assessment of the results of the Harwell experiment was undertaken so that developments since the original publication could be taken into account.

The following results were obtained from this re-assessment:-

	^{239}Pu	^{240}Pu	^{241}Pu
Absorption cross section (barns)	1203.8 ± 42.1		1522.1 ± 29.8
Capture cross section (barns)	368.2 ± 8.3	297.2 ± 14.2	388.7 ± 9.2
Ratio of absorption to capture	3.269 ± 0.089		3.916 ± 0.075
Ratio of capture to fission	0.4407 ± 0.0173		0.3429 ± 0.0088

In addition the difference between the absorption cross sections of ^{241}Pu and ^{239}Pu was found to be 325.6 ± 25.8 barns.

Gamma-ray spectrometric measurements of the capture cross section of ^{198}Au for reactor neutrons (M. J. Cabell and M. Wilkins)

The fact that ^{198}Au has a very large capture cross section for reactor neutrons, and that this cross section has been known only imprecisely, has limited the use of gold as a neutron flux monitor to relatively small neutron dose irradiations in neutron fluxes of only moderate intensity. Earlier measurements of this quantity have been good to ± 8 per cent at best; its variation with the epithermal content of the reactor spectrum has been known too imprecisely for any firm conclusions to be drawn.

By using a calibrated gamma-ray spectrometer to measure the absolute disintegration rate of ^{198}Au and ^{199}Au in mixtures of the two, the capture cross section of ^{198}Au for reactor neutrons, $\hat{\sigma}_8$, has been measured as a function of Westcott's epithermal index-parameter, $r\sqrt{T/T_0}$ over the range encountered in the high-flux irradiation positions of the PLUTO reactor ($r\sqrt{T/T_0}$ = 0.015 to 0.106). Assuming the 2200 m/sec capture cross section of ^{59}Co to be 37.4 barns it was found that

$$\hat{\sigma}_8 \text{ (barns)} = 25102 - 46535\ r\sqrt{T/T_0}$$

The capture cross section of Maxwellian neutrons (T = 70°C) was found to be 25102 ± 371 barns.

Publications

CABELL, M. J. A re-assessment of Harwell mass spectrometric measurements of the cross sections of ^{239}Pu, ^{240}Pu and ^{241}Pu for Maxwellian neutrons. AERE-R 5874 (August, 1968).

CABELL, M. J. & WILKINS, M. Mass spectrometric measurements of the neutron capture cross sections of ^{142}Nd, ^{143}Nd, ^{144}Nd and ^{145}Nd for reactor and Maxwellian neutrons. J. Inorg. Nucl. Chem. 30. pp. 897-905, 1968.

CABELL, M. J. A mass spectrometric measurement of the half-life of plutonium-241. J. Inorg. & Nuclear Chemistry, 30, pp. 2583-2589, 1968.

CHEMISTRY DIVISION A. E. R. E.
(Division Head: Dr. W. Wild)

V.E.C. Studies

Fission of the Compound Nucleus ^{210}Po Formed with Varying Amounts of Angular Momentum
(J. G. Cuninghame, I. F. Croall and J. P. Unik)

The fission of ^{210}Po produced by two reactions

$$^{209}Bi + {}^{1}He \rightarrow {}^{210}Po^*$$

$$^{206}Pb + {}^{4}He \rightarrow {}^{210}Po^*$$

each with the three excitation energies 40, 45 and 58 MeV for the compound nucleus ^{210}Po, has been studied. It has been found that there is no change in the fragment mass distributions between the pairs of reactions at any of the excitation energies. However, the fragment total kinetic energy release does increase, both with increase in excitation energy, and with increase in angular momentum. These results are being finally computed for presentation at the I.A.E.A. Conference on Fission to be held in Vienna in July 1969.

A target of ^{198}Pt has been obtained from the Mass Separator Group, and it is intended to produce $^{210}Po^*$ from this target also, by the reaction

$$^{198}Pt + {}^{12}C \rightarrow {}^{210}Po^*.$$

Since this will increase the angular momentum by a factor of ~ 3-4 over the ^{4}He reaction, an even larger increase in the total kinetic energy may be expected.

Mass Spectrometry

Multiple Neutron Capture in ^{239}Pu (E. A. C. Crouch, I. C. McKean and M. Brownsword)

In the analysis of the series of samples of highly irradiated ^{239}Pu from the DIDO reactor it has not proved possible, with existing nuclear data, to fit the experimental ratios of the mass number 238, 239, 240, 241 and 242 isotopes of Pu, using the exact solutions to the equations of formation. It is possible to get a good fit up to a neutron dose of about 2×10^{21} n/cm^2 except in the case of ^{238}Pu which up to 1×10^{21} n/cm^2 is found in greater quantity that the equations of formation predict. For a dose of 6×10^{21} n/cm^2 the ^{241}Pu is also calculated to be greater than the experimental findings by about 10%. These results are consistent with the existence of a ^{241}Pu isomer of half-life ≈5 years which would be formed to the extent of about 15% of the ^{241}Pu total. Alternatively there may be a method of ^{238}Pu formation other than the route $^{239}Pu \rightarrow {}^{240}Pu \rightarrow {}^{241}Pu \rightarrow {}^{241}Am \rightarrow {}^{242}Am \rightarrow {}^{242}Cm \rightarrow {}^{238}Pu$, but existing nuclear data allow of no such alternative route with decay constants and capture cross-sections of magnitude necessary to explain the ^{238}Pu found.

However, for any assumed half-life for ^{241}Pu between 10 and 15 years the best fit to the experimental results yields the information that at a dose of 6×10^{21} (about 24 months irradiation at 1.28×10^{14} n/cm^2/sec.), about 75% of all fissions have occurred in ^{239}Pu and 25% in ^{241}Pu. The ^{239}Pu fissions occur first in time.

From these findings it is clear than failure exactly to fit the Pu isotopic ratios at all irradiation periods, will not much affect the examination of the Fission Product results, which is continuing.

The part of this work dealing with the Pu isotopes is being reported.

Calculated Independent Fission Yields (E. A. C. Crouch)

At the request of Nuclear Data Group, Fast Reactor Physics Division, Winfrith, the calculated independent fission yields of AERE-R 5488 were extended and now include ^{232}Th, ^{233}U, ^{235}U, ^{238}U, ^{239}Pu, ^{240}Pu and ^{241}Pu. At the same time opportunity was taken to review the basis of the calculation in AERE-R 5488. The method has been slightly modified in the new calculation in that the available experimental values for ν were used to find the fission fragment masses. The widths of the gaussian distribution curve for Z about Zp from the new procedure plotted against mass number show a distribution which could be interpreted as indicating the effect of nuclear shell structure on the distribution of independent yields round Zp. The calculated values of the independent yields now agree closely with the experimental values in most cases. This work is being reported.

Delayed Neutrons (Fission Product Emission)

Fission Product Selenium (L. Tomlinson and M. H. Hurdus)

Selenium is the precursor to bromine from which a major fraction of delayed neutrons originate.

The new radiochemical method based on isotopic exchange with hydrogen selenide gas has been written up for publication. Equipment is being constructed to allow this method to be operated in the LIDO reactor using a new rig incorporating a cadmium shutter. A timing system is being constructed which will allow the shutter, chemical operations and counting to be started automatically when the LIDO reactor shut-down button is pressed. This should further improve reliability and timing accuracy.

Pulsing Reactor Model (G. N. Walton and P. J. Silver)

Further work has continued on the proposal to obtain mechanical work from a reactor core by oscillating the moderator and coolant. To increase the efficiency of an electrically heated model the working gas (helium) was replaced by a boiling fluid. To avoid corrosion by water "fluoron" ($C_2Cl_3F_3$) which boils at 48°C was used. A more vigorous power stroke is obtained at lower temperatures, than when helium is used, and control aspects are being investigated.

Publication

Fragment Distribution in Fission of ^{232}Th by Protons of Energy 13-53 MeV. I. F. Croall and J. G. Cuninghame. Nuclear Physics A125, 402, 1969.

NUCLEAR RESEARCH DIVISION, A. W. R. E.

(Chief of Nuclear Research: Dr. H. R. Hulme)

1. Elastic and Inelastic scattering of Neutrons in the Energy Range 2 to 5 MeV by ^{10}B and ^{11}B. (D. Porter, R. E. Coles and K. Wyld).

A paper with the following abstract has been submitted for publication:

"The time of flight method has been used to study fast neutron elastic and inelastic scattering on ^{10}B and ^{11}B in the energy region between 2 and 5 MeV. The elastic angular distributions have been compared with the predictions of a non-local optical model. Calculations show qualitative agreement with experiment. The results obtained for neutron excitation of the 0.717 MeV state in ^{10}B substantiate previous findings and in addition excitation functions have been determined for the 1.740, 2.154 and 3.590 MeV states in ^{10}B. Comparisons of the differential and integrated inelastic cross-sections have been made with compound nucleus calculations derived from Hauser-Feshbach theory with fluctuations (HFW) using neutron optical potentials obtained from fits to the elastic angular distributions with estimates of optical potentials for (n,p), (n,t) and (n,α) reaction modes included. Apart from resonance effects, agreement is fair.

For ^{11}B, the excitation of the 2.140 MeV state has been determined and compared with existing data. Finally comparisons are given of the differential and integrated cross-section for inelastic scattering to this state with the HFW theory utilising the neutron optical model parameters deduced from fits to the elastic angular distributions. The rise of the cross-section above threshold is shown to be much slower than that theoretically predicted."

2. Elastic and Inelastic Scattering of 9.72 MeV Neutrons by ^{10}B and ^{11}B. (J. A. Cookson and J. G. Locke).

A paper with the following abstract has been submitted for publication.

"Differential cross-sections for elastic and inelastic scattering of 9.72 MeV neutrons from ^{10}B and ^{11}B were measured using the time-of-flight technique. The integrated elastic cross-sections were 933 ± 68 mb and 895 ± 63 mb for ^{10}B and ^{11}B respectively (the former including inelastic scattering to the 0.717 MeV state). For the excited state of ^{10}B and ^{11}B below 6.8 MeV excitation the integrated inelastic cross-sections were 239 ± 27 mb and 385 ± 29 mb respectively. The inelastic angular distributions showed little sign of the forward peaking expected for a direct interaction. Comparison with Hauser-Feshbach theory gave, rather surprisingly, better agreement for ^{11}B than for ^{10}B."

3. Neutron scattering by ^{93}Nb and Mo. (D. Porter and R. E. Coles).

Fast neutron scattering by ^{93}Nb and Mo for incident neutrons in the energy range 1.5 MeV to 5 MeV has been studied. Time-of-flight data at various scattering angles and at 0.5 MeV energy intervals have been taken and data analysis is in progress.

4. Neutron scattering by ^{23}Na. (D. Porter and R. E. Coles).

An angular distribution of the elastic and inelastic neutron groups has been run a 5 MeV incident energy and analysis is in progress.

5. Gamma Rays following inelastic neutron scattering. (D. Porter, R. E. Coles, W. B. Gilboy*).

Analysis of data obtained on ^{51}V and ^{89}Y using a Ge(Li) detector is progressing slowly.

---

* Presently at University of Surrey.

6. ν measurement on Pu^{239}. (P. F. Bampton, G. James, P. J. Nind and D. S. Mather).

Measurements of promp ν averaged over energy bands 40-120 Kev, 120-300 Kev and 100 Kev wide, between 300 KeV and 1.2 MeV have been continued. The relative accuracy is about 1%. In addition, the energy region 500-800 Kev has been scanned with a reduced energy spread of 50 KeV. Data acquisition is now complete.

7. Measurement of (n,2n) and (n,3n) cross-sections. (D. S. Mather, P. J. Nind).

Following the publication of AWRE 0 47/69, the programme of measurements of (n,2n) and (n,3n) cross-sections has been re-considered. Further measurements using the giant scintillator facility will commence shortly.

8 Neutron cross-section measurements using neutrons from nuclear explosions. (A. Moat, R. R. Harris, S. Le Flem).

Analysis of the data gathered at the 1967 and 1968 USA Physics Shot has continued slowly. The Pu^{238} fission cross-section analysis is now at an advanced stage and the data are showing good agreement with results from LASL. Some residual problem areas are being worked upon.

There has been a preliminary analysis of the Pu^{241} fission cross-section data. In some regions of low signal level there may be difficulties due to base line movements, but the time resolution is excellent and a full analysis is desirable. Difficulties in interpretation of the Pu^{241} α measurements have halted further analysis of the data, but hopefully, some insight to these problems may result from a completed analysis of the fission data for that nucleus.

A second version of the film disc assessor has been designed.

9. The (n,α) cross-sections for natural nickel, iron, chromium and molybdenum in a Fission Neutron Spectrum. (N. J. Freeman, J. F. Barry and N. L. Campbell).

A paper on this topic has been accepted for publication Journal of Nuclear Energy. The final results are:

Ni 4.7 $\pm$ 0.6 mb, Fe 0.18 $\pm$ 0.04 mb

Cr 0.17 $\pm$ 0.06 mb, Mo 0.13 $\pm$ 0.03 mb

10. Alpha and Fission counting of Thin Foils of Fissile Material. (P. H. White).

A paper with the following abstract has been accepted for publication in Nuclear Instruments and Methods.

"In 2π alpha and fission counting of active foils corrections are necessary for particles which do not enter the counting volume but dissipate their energy in the thickness of the foil. Measurements of these corrections have been made for foils of uranium oxide prepared by a painting technique, by vacuum evaporation and by electro-spraying. A comparison of the measurements with calculated values of the corrections gives discrepancies of up to 5%/mg cm^{-2}. For both alpha and fission counting this discrepancy can be explained by assuming that the foils have a non-uniformity of the same order as their thickness. The relationship of this 'non-uniformity' to the method of preparation is discussed. The backscattering correction applied to alpha particle counting has been re-calculated and shown to be a function of the foil thickness. Corrections for low geometry counting are also discussed.

Typical fission fragment and alpha particle spectra are shown for both 2π and low geometry assay."

11. The SCORE Programme. (J. Camerson).

SCORE is a semi automatic neutron data evaluation program. It was written by a group at Atomics International as part of the ENDF effort. It uses IBM system 360 equipment featuring an IBM 2250 graphical display unit.

An operational description of the program is given in report AI-AEC-12757. Briefly SCORE retrieves data in the SCISRS-I format and displays it as a graph on the 2250 screen. The data can be easily re-plotted with different scales or different selections of experimenter or the data modified. Curves from evaluations or from resonance parameters can be displayed with the experimental points so the evaluator can construct his own curve and display it.

A few modifications have been made to the program to suit the AWRE computer system. Data are now acceptable from the CCDN NE DADA format. Routines have been added to make SD4060 hard copy prints of the graphs appearing on the screen. Other routines allow output to be taken in the format of the UKAEA nuclear data library, but these are still under development.

SCORE runs at AWRE with little trouble and is being increasingly used for practical evaluation work.

12. Evaluation of the neutron cross-sections of Carbon. (D. Porter, K. Wyld).

A start has been made using the SCORE program to retrieve and plot data supplied by CCDN prior to an evaluation for carbon in the energy region 1 ev to 7 MeV.

13. Fission Parameter Evaluations. (D. Mather, P. Bampton).

Preliminary investigations into the evaluations of selected fission parameters have been made. It is planned to collaborate with AERE, on evaluations of σ_{nf} U^{235}, U^{238} and Pu^{239}.

Publications

MATHER, D. S. and PAIN, L. F. Measurement of (n,2n) and (n,3n) cross-sections at 14 MeV incident energy, UKAEA Report AWRE O 47/69.

BATCHELOR, R. and WYLD, K. Neutron scattering by ^{235}U and ^{239}Pu for incident neutrons of 2, 3 and 4 MeV, UKAEA Report AWRE O 55/69.

TOWLE, J. H. The Inelastic Scattering of Neutrons from ^{89}Y, Nuclear Physics A131, 561 (1969).

HOWE, F. A. Magnetically suppressed accelerator tubes for electrostatic accelerators, IEEE Journal, 1969 Particle Accelerator Conference, 5-7 March 1969, Washington D.C.

RADIATION DIVISION, N.P.L.

(Superintendent: Dr. P. Campion)

Measurements of thermal activation cross-sections and activation resonance integrals (less 1/v) (T. B. Ryves)

The provisional results previously given in EANDC(UK) 110A have been revised. The neutron flux was re-measured by the activation of thin gold foils, and other corrections applied in several cases (^{124}Sb and ^{64}Cu). The ^{28}Al half-life was re-measured as 2.25 ± 0.02m, which has the effect of increasing the Al cross-section by about 4%. σ_0 is the 2200 m/s capture cross-section, I' the resonance integral (less 1/v part) relative to Au σ_0 = 98.86, I' = 1514 b.

Product nucleus from (n,)	σ_0	I'
^{24}Na	529 ± 7 mb	80 ± 12 mb
^{27}Mg	38.2 ± 0.8 mb	8.0 ± 1.2 mb
^{28}Al	233 ± 5 mb	66 ± 9 mb
^{31}Si	108 ± 2 mb	
^{38}Cl	423 ± 7 mb	120 ± 60 mb
^{42}k	1.46 ± 0.03 b	0.77 ± 0.15 b
^{51}Ti	179 ± 3 mb	38 ± 11 mb
^{52}V	4.93 ± 0.06 b	0.48 ± 0.09 b
^{59}Fe	1.14 ± 0.02 b	
^{65}Ni	1.49 ± 0.14 b	0.44 ± 0.14 b
^{64}Cu	4.4 ± 0.2 b	2.5 ± 0.2 b
^{66}Cu	2.17 ± 0.03 b	1.17 ± 0.12 b
^{80}Br	8.70 ± 0.30 b	92 ± 10 b
^{80}Br	(2.7 ± 0.2 b) assumed	34.5 ± 4b
^{82}Br	2.69 ± 0.09 b	50 ± 5b
^{116m}In	161 ± 3	2710 ± 200 b
^{122}Sb	6.21 ± 0.10 b	206 ± 15 b
^{124}Sb	4.14 ± 0.12 b	120 ± 12 b
^{128}I	6.12 ± 0.12 b	145 ± 9 b
^{134m}CS	(2.6 ± 0.2 b) assumed	30 ± 6 b

The errors in σ_0 are the sums of the standard errors of the mean and the estimated systematic errors. The values of Na, Al, ^{37}Cl and 51V have been recently re-measured to higher precision.

Measurement of $\bar{\nu}$ for spontaneous fission of ^{252}Cf. (E. J. Axton, B. N. Audric, A. G. Bardell).

The measurements described in the previous report (EANDC(UK)110AL) were made with an old sample of ^{252}Cf kindly loaned by Dr. K. F. Lauer of BCMN, Euratom. This sample contained only 30% of ^{252}Cf and 70% of the other Californian isotopes. A more recent sample from Oak Ridge containing 70% ^{252}Cf proved to be too small for accurate measurements, and experiments with this sample were discontinued. Recently much larger samples have been acquired and measurements are in progress with these. No further results are available.

Intercomparisons of fission counting are in progress with Argonne National Laboratories and with BCMN, GEEL. No results are available to date.

Measurement of ^{238}U activation cross section in the energy range 150 kev to 600 kev. (J. C. Robertson, J. B. Hunt, T. B. Ryves).

The calibration of the long counter in this energy range is in progress using a vanadium sulphate bath to determine the angular distribution and the total yield of neutrons from the ^{7}Li (p,n) reaction. The feasibility of determining the ^{238}U (n γ) cross section by activation measurements at the same time is being investigated.

NUCLEAR DATA FOR FAST REACTORS

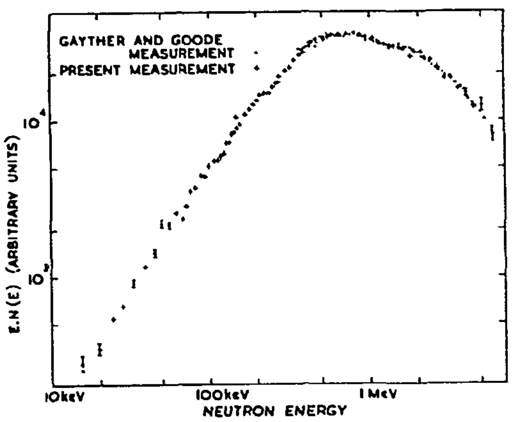

Fig. 1. Spectrum from 6 cm uranium target.

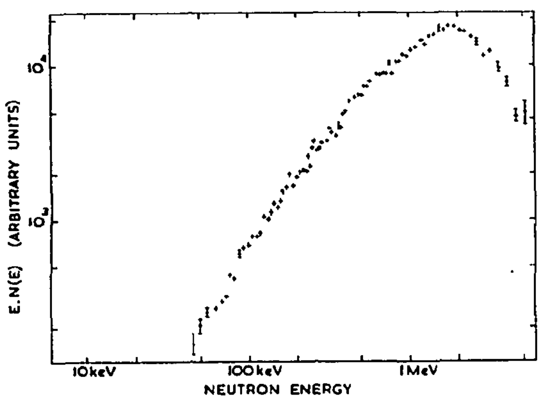

Fig. 2. Spectrum from 7.6 cm lead target.

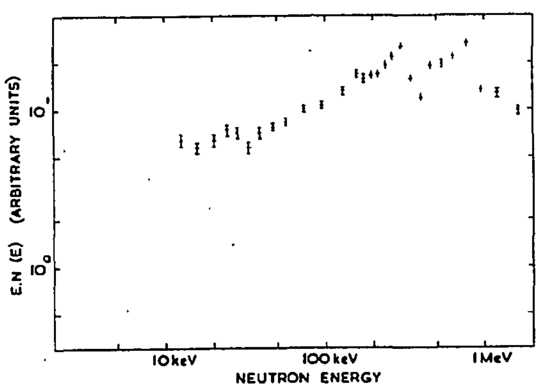

Fig. 3. Wall return spectrum.

E. Fast neutron spectrum measurements (A. J. H. Goddard and J. G. Williams (Imperial College) and H. Lichtblau (University of Birmingham))

We have measured the following spectra by the time of flight method using a 60 meter flight path:-

(1) The leakage spectrum from the 6.0 cm diameter natural uranium target developed by Gayther and Goode(1). The measurement was made using the boron-vaseline plug detector and a plastic scintillator (both detectors are described by Coates et al.(2)) and covered the energy range 15 keV to 5 MeV. In Fig. 1 our values for the function E.N(E) (proportional to flux/unit lethargy) are plotted, together with the results obtained by Gayther and Goode using a ^{10}B detector and the same plastic scintillator. The two spectra are arbitrarily normalised at 750 keV. The present measurements were extended to lower energies than those covered by Gayther and Goode to assist the interpretation of future measurements of the spectra of neutrons passing through shells of materials placed round the neutron target.

(2) The leakage spectrum from a 7.6 cm diameter spherical lead target, again of the type described in (1). No previous measurement was available for this target. The spectrum is shown in Fig. 2.

(3) The spectrum of neutrons emerging from a small area of the concrete wall of Cell III, at a distance of 75 cm from the 6.0 cm uranium target. The spectrum was observed in a direction close to the radius vector from the element of wall to the target. This measurement was made with the boron-vaseline plug detector and the spectrum is shown in Fig. 3.

The error bars shown indicate contributions from counting statistics and from systematic errors in the background subtraction only. All the spectra are subject to additional systematic errors due to detector calibrations (± 5%) and the spectra in Figs. 1 and 2 also have errors associated with the uranium filter correction (±5%).

During these runs nickel foil activation measurements were also made. They provide more accurate normalisation (± 5%) between spectra than can be achieved with beam current measurements and also confirm the spatial symmetry of the neutron production in the targets.

After these measurements were made the electron beam handling system was altered to move the target about half a metre further from the nearest wall. The uranium target measurement with the boron-vaseline plug detector has since been repeated, but no significant change in the leakage spectrum was found.

(1) Gayther D. B. and Goode P. D. J. Nucl. Energy 21, 733 (1967).

(2) Coates M. S., Gayther D. B. and Goode P. D. AERE - R 5364 (1968).

E. Design of a neutron detector with a flat energy response for use in time of flight experiments (M. S. Coates and W. Hart (Risley))

Detailed Monte Carlo calculations of the detection efficiency of a 12 cm radius spherical neutron counter have been reported earlier(1). The neutrons are moderated in a homogeneous ^{10}B-vaseline mixture, captured in ^{10}B, and the 480 keV γ-rays produced in the $^{10}B(n\alpha)^7Li^*$, γ^7Li reaction are detected at the sphere surface. The construction of this counter is almost complete. The calculations were limited to a ^{10}B content of 1 kg and it was noted that a higher ^{10}B concentration would be desirable because this leads to a proportionally faster time response. However, further calculations which have been made to obtain the detection efficiency for a counter containing 2 kg ^{10}B show that the increased concentration results in a much less acceptable efficiency variation at high incident neutron energies

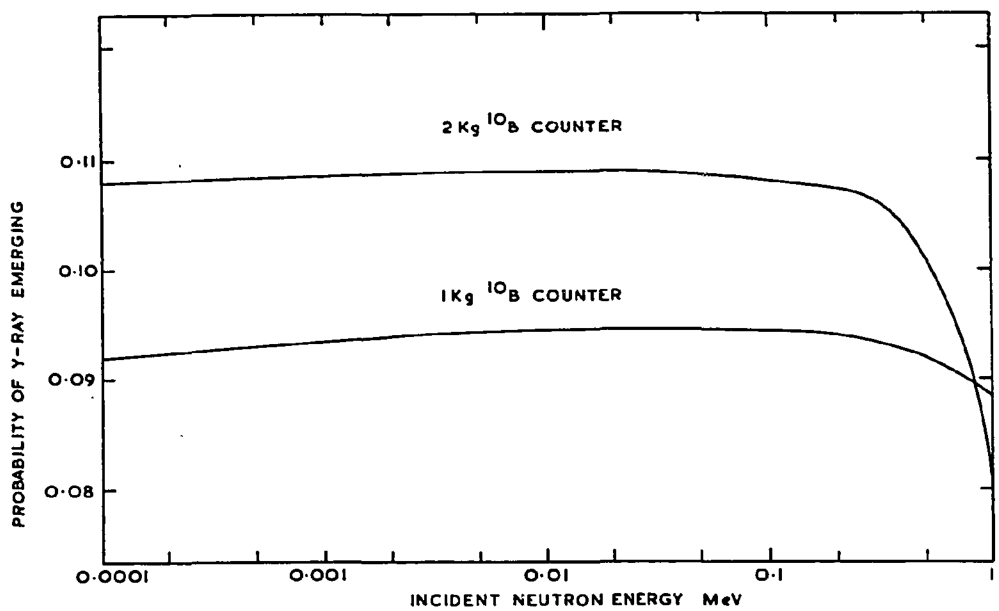

Fig. 1. Probability that gamma rays in energy range 400 → 480 keV will emerge from sections 2-3 (see text) as a function of incident neutron energy.

than that obtained for the 1 kg ^{10}B counter. The results for both counters are shown in Fig. 1, where the γ-rays are accepted from an area comprising half each of regions 2 and 3 of Fig. 1 of Ref. 1. It is seen that the response for the 2 kg ^{10}B counter falls off more rapidly at high energies than that for the 1 kg ^{10}B counter, the regions over which the efficiencies are flat to within ~ 4% being respectively

(100 eV → 300 keV) and (100 eV → 700 keV). The calculations are most accurate in the region of flat energy response, since they are insensitive there to the inaccuracies in the input nuclear data[1].

---

(1) Coates M. S. and Hart W. Nuclear Physics Division Progress Report AERE - PR/NP 15, p. 1 (1968).

B. Measurement of the absolute sensitivity of neutron detectors (J. M. Adams, A. T. G. Ferguson and G. D. McKenzie*)

The analysis of the experimental work on the calibration of a Harwell long counter has now been completed[1], and will shortly be written up for publication. In the neutron energy range covered by the experiments, viz. 50 keV to 1.3 MeV, the results are in good agreement with the previous relative efficiency curve of Allen and Ferguson[2,3]. However the activation techniques adopted for this experimental work provide a better foundation for the relative efficiency curves of the Harwell long counters.

---

(1) Adams J. M., Ferguson A. T. G. and McKenzie C. D. AERE - PR/NP 14 and 15.

(2) Allen W. D. and Ferguson A. T. G. Proc. Phys. Soc. (London) 70A, 639 (1957).

(3) Allen W. D. Fast Neutron Physics (Interscience), Chap. 3A, 361 (1960).

*On leave from the University of Melbourne, Australia. Since returned.

B. Intercalibration of Harwell long counters (J. M. Adams)

By using a Harwell long counter, calibrated by the method of reference[1], an inter-comparison with other Harwell long counters has been carried out. The experimental technique adopted involved using each long counter in turn under the same experimental conditions to measure the neutron angular distributions from the monoenergetic neutron producing reactions $^7Li(p,n)^7Be$ and $T(p,n)^3He$. Various incident proton energies were used in order to cover the neutron energy range from 100 keV to 1.3 MeV.

From the known curve of relative efficiency versus energy for the calibrated long counter, those for the other long counters could be calculated using the relation

$$S = \frac{(R + R_0)^2}{\epsilon a} C$$

where S is the neutron source strength/steradian/unit monitor count (calculated from the standard long counter data), ϵ is the relative efficiency, a is the effective sensitive area of the long counter, R is the distance from the target to the Cd front plate, R_0 is the effective depth of neutron penetration into the long counter measured from the Cd front plate and C is the experimentally determined count rate/unit monitor count. In fact the quantity ϵa, the count rate in a uniform unit neutron flux, is used for the intercomparison calculations. The analysis of the experimental data is at present in progress.

---

(1) Adams J. M., Ferguson A. T. G. and McKenzie C. D. AERE - PR/NP 14, p. 16.

E. The neutron absorption cross section of ^6Li (K. M. Diment and C. A. Uttley)

In the previous progress report[1] it was concluded that the absorption cross section of ^6Li for energies below 1.7 MeV laboratory neutron energy could be obtained by subtracting the scattering cross section from the measured total cross section. The result is shown in Fig. 1 (overleaf), in which the points are the values of the total cross section minus scattering and the full curve is the sum of the calculated s-wave absorption and the 250 keV p-wave resonance absorption obtained from the measured resonance parameters. The s-wave scattering cross section below 1 MeV was calculated from the parameters of a $\frac{1}{2}^+$ s-state at 6.56 MeV excitation in the compound nucleus ^7Li plus a very small contribution from a $^3/_2{}^+$ state at positive energy, assumed to be the level at 9.68 MeV excitation. The calculated scattering cross section below 1 MeV is in very good agreement with the data of Lane et al.[2] which in turn agrees very well above 1 MeV with the more recent scattering data of Knitter and Cappola[3], taken between 1 and 2 MeV. Subsequent to the calculation of the s-wave interaction it was found that the

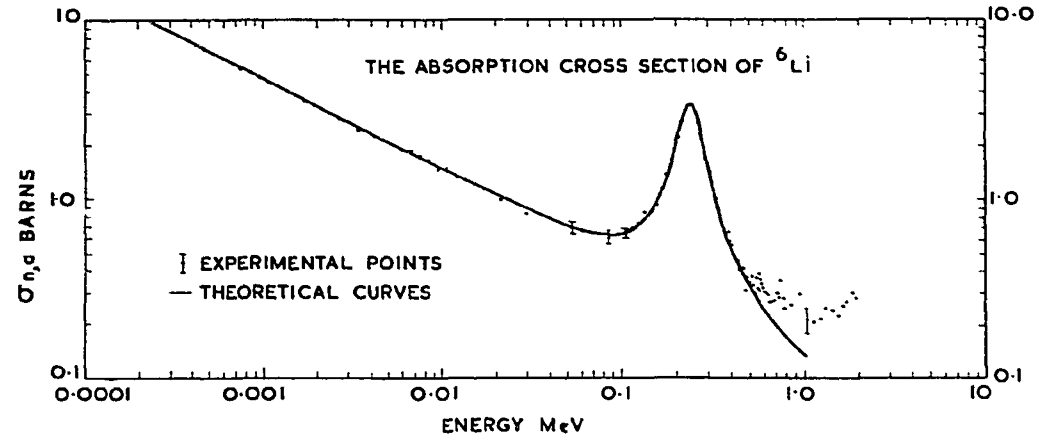

Fig. 1. The absorption cross section of ^{6}Li.

level in ^{7}Li at 9.68 MeV had been assigned as $^7/_2{}^-$ by Spiger and Tombrello[4]. This fact does not affect the conclusions on the s-wave scattering cross section, since the contribution to scattering in channel spin $^3/_2$ is very small and the same contribution below 1 MeV could be obtained from a $^3/_2{}^+$ state at higher energy. However this $^7/_2{}^-$ state, which lies at about 3 MeV laboratory neutron energy and is probably an f-state, should now account for the rising cross section above 1 MeV and also for the small contribution to the absorption cross section below 1MeV which was observed to be required after including the s-wave and p-wave resonance absorption cross sections. This effect is seen in Fig. 1, where the experimental data deviate increasingly from the calculated curve above about 500 keV.

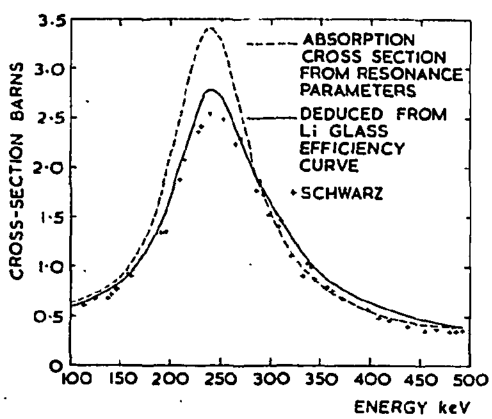

Fig. 2. Comparison of absorption cross section with the ^{6}Li(n,α)r cross section deduced from lithium loaded glass scintillators.

A significant discrepancy exists at present between the p-wave resonance absorption cross section and the measured ^{6}Li(n,α)t cross section deduced from the response of lithium loaded glass scintillators[5,6]. This is illustrated in Fig. 2, where the full curve[6] and the experimental points of Schwarz[5] were obtained from glass scintillator data, while the dotted curve was obtained from the measured resonance parameters plus the very small (0.3 barn at 250 keV) s-wave absorption cross section. Clearly the absorption and (n,α) cross sections are in agreement on both sides of the resonance, particularly if allowance is made for a slight shift in energy. Furthermore it is not expected that radiative neutron capture can contribute significantly to the absorption cross section as is indicated by the value of the radiation width $\Gamma_\gamma \approx 100$ eV which is obtained if most of the thermal capture cross section of 40 m barns is due to a $^1/_2{}^+$ state 6.56 MeV.

It is not possible at present to comment on the relative deviation with energy between the two sets of data across the resonance, but interesting conclusions can be reached concerning the peak observed cross sections. The observed peak total cross section is 10.8 barns. Subtracting an s-wave cross section comprising 0.7 barn of scattering and 0.3 barn of absorption leads to a peak p-wave total cross section of 9.8 barns. This peak total cross section is given by $4\pi g\Gamma_n/k^2\Gamma$, where g (=1) is the statistical weight factor for the $J = 5/2$ level, Γ_n and Γ are the neutron and total widths respectively and k is the neutron wave number. At resonance $4\pi g/k^2$ = 14.25 barns so that $\Gamma_n/\Gamma = 0.68$. The peak scattering cross section is $4\pi g\Gamma_n^2/k^2\Gamma^2 = 6.76$ barns which when added to the 0.7 barns s-wave scattering gives an observed peak scattering cross section of 7.46 barns in agreement with the value of 7.2 ± 0.4 barns of Lane et al.(2). Similarly the peak resonance absorption cross section is given by $4\pi g\Gamma_n(1 - \Gamma_n/\Gamma)/k^2\Gamma = 3.11$ barns which, when added to the 0.3 barn s-wave absorption gives the 3.41 barn peak cross section shown in Figs. 1 and 2. However Schwarz(5) in fitting his measured (n,α) resonance data found the parameters $\Gamma_n = 111$ keV and $\Gamma_\alpha = 30$ keV at resonance, giving a ratio $\Gamma_n/\Gamma = 0.79$. This ratio corresponds to a peak total cross section of 12.2 barns and a peak scattering cross section of 9.5 barns, which are inconsistent with the measured values.

(1) Nuclear Physics Divisional Progress Report AERE - PR/NP 15 (1968).

(2) Lane R. O., Langsdorf A., Monahan J. E. and Elwyn A. J. Ann. Phys. 12, 135 (1961).

(3) Knitter H. H. and Cappola M. EANDC(E)100 AL (1967).

(4) Spiger and Tombrello B.A.P.S. 11, 300 (4/66).

(5) Schwarz S., Stromberg L. G. and Bergstrom A. Nuc. Phys. 63, 593 (1965) and Neutron Data Compilation Centre, Newsletter No. 3, Oct. 1966.

(6) Leroy J. L. et al. EANDC(E)115 U, p. 147 (1968).

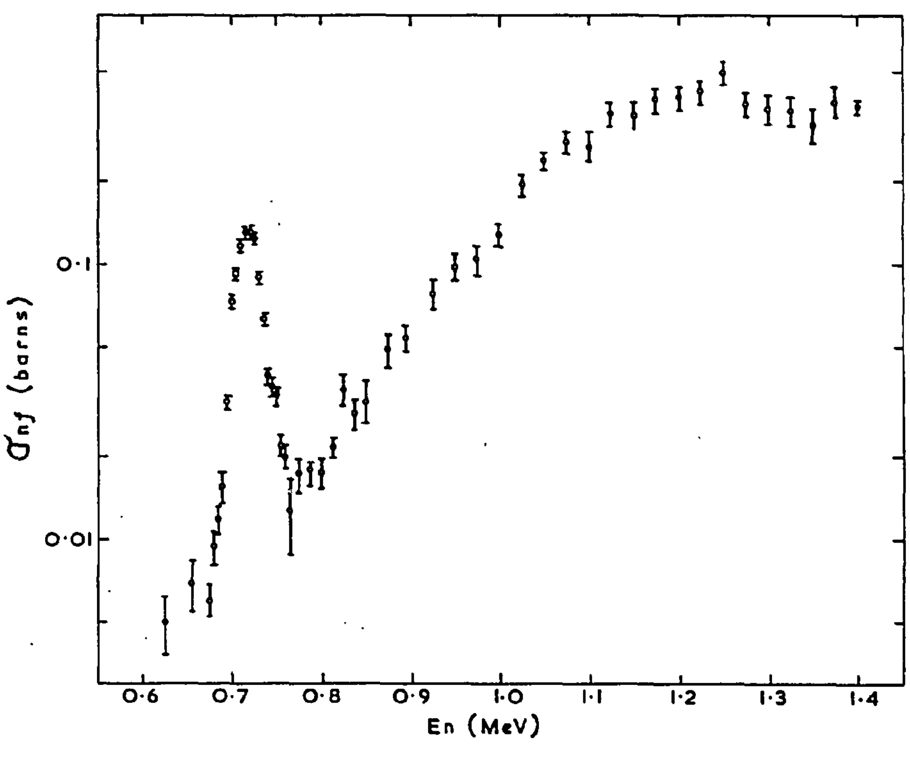

Fig. 1. ^{230}Th fission cross section.

B. The ^{230}Th fission cross section from 600 keV to 1.4 MeV (L. G. Earwaker, G. D. James and D. A. J. Endacott)

A measurement of the fission cross section of ^{230}Th over the energy range 600 keV to 1.4 MeV has been carried out on the IBIS accelerator using the $^7Li(p,n)$ reaction to generate neutrons and a Si-Au surface barrier detector of 6.5 cm^2 sensitive area to detect fission fragments from the ^{230}Th. Measurements were made with 5 keV energy resolution and the results obtained are shown in Fig. 1. The primary aim of the measurement was to determine the width of the resonance at 715 keV. This peak was first observed by Gokhberg et al.[1] and later remeasured by Vorotnikov et al.[2] and also by Evans and Jones[3] at an energy resolution of about 50 keV. It has been shown by Lynn[4] that it is very difficult to explain the decrease in fission cross section with increasing neutron energy beyond the peak of this resonance on the theory of inelastic neutron competition after a channel has become fully open for fission[5]. A second minimum in the fission potential barrier can provide a ready explanation of the resonance, and an analysis of the data on these lines is being carried out.

---

(1) Gokhberg B. M., Ostroshchenko G. A. and Shigin V. A. DAN SSSR 128, 1156 (1958).

(2) Vorotnikov P. E., Dubrovina S. M., Ostroshchenko G. A. and Shigin V. A. Soviet JNP 5, 207 (1967).

(3) Evans J. E. and Jones G. A. Unpublished, see ref. (4).

(4) Lynn J. E. Nuclear Data for Reactors II, (IAEA, Vienna), 89 (1967).

(5) Wheeler J. A. Physica 22, 1103 (1956), Fast Neutron Physics (New York, Interscience), 2051 (1963).

E. The total cross section of ^{234}U and the parameters of its sub-threshold fission resonances (G. D. James, G. G. Slaughter (ORNL) and D. A. J. Endacott)

A measurement of the total cross section of ^{234}U, at an energy resolution similar to that used by James and Rae[1] in their measurement of the ^{234}U fission cross section, has led to the determination of the neutron widths of 38 resonances below 687 eV. These results have been combined with the data of James and Rae to yield the fission widths of the resonances which are given in Table I. The data give a level spacing of 12.3 ± 1.5 eV and a neutron strength function of $(1.09 \pm 0.36) \times 10^{-4}$. The energy dependence of the fission widths is illustrated in Fig. 1 (see page 8). These fine structure resonances form the major part of a narrow intermediate structure resonance in the sub-threshold fission cross section of ^{234}U. Weigmann[2] and Lynn[3] predict that the fission widths should have a Lorentzian energy dependence superimposed on a Porter-Thomas distribution. The solid line in Fig. 1 shows a Lorentzian energy dependence of the mean fission width defined by the parameters given in Table II (see page 9). Here E_0 is the class II resonance energy, W the half width and K the numerator of the Lorentzian expression. These parameters were deduced by assuming that the peak of the curve passes through the measured fission width at 638.4 eV and that the sum of the observed fission widths is equal to the sum of the mean fission widths defined by the curve at each resonance energy. The assumptions made here are justified by observing that the resonance at 638.4 eV is predominantly a class II resonance because of its large fission width and small neutron width. The class II resonance energy is therefore close to 638.4 eV, and the observed fission width at this energy is not expected to differ greatly from the mean value defined by the Lorentzian curve. The parameters deduced after changing the peak fission width up and down by one standard deviation have been found and are also given in Table II. Five of the measured fission widths are negative, and it was found that the parameters of the Lorentzian curve are insensitive to changes in the fission widths of these five resonances from 10^{-6} meV to the values found by increasing the measured values by one standard deviation. In Table II we also give the degree of freedom, ν, of χ^2 distributions of the fission widths deduced by the maximum likelihood method of Porter and Thomas[4] for mean widths having a Lorentzian energy dependence ($\nu^{(a)}$ and $\nu^{(b)}$) and for an energy independent mean fission width ($\nu^{(c)}$). It is clear that the values of $\nu^{(c)}$ are inconsistent with a Porter-Thomas distribution for which $\nu = 1$. The values of $\nu^{(a)}$ were obtained by setting the five negative fission widths to 0.001 meV and those of $\nu^{(b)}$ by setting these widths to one standard deviation above their measured values. As expected, the values of ν are sensitive to the small positive values adopted for the negative fission widths but they are all near unity. It should be noted that for all the Lorentzian curves (A, B and C), $\nu^{(a)}$ is less than one and $\nu^{(b)}$ is greater than one. Thus it would be possible to choose values for these five fission widths within one standard deviation of their measured values which would give ν arbitrarily close to unity for any one of the Lorentzian energy dependent mean fission widths. Such a result would, of course, be improbably accurate for only 38 data points.

TABLE I

^{234}U Resonance Parameters

E_0 (eV)	Γ_n (meV)	$\sigma_0\Gamma_f$ (b.eV)	Γ_f (meV)
5.19	3.92 ± 0.019	1.250 ± 0.085	0.019 ± 0.001
22.74	0.018 ± 0.002	−0.003 ± 0.011	−0.037 ± 0.134
23.42	0.16 ± 0.02	−0.009 ± 0.011	−0.013 ± 0.016
31.21	6.50 ± 0.25	0.204 ± 0.025	0.012 ± 0.001
36.86	0.058 ± 0.005	−0.013 ± 0.023	−0.080 ± 0.142
45.83	0.297 ± 0.014	0.071 ± 0.026	0.108 ± 0.039
48.75	8.0 ± 0.7	0.050 ± 0.030	0.004 ± 0.002
77.66	7.9 ± 0.3	0.091 ± 0.047	0.011 ± 0.005
94.75	41 ± 2	0.683 ± 0.087	0.040 ± 0.005
106.65	3.2 ± 0.3	0.302 ± 0.080	0.110 ± 0.029
111.49	17.8 ± 0.6	2.85 ± 0.23	0.297 ± 0.024
146.75	8.7 ± 1.4	0.031 ± 0.071	0.007 ± 0.016
152.81	19.7 ± 0.6	0.175 ± 0.070	0.023 ± 0.009
177.25	28 ± 4	0.92 ± 0.13	0.120 ± 0.017
183.5	40 ± 6	1.15 ± 0.15	0.133 ± 0.017
188.3	52 ± 1	0.297 ± 0.097	0.032 ± 0.010
209.5	6.4 ± 1.5	0.006 ± 0.076	0.002 ± 0.030
238.7	3.9 ± 0.8	0.132 ± 0.092	0.091 ± 0.063
259.1	7.0 ± 1.4	0.91 ± 0.17	0.422 ± 0.080
277.8	3.2 ± 0.3	0.226 ± 0.105	0.216 ± 0.101
291.4	29 ± 2	0.99 ± 0.15	0.209 ± 0.032
309.8	11.3 ± 1.2	0.33 ± 0.14	0.127 ± 0.054
324.5	16.2 ± 0.4	0.052 ± 0.122	0.017 ± 0.039
332.9	2.7 ± 0.2	0.125 ± 0.107	0.166 ± 0.143
350.8	27 ± 6	0.66 ± 0.20	0.173 ± 0.053
360.3	37 ± 5.	0.00 ± 0.21	0.0 ± 0.049
393.1	10 ± 1.5	1.31 ± 0.25	0.711 ± 0.138
414.1	4.1 ± 0.1	0.574 ± 0.195	0.667 ± 0.232
439.1	2.2 ± 0.8	0.560 ± 0.193	1.229 ± 0.443
457.0	10.0 ± 1.7	11.90 ± 0.93	9.320 ± 0.924
466.4	12.5 ± 1.6	0.573 ± 0.359	0.313 ± 0.197
491.1	36 ± 11	5.05 ± 0.48	1.669 ± 0.164
515.0	70 ± 30	17.75 ± 1.32	5.053 ± 0.406
549.8	47 ± 13	0.0 ± 0.5	0.0 ± 0.16
559.1	72 ± 26	18.30 ± 1.36	5.640 ± 0.454
578.3	44 ± 10	14.20 ± 1.10	5.367 ± 0.452
638.4	$2^{+8}_{-0.7}$	5.30 ± 0.57	$51.1^{-16.2}_{+700}$
686.7	12 ± 8	8.89 ± 0.79	$9.06^{-0.84}_{+500}$
722.0		3.85 ± 0.51	
770.0	710 ± 85		
817.6	260 ± 100		

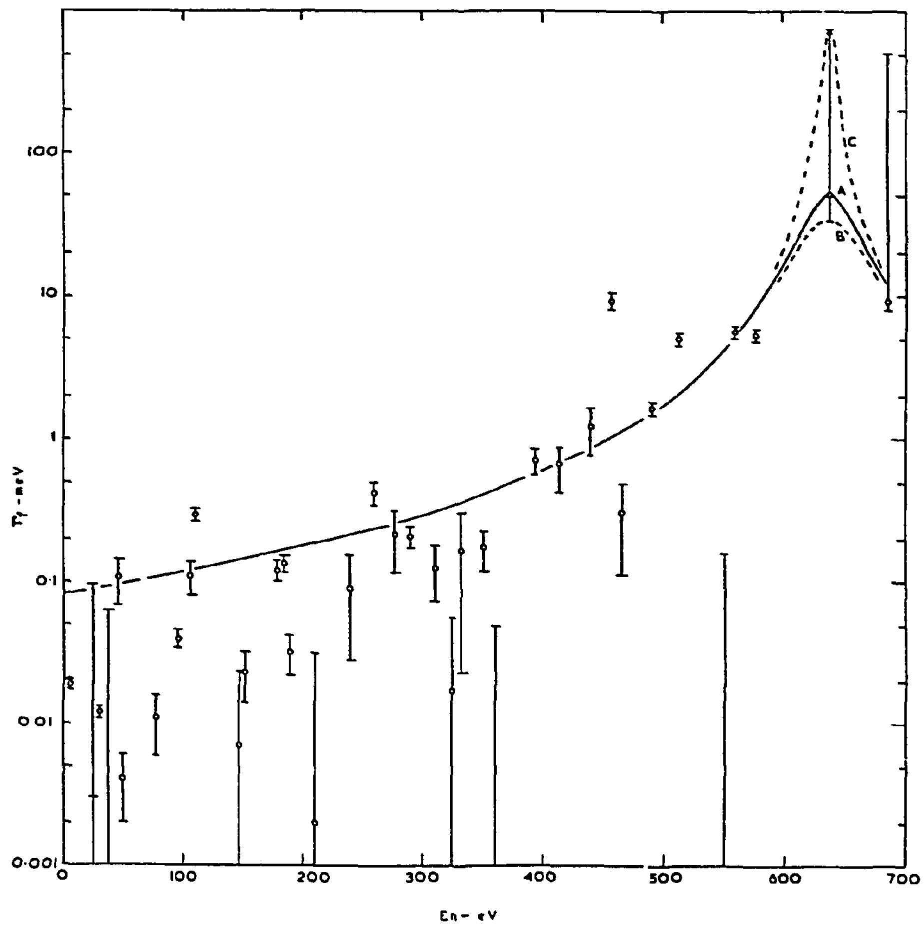

Fig. 1. The energy dependence of the observed fission widths for ^{234}U resonances. Curves A, B and C show a Lorentzian energy dependence of the mean fission width defined by the parameters in Table II. Curve A goes through the measured fission width at 638.4 eV whereas curves B and C go through points at one standard deviation from this datum.

TABLE II

Parameters of Lorentzian dependence of fission widths

Curve in Fig. 1	Γ_f at 638.4 eV (meV)	E_0 (eV)	W (eV)	K (eV^3)	$\nu^{(a)}$	$\nu^{(b)}$	$\nu^{(c)}$
A	51.1	638.4	25.9	34.4	0.92 ± 0.19	1.34 ± 0.26	0.46 ± 0.08
B	34.9	638.4	32.4	36.6	0.88 ± 0.16	1.27 ± 0.24	0.48 ± 0.08
C	751	638.4	6.36	30.4	0.98 ± 0.18	1.48 ± 0.28	0.30 ± 0.06

(a) ν is the degree of freedom of a χ^2 distribution describing the fluctuation of the fission widths. The results in this column are obtained by taking the mean fission width to have a Lorentzian energy dependence described by the parameters E_0, W and K and by setting the five negative values of fission widths given in Table I to 0.001 meV.

(b) These results are obtained by allowing for the Lorentzian energy dependence of the mean fission width and increasing all the negative values of fission width by one standard deviation.

(c) These values of ν are obtained when the mean fission width is assumed to be energy independent and the five negative fission widths are set to 0.001 meV.

The half widths given in Table II imply either very weak coupling to a broad class II level with class II fission width $\Gamma_f^{II} = 52.2^{+3.0}_{-39.4}$ eV and mean coupling matrix element $\overline{\langle H''\rangle^2} = 0.67^{-0.10}_{+1.73}$ $(eV)^2$ or weak coupling with $\Gamma_f^{II} = 0.30^{-0.05}_{+1.03}$ eV and $\overline{\langle H''\rangle^2} = 115^{+31}_{-92}$ $(eV)^2$. There is evidence that the latter coupling is the more likely.

(1) James G. D. and Rae E. R. Nucl. Phys. A118, 313 (1965).

(2) Weigmann H. Z. Phys. 114, 7 (1968).

(3) Lynn J. E. Structure in sub-threshold fission modes Report AERE - R 5891 (1968).

(4) Porter C. E. and Thomas R. G. Phys. Rev. 104, 483 (1956).

E. <u>Total cross section of ^{238}U (M. C. Moxon and M. B. Hughes)</u>

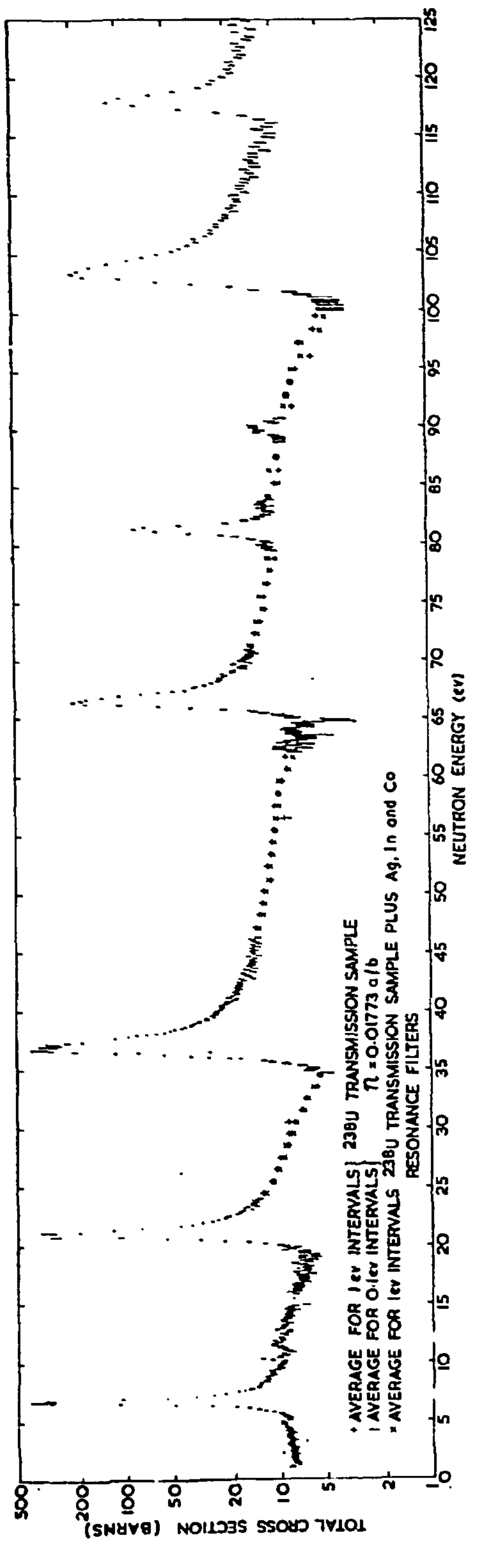

Fig. 1. Total cross section of ^{238}U.

Transmission measurements have been carried out on samples of ^{238}U (99.97% ^{238}U) obtained from Los Alamos Scientific Laboratory using a 14 m flight path on the booster target of the neutron time of flight spectrometer. Preliminary results obtained from the thickest sample (n = 0.01773 a/b) covering an energy range 1 to 125 eV are shown in Fig. 1. They are in reasonable agreement with the data given in BNL-325. The peak cross sections are not meaningful due to the effects of resolution and self-screening. It is hoped that the analysis of these data combined with the capture data will yield accurate values of the resonance parameters in the energy region below 300 eV.

E. <u>Neutron capture measurements in the keV region (M. C. Moxon and M. B. Hughes)</u>

(a) <u>Uranium</u>

The measurement and analysis of the neutron capture cross section of ^{238}U in the energy region 0.5 to 100 keV has been completed[(1)]. Values averaged over convenient energy regions are given in Table I and are shown in Fig. 1 (see page 12) together with previous data in this energy region. Estimates of the uncertainties are given in Table II. The total uncertainty in column 5 of Table I was determined from the quadratic sum of all the known uncertainties and varies from 5.7% at 100 keV down to 3.4% at 1 keV.

A quantitative comparison of these previous sets of data and the present results is most easily made at 30 keV. An extrapolation or interpolation was carried out on any measurements not having a data point at 30 keV, assuming that the present results give the correct shape of the ^{238}cross section and the magnitude was adjusted to fit the measurement. The weighted mean of previous data[(2-12)], using the quoted errors, is (441 ± 10)mb with a χ^2 of 35.2 for 9 degrees of freedom. Because of possible systematic errors in the measurements carried out with the ^{7}Li(p,n)^{7}Be threshold neutrons, the errors on these measurements were increased by 5%. The uncertainties on the shell transmission results were also increased by 5% to take into account the fact that fluctuation about the average value will be observed when the cross section is averaged over a finite number of resonances. Using these uncertainties a further weighted mean of (425 ± 15) mb was obtained. As the chi-squared value at 20.4 is still high for 9 degrees of freedom, it would appear to be necessary to increase the

TABLE I

Initial Energy (keV)	Final Energy (keV)	Capture Cross Section (b)	Statistical Error (b)	Systematic Error (b)	Total Error (b)
0.5	0.6	3.845	0.031	0.122	0.126
0.6	0.7	2.995	0.029	0.101	0.105
0.7	0.8	1.712	0.025	0.074	0.078
0.8	0.9	2.782	0.029	0.097	0.102
0.9	1.0	3.121	0.030	0.105	0.109
1.0	2.0	1.772	0.009	0.074	0.075
2.0	3.0	1.372	0.009	0.064	0.064
3.0	4.0	1.156	0.009	0.058	0.059
4.0	5.0	0.921	0.009	0.051	0.052
5.0	6.0	0.856	0.019	0.050	0.054
6.0	7.0	0.825	0.010	0.048	0.049
7.0	8.0	0.760	0.010	0.045	0.046
8.0	9.0	0.701	0.010	0.043	0.045
9.0	10.0	0.701	0.009	0.042	0.043
10.0	20.0	0.594	0.003	0.035	0.035
20.0	30.0	0.460	0.008	0.028	0.028
30.0	40.0	0.380	0.025	0.024	0.033
40.0	50.0	0.351	0.006	0.021	0.022
50.0	60.0	0.305	0.003	0.018	0.018
60.0	70.0	0.253	0.002	0.015	0.015
70.0	80.0	0.208	0.002	0.013	0.013
80.0	90.0	0.192	0.010	0.012	0.016
90.0	100.0	0.183	0.010	0.011	0.015

TABLE II

Uncertainties in the Measurement of the Uranium Capture Cross Section.

Energy (keV)	Statistical %	Background (mb)	$^{10}B(n\alpha\gamma)^{7}Li$ Cross Section %	Normalisation %	^{10}B Yield Calc. %	^{10}B n Value %
100	1.0	8.5	3.0	)	)	)
50	0.8	10.0	3.0	)	)	)
20	0.6	24.0	3.0	)	)	)
10	0.9	33.0	3.0	) 1.25	) 1.5	) 1.0
5	1.0	41.0	2.6	)	)	)
2	0.6	47.5	2.3	)	)	)
1	0.4	54.0	2.0	)	)	)

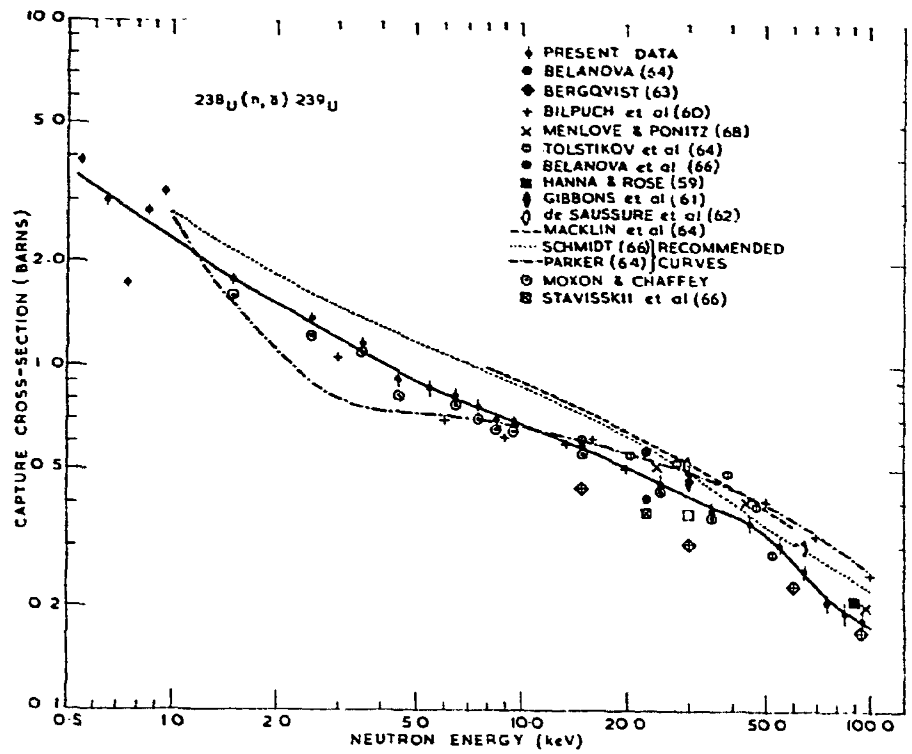

Fig. 1. Neutron capture cross section of ^{238}U.

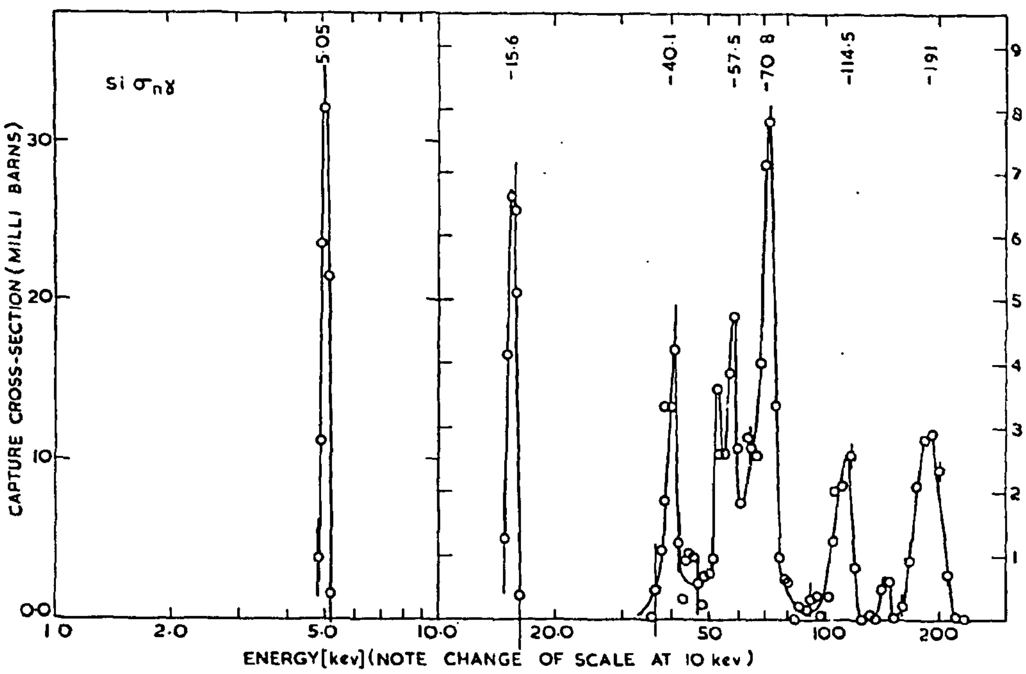

Fig. 2. Neutron capture cross section of natural Si.

uncertainty on this mean value by the square root of the ratio of χ^2 to the number of degrees of freedom, i.e. by a factor of 1.51 to ± 23 mb.

This mean value from previous measurement of 425 ± 23 mb is in good agreement with the value of 418 ± 29 mb given by the present data when averaged over the energy range 22 to 38 keV, i.e. similar to the energy spread quoted for threshold measurements.

(b) Silicon

Several runs have been carried out on samples of pure silicon. In the neutron energy region below 5 keV no significant resonance structure was observed, while from 5 keV to 200 keV several resonances were seen (see Fig. 2). Most of these resonances have not been seen in total cross section measurements[16] but some could be associated with levels observed in charged particle reactions[17].

The neutron capture resonance integral for silicon from the observed resonances is 3.8 ± 1.0 mb. The statistical uncertainty on the remaining data points does not eliminate the possibility of further weak resonance structure. A statistical estimate of the upper limit for such structure is 6^{+50}_{-2} and we conclude that the resonance integral for pure silicon is $10^{+51}_{-2.5}$.

---

(1) Moxon M. C. The neutron capture cross section of uranium-238 in the energy region 0.5 to 100 keV. AERE - R 6074.

(2) Gibbons J. H., Macklin R. L., Miller P. D. and Neiler J. H. Phys. Rev. 122, 182 (1961).

(3) Hanna R. C. and Rose B. J. Nuc. Energy 8, 197 (1959).

(4) Bilpuch E. G., Weston L. W. and Newson H. W. ANN Phys. 10, 455 (1960).

(5) De Saussure G., Weston L. W., Kington J. D., Smiddie R. D. and Lyon W. S. taken from BNL 325, 2nd Edition, Vol. III and ORNL-3360, p. 51 (1962).

(6) Macklin R. L. and Gibbons J. H. ORNL-TM-761 (1964) and private communication (1968).

(7) Tolstikov V. A., Sherman L. E. and Stavisskii Yu. Ya. J. Nuc. Energy 18, 599 (1964).

(8) Belanova T. S. Atomnaya Energiya 8, 549 (1960).

(9) Belanova T. S., Van'kov A. A., Mikhailus F. F. and Stavisskii Yu. Ya. J. Nuc. Energy 20, 411 (1966).

(10) Menlove H. O. and Poenitz W. P. Nuc. Sci. and Eng. 33, 24 (1968).

(11) Stavisskii Yu. Ya. et al. Soviet Atomic Energy 20, 431 (1966).

(12) Bergquist I. Arkiv for Fysik 23, 425 (1963).

(13) Moxon M. C. and Chaffey C. H. TRDWP/P8, The neutron capture cross section of iron, rhodium, silver, indium, gold, thorium and uranium from 1-30 keV.

(14) Schmidt J. J. Neutron cross sections for fast reactor materials (1966) EANDC(E) 35 U.

(15) Parker K. AWRE 0-79/63 (1964).

(16) Neutron cross sections. Sigma Centre, Brookhaven National Laboratory BNL-325.

(17) Story J. S. The thermal neutron absorption cross section resonance integrals and resonance parameters of silicon and its stable isotopes. (Unpublished, 1969).

Capture cross section for ^{238}U (D. W. Colvin and P. H. Bowen)

The A.W.R.E. 80 cm liquid scintillator has been set up on the electron linac and is now ready to be used for measurements of the capture cross section of ^{238}U to higher energies.

E. The direct measurement of alpha for ^{239}Pu over the energy range 10 eV to 30 keV (M. G. Schomberg, M. G. Sowerby, D. A. Boyce, K. J. Murray and D. L. Sutton)

The collection of data for this measurement[1] is now complete and analysis is in progress.

(1) Schomberg M. G., Sowerby M. G. and Boyce D. A. Nuclear Physics Division Progress Report AERE - PR/NP 15 (1968), p.5.

GENERAL NUCLEAR DATA FOR REACTORS

E. Correlation analyses of the total and fission cross sections of ^{239}Pu (G. D. James and B. H. Patrick)

A correlation analysis, of the type suggested by Egelstaff, of high resolution ^{239}Pu total cross section data indicates a modulation of the cross section with a spacing of about 460 eV. The correlations are not so significant as those discovered for the fission cross section, but they cannot be explained by a modulation of the fission widths and suggest a modulation of the neutron widths. A comparison of the fission and total cross sections shows that two of the several regions of high fission cross sections are also regions of high total cross section. These two regions, spaced about 460 eV apart, are adequate to explain the weak correlation found for the total cross section but do not invalidate our earlier conclusion that there exists a periodic modulation of the fission widths with a spacing of 460 eV.

E. Transmission measurements on ^{107}Ag and ^{109}Ag (N. J. Pattenden and J. E. Jolly)

A modified version of the Atta-Harvey area analysis program[1] has been used to obtain neutron widths from the transmission measurements on separated ^{107}Ag and ^{109}Ag metallic foil samples previously reported[2]. The values are shown in Tables I and II. The results give s-wave neutron strength functions of $(0.35 \pm 0.07) \times 10^{-4}$ and $(0.46 \pm 0.09) \times 10^{-4}$ for ^{107}Ag and ^{109}Ag respectively, over the range below 2600 eV, and Table III (see page 16) shows the neutron strength function in 500 eV energy intervals. The errors indicated are due to the limited number of resonances in the sample and not to the experimental uncertainty.

The results show that the conclusion reached from an earlier set of measurements made on ^{109}Ag only[3], namely, that the ^{109}Ag neutron strength function is about double that for ^{107}Ag, is no longer tenable. The earlier set covered an energy range below 600 eV; the present results show that for ^{109}Ag the strength function in this region is abnormally large.

These results greatly extend the range over which isotopic assignments of the silver resonances have been made[4] (previously to ~ 600 eV). They show that at energies of about 174, 252, 471 and 556 eV, there are resonances in both isotopes, and the 265 eV resonance previously attributed to ^{109}Ag (ref. 4) is really in ^{107}Ag. The results will later be used combined with capture and scattering measurements to obtain values of neutron and radiation widths.

(1) Atta S. E. and Harvey J. A. ORNL-3205 (1961).

(2) Nuclear Physics Division Progress Report AERE - PR/NP 13, p. 6 (1968).

(3) Pattenden N. J. Nuclear Structure with Neutrons Vol. I, paper 92, EANDC-50.S (1965).

(4) Goldberg M. D. et al. Neutron Cross Sections, Vol. IIB, BNL-325 Second Edition, Supplement No. 2 (1966).

TABLE I

^{107}Ag neutron widths

(Assuming $\Gamma_{\gamma} = 140$ meV)

E_R (eV)	$g\Gamma_n^o$ (meV)	$\Delta g\Gamma_n^o$ (%)	E_R (eV)	$g\Gamma_n^o$ (meV)	$\Delta g\Gamma_n^o$ (%)
41.58	0.52	3	697.2	0.42	20
44.93	0.119	6	754.0	1.41	8
51.52	2.30	5	935.5	4.8	6
144.4	0.45	5	947.1	1.02	14
174.0	0.37	5	991.8	1.8	12
203.0	0.743	4	1049	1.6	12
228.0	0.056	35	1137	1.1	18
251.8	0.78	5	1151	0.5	35
264.9	0.17	18	1181	2.9	10
311.6	4.2	6	1419	2.0	15
362.2	0.71	7	1592	1.0	28
445.3	0.71	10	1630	1.5	18
462.2	0.45	15	1645	2.4	15
467.5	2.76	5	1722	1.5	20
472.8	0.63	14	1837	1.3	24
516.2	1.71	6	1909	3.5	12
555.6	4.2	6	1941	8.2	8
577.8	0.93	12	1993	1.7	30
588.6	2.11	6	2050	4.2	15
626.8	0.51	14	2179	4.1	14
654.4	0.21	28	2318	1.0	50
675.3	0.85	10	2399	9.6	8
			2665	7.6	12

TABLE II

^{109}Ag neutron widths

(Assuming γ = 140 meV)

E_R (eV)	$g\Gamma_n^o$ (meV)	$\Delta g\Gamma_n^o$ (%)	E_R (eV)	$g\Gamma_n^o$ (meV)	$\Delta g\Gamma_n^o$ (%)
55.84	1.39	3	748.8	2.11	6
71.07	2.22	5	786.2	4.90	4
87.73	0.48	3	883.8	1.72	10
134.1	4.80	5	932.8	1.82	10
139.9	0.126	12	949.3	0.32	40
173.3	2.43	3	962.9	0.64	25
209.6	1.33	4	976.8	1.76	10
251.8	0.53	6	1011	2.16	10
259.4	0.10	28	1059	1.41	14
273.2	0.06	50	1063	1.33	18
291.4	0.50	9	1118	1.36	17
317.0	5.87	4	1206	4.51	7
328.2	0.19	22	1222	4.73	7
387.5	1.63	5	1238	2.3	11
398.4	0.88	9	1302	1.8	14
404.9	2.48	5	1385	1.4	20
429.1	0.43	12	1417	2.6	13
470.2	1.74	5	1486	1.2	23
488.2	0.53	12	1514	2.1	15
501.3	4.43	3	1590	3.0	12
513.1	0.68	11	1681	1.9	18
557.2	0.57	15	1918	6.0	10
561.5	2.55	4	2093	2.4	23
565.5	2.73	7	2133	4.6	14
608.8	0.85	11	2329	5.3	15
623.3	1.93	6	2351	1.0	70
670.7	0.67	14	2511	3.2	35
727.5	0.69	13	2587	4.3	20

TABLE III

Variation of neutron strength functions with energy

Energy range (eV)	s-wave neutron strength function (× 10^4)	
	^{107}Ag	^{109}Ag
0 - 500	0.35 ± 0.12	0.65 ± 0.20
500 - 1000	0.38 ± 0.16	0.58 ± 0.15
1000 - 1500	0.19 ± 0.12	0.49 ± 0.15
1500 - 2000	0.35 ± 0.18	0.30 ± 0.15
2000 - 2500	0.47 ± 0.33	0.31 ± 0.16

E. Spin assignments of resonances in ^{165}Ho using a polarized target (H. Marshak (N.B.S., Washington), C. A. Uttley and K. M. Diment)

The object of this measurement is to determine the total angular momentum J of s-wave neutron resonances in ^{165}Ho by measuring the change in transmission of unpolarized neutrons through an unpolarized and a polarized sample of holmium. The effect to be observed is relatively small and can only be detected with thick samples. It is hoped to be able to determine the spins of at least 100 resonances to see if a significant J-dependence in the s-wave neutron strength function exists and for this purpose the 120 meter detector station on the 300 meter flight path is being used to obtain the required resolution. The helium-3 refrigerator[1] is placed at the 60 meters point, along with a thin boron-10 plug which acts both as an overlap filter for 120 meters and also as a detector at 60 meters to enable transmission measurements to be extended down to about 13 eV. In this way the measurements include the low energy resonances whose spins have been determined by other methods. The refrigerator is cycled in and out of the neutron beam in order to achieve accurate transmission data. Measurements have already been made on a 2.5 cm thick sample and data are now being taken with a 5 cm thick holmium sample.

---

(1) Marshak H., Langsford A., Wong C. Y. and Tamura T. Phys. Rev. Lett. 20, 554 (1968).

E. Partial radiation widths for neutron resonance capture by ^{238}U (B. W. Thomas, J. Murray, E. R. Rae and P. Riehs (Seibersdorf))

The study of ^{238}U capture gamma-ray spectra for individual resonances has remained a subject of interest for several years. The main reason for this has been the inability to resolve completely the complex spectra that are observed. The spectra are dominated by several strong gamma-rays at 4 MeV, which represent transitions to final states in ^{239}U with excitation energies in the range 700-800 keV.

Early experiments with NaI detectors[1,2], which did not resolve the individual gamma-rays in the neighbourhood of 4 MeV, showed small fluctuations in the gamma-ray strength in this area which corresponded to a χ^2 distribution for the group with a number of degrees of freedom varying from 11 to 90. Later careful work with NaI by Jackson[3], in which 12 resonances were studied, showed much stronger fluctuations corresponding to 5.8 ± 2.3 degrees of freedom for the gamma ray lines lying between 3.8 and 4.2 MeV. By this time it was known that there were four strong lines in this energy interval, so that Jackson's result was consistent with a Porter Thomas distribution (ν = number of degrees of freedom = 1) for the individual lines, as expected from the statistical model.

More recently the controversy over the applicability of the statistical model to neutron capture in ^{238}U has been re-opened by the work of Price et al.[4], who examined the resonance spectra with a Ge(Li) detector, using the fast chopper on the Brookhaven High Flux Reactor. Spectra were obtained for individual resonances up to 100 eV, and the distribution of 18 partial widths for each of 5 resonances was consistent with a ν value of $4.6^{+1.9}_{-1.2}$ for the individual transitions. The distribution for the four strongest gamma-ray lines at 3982, 3991, 4059 and 4068 keV gave a ν value of $3.7^{+2.1}_{-1.6}$ for the individual transitions. Though the latter result is not strongly discrepant from the above result of Jackson, it disagrees with the Porter Thomas distribution ($\nu = 1$).

A similar experiment on a 10 metre flight path of the Harwell linac was reported previously[5]. Capture gamma-ray spectra for 15 resonances in ^{238}U up to 350 eV have now been analysed and the partial radiation widths for the two strong doublets at 4 MeV are listed in Table I (overleaf) together with published data from ref. (4). The individual components of each doublet were not resolved in this experiment, but their existence is obvious from the line shapes. The present data are normalised to the strong 3982, 3991 keV doublet observed in the 6.7 eV resonance in ref. (4).

There is reasonable agreement between the two sets of data for the first three resonances, but not for those at 66 eV and 81 eV. This may be due to overlapping of resonances in ref. (4) because of poor timing resolution. This fact may also explain the high value of ν obtained by the Brookhaven group for the four lines around 4 MeV.

TABLE I

Partial radiation widths for $^{238}U(n,\gamma)^{239}U$ in meV

[Only the strong lines near 4 MeV are listed]

Resonance energy (eV)	Gamma-ray energy keV			
	3982 + 3991		4059 + 4068	
	This work	ref. 4	This work	ref. 4
6.67	1.89 ± 0.06	1.89 ± 0.09	0.55 ± 0.05	0.66 ± 0.04
21	0.64 ± 0.06	0.82 ± 0.05	0.85 ± 0.06	1.19 ± 0.06
36.7	0.39 ± 0.05	0.47 ± 0.05	0.23 ± 0.05	0.34 ± 0.04
66.2	0.10 ± 0.08	0.36 ± 0.08	0.51 ± 0.10	0.80 ± 0.18
81.1	0.06 ± 0.15	0.61 ± 0.24	0.29 ± 0.14	0.80 ± 0.15
102.7	0.02 ± 0.10		0.75 ± 0.10	
116.9	0.10 ± 0.14		0.25 ± 0.12	
145.7	−0.22 ± 0.20		0.19 ± 0.38	
165.4	0.14 ± 0.28		0.24 ± 0.30	
189.6	0.25 ± 0.25		−0.02 ± 0.24	
208.6	0.53 ± 0.26		0.58 ± 0.23	
237.4	1.91 ± 0.30		0.13 ± 0.20	
273.7	−0.04 ± 0.36		0.55 ± 0.30	
291	1.36 ± 0.40		0.33 ± 0.34	
347.9	0.16 ± 0.40		1.33 ± 0.60	

N.B. The errors quoted are statistical

The present data on the two doublets for 15 resonances (i.e. sample of 30 doublet strengths) have been analysed by the maximum likelihood method, and their population corresponds to a χ^2 distribution of 1.3 ± 0.6 degrees of freedom (10 and 90% limits). This result, although low, is not inconsistent with a Porter Thomas distribution for the individual widths, which would predict 2 degrees of freedom for uncorrelated pairs. An analysis of all transitions observed in the 15 resonance spectra is almost completed and will provide a more accurate estimate of ν for the individual transitions.

The number of resonance spectra obtained in this experiment is sufficient to provide an estimate of ν for each doublet (sample of 15 widths). The results obtained in this case are:-

$$\begin{array}{lll} (1)\ 3982,\ 3991\ \text{keV} & \nu = 0.7 \pm 0.4 & \multirow{2}{*}{} \\ (2)\ 4059,\ 4068\ \text{keV} & \nu = 2.5 \pm 1.3 & \end{array} \Bigg\}\ 10\%\text{-}90\%\ \text{limits}$$

The second case is in good agreement with theory ($\nu = 2$) but the value of 0.7 for the first pair suggests that the 3982 and 3991 keV transitions are correlated, the probability of ν being 2 in this case is less than 1%.

(1) Hughes D. J. et al. Proc. Int. Conf. on Nuclear Structure, Ed. Bromley and Vogt, University of Toronto Press (1960), p. 771.

(2) Corge C. et al. J. Phys. Rad. 22, 722 (1961).

(3) Jackson H. E. Phys. Rev. 134B, 931 (1964).

(4) Price D. L. et al. Nucl. Phys. A121, 630 (1968).

(5) Thomas B. W., Uttley C. A. and Rae E. R. Nuclear Physics Division Progress Report AERE - PR/NP 14, p. 23 (1968).

E. High resolution gamma ray studies of resonant capture (J. Murray, B. W. Thomas and P. Riehs (Seibersdorf)

The thermal neutron capture gamma ray spectra of even even target nuclei in the mass region with $A \approx 180$ appear to show a systematic feature which is at variance with the decay properties expected from highly complex compound states[1].

The nuclei in this region are highly deformed and the levels near the ground state have been interpreted in terms of rotational bands built on Nilsson states. The intrinsic states in the Nilsson model are labelled by the asymptotic quantum numbers (N, n_3, Λ) where N is the total oscillator quantum number, n_3 is the number of oscillator quanta along the symmetry axis and Λ is the projection of the orbital angular momentum on to the symmetry axis. A nuclear level in this model is characterised by the quantum numbers $J^{\pi}[N\, n_3\, \Lambda]$ where J is the total angular momentum and π is the parity of the level.

For even target nuclei the s-wave resonances will have spin and parity $\frac{1}{2}^{+}$ and will decay by E1 transitions to levels with J^{π} of $\frac{1}{2}^{-}$ or $\frac{3}{2}^{-}$. The tungsten isotopes with A = 183, 185 and 187 have low lying levels which have been assigned on the basis of (d,p) studies[2] as belonging to the [510] and the [512] bands. The $\frac{1}{2}^{-}[510]$, $\frac{3}{2}^{-}[510]$ and $\frac{3}{2}^{-}[512]$ members of these bands should be strongly excited by the (n,γ) reaction.

Namenson and Bolotin[1] have noted that in the thermal spectra for capture by ^{178}Hf, ^{180}Hf, ^{182}W, ^{184}W and ^{186}W the [510] band is much more strongly excited than the [512] band. They suggested that it could be explained by a selection rule operating on Λ, i.e. $\Delta\Lambda = 0, \pm 1$. This implies that the resonances which cause the thermal capture cross section in these nuclei retain to a significant degree their original structure of an s-wave neutron (with l and therefore $\Lambda = 0$) orbiting an even core.

However, when the spectra of the 4, 21 and 114 eV resonances in ^{182}W were studied[3] it was shown that the [510] band is not in general excited more strongly than the [512] band. There remains the possibility that resonances which decay strongly to the [510] band decay weakly to the [512] band and vice versa. This effect will manifest itself as an anticorrelation between the strengths to the two bands from different resonances.

Using a 20 metre flight path on the Harwell linac and a natural tungsten target, capture spectra for the 4, 21, 114, 249, 377 and 486 eV resonances in ^{182}W, the 184, 311 and 425 eV resonances in ^{184}W and the 19, 171, 219, 288 and 511 eV resonances in ^{186}W have been obtained. The results of a correlation analysis for the three levels discussed above are given in Table I (overleaf).

The correlation coefficient, t_{ij}, between the reduced widths to the levels designated by i and j is as usual defined as

$$t_{ij} = \frac{\Sigma\,(\Gamma_{\gamma ki} - \bar{\Gamma}_{\gamma i})\,(\Gamma_{\gamma kj} - \bar{\Gamma}_{\gamma j})}{\sqrt{\sum_k (\Gamma_{\gamma ki} - \bar{\Gamma}_{\gamma i})^2\, \Sigma(\Gamma_{\gamma kj} - \bar{\Gamma}_{\gamma j})^2}}$$

where $\Gamma_{\gamma ki}$ is the reduced radiation width from resonance k to level i and $\bar{\Gamma}_{\gamma i}$ is the mean width to level i. The probability that a value for the correlation coefficient which is greater than t_{ij} will obtain in a random sample is denoted by $P(t_{ij})$.

Since the reduced radiation widths are expected to be drawn from a population with a χ^2 distribution with one degree of freedom, and the sample size is small, the values of P are obtained using Monte Carlo techniques.

Although there is evidence for an anticorrelation between the widths to the two $\frac{3}{2}^{-}$ states there is no evidence for a similar relationship between the widths to the $\frac{1}{2}^{-}[510]$ and the $\frac{3}{2}^{-}[512]$. It is therefore unlikely that it is a selection rule on Λ which is causing the anticorrelation.

TABLE I

	i	j	t_{ij}	$P(t_{ij})$
^{182}W	$3/2^-$[510]	$1/2^-$[510]	−0.218	65%
	$3/2^-$[510]	$3/2^-$[512]	−0.548	90%
	$1/2^-$[510]	$3/2^-$[512]	0.203	30%
^{186}W	$3/2^-$[510]	$1/2^-$[510]	0.580	17%
	$3/2^-$[510]	$3/2^-$[512]	−0.868	98%
	$1/2^-$[510]	$3/2^-$[512]	−0.612	90%

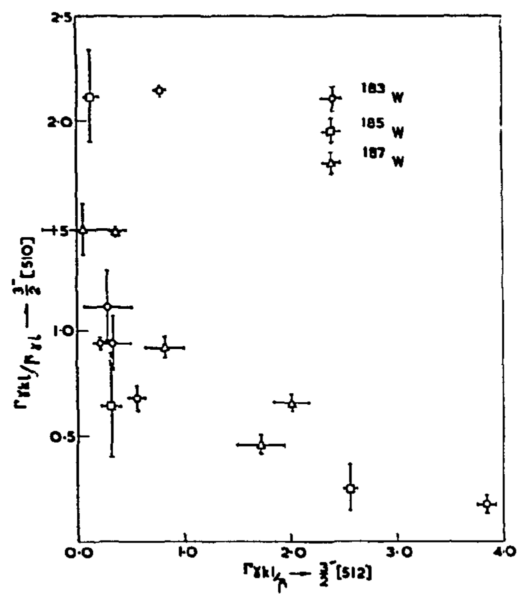

Fig. 1. Correlation between the reduced radiation widths $\Gamma_{\gamma ki}$ from various resonance levels k to the $3/2^-$ members of the [510] and [512] rotational bands.

Fig. 1 is a plot of the width from a resonance to the $3/2^-$[510] as a function of the width from the same resonance to the $3/2^-$[512] for the 14 resonances studied. The negative correlation is clearly demonstrated.

Prestwich and Cote[3] have suggested that the relative strengths to the [510] and the [512] bands from a resonance may depend on the reduced neutron width of the resonance. Therefore a similar analysis has been made for the correlation coefficient between the reduced neutron width and the radiation width to each of the three levels above. The results are given in Table II. They do not appear to be significant.

The apparent breakdown of the statistical model as evidenced by Fig. 1 is difficult to explain. If it is related to the collective nature of the $3/2^-$[510] level then one would expect a negative correlation between the widths to the $3/2^-$[510] level and the $1/2^-$[510] level which is not seen. If on the other hand it is related to the difference in the intrinsic states, then one would expect a negative correlation between the widths to the $3/2^-$[512] level and the $1/2^-$[510] level, which also is not seen.

(1) Namenson A. I. and Bolotin H. H. Phys. Rev. 158, 1206 (1967).

(2) Erskine J. R. Phys. Rev. 138, B66 (1967).

(3) Prestwich W. V. and Cote R. E. Phys. Rev. 160, 1038 (1967).

TABLE II

	i	r_i	$P(r_i)$
^{182}W	$3/2^-[510]$	−0.397	80%
	$1/2^-[510]$	−0.696	97%
	$3/2^-[512]$	+0.124	35%
^{186}W	$3/2^-[510]$	0.417	23%
	$1/2^-[510]$	−0.183	55%
	$3/2^-[512]$	−0.096	50%

A. Studies of fission isomer production in neutron bombardment (A. J. Elwyn+ and A. T. G. Ferguson)

The discovery of isomers having short lifetimes against fission and other experimental studies in the region of sub-barrier fission have led to new theoretical insights into the properties of heavy nuclei, and into the mechanism of the fission process itself. In an effort to synthesize new fissioning isomers we are searching for isomeric states with lifetimes in the range 10-1000 ns in the neutron induced fission of various isotopes of Uranium and ^{239}Pu.

In the experiment, foils (~ 1.5 mg/cm^2) of ^{233}U, ^{234}U, ^{235}U, ^{238}U and ^{239}Pu are bombarded by neutrons with energies of 0.5 and 2.2 MeV produced in the $^7Li(p,n)^7Be$ and $T(p,n)^3He$ reactions initiated by the pulsed proton beam from the I.B.I.S. electrostatic accelerator. The time distribution of the pulses due to the detection of fission fragments is studied using Si surface barrier counters. With the addition of a second set of beam deflection plates (supplementing the usual beam sweeping and bunching arrangement of I.B.I.S.) it has been possible to reduce the intensity of the residual beam between beam bursts to less than 10^{-5} of the main beam intensity, at least over a time interval of about 500 ns after the main beam burst.

Preliminary results suggest that fission isomers have been observed with half-lives in the range 24-67 ns. The cross sections for the production of such isomeric states lie between 10^{-5} and 2×10^{-4} of those for neutron induced prompt fission. Preliminary results at an energy of 2.2 MeV are shown in Table I (overleaf). Analysis of results obtained at 0.5 MeV are in progress.

+On leave from Argonne National Laboratory, Argonne, Illinois, U.S.A.

E. Fission fragment angular distributions from resonance fission with oriented nuclei (N. J. Pattenden and J. E. Jolly; H. Postma, R. Kuiken and K. Ravensberg (F.O.M. Netherlands); J. C. Waldron (Chemistry))

This experiment was first reported in the previous progress report. The semiconductor detectors (eight multidiffused-junction silicon detectors, each of 4 cm^2 active area, obtained from the Harshaw Chemical Company) were tested at ~1°K, their operating temperature in the experiment. They were shown to operate with sufficient stability and reliability for our purposes. It was noticed that at ~1°K (a) the γ-ray sensitivity was greater than at room temperature, relative to α-particle pulses, (b) for a given bias, the α pulse height distribution had a lower mean value than at room temperature, with a high energy tail going up to about the room temperature value, (c) the bias could be increased to greater values than at room temperature without fear of breakdown, and increasing the bias caused the mean value of the α pulse height distribution to increase without increasing the high energy tail, until the distribution resembled the room temperature distribution more closely.

TABLE I

Target Nucleus	$E_n = 2.2$ MeV	
	Half-life (± 10-15%) (nsec)	Intensity Ratio (Isomer/Prompt Fission) ($\times 10^{-4}$)
^{233}U	35	1.2
^{234}U	24	0.15
^{235}U	67	1.3
^{238}U	No isomeric decay observed	
^{239}Pu	56	0.8

During November-December, a preliminary series of measurements were performed, using four rubidium uranyl nitrate (RUN) crystals with a ^{235}U content of 5.5 mg (determined by α counting) and average thickness 1.2 mg/cm^2. This showed that at temperatures of ~0.1°K significant anisotropies could be observed, which varied from resonance to resonance by up to ~40%.

Another sample was prepared, consisting of 21 RUN crystals containing 27.7 mg ^{235}U and having an average thickness of 1.3 mg/cm^2 and 15 crystals containing 9.6 mg ^{235}U and having an average thickness of 0.75 mg/cm^2. These two groups were attached to opposite sides of a copper plate and observed by different groups of detectors (see Fig. 1). Measurements were started in January and continued until April. The measurements give fission fragment count rates as a function of incident neutron time-of-flight, observed with detectors parallel and perpendicular to the RUN crystal c-axis, and these are measured at different temperatures. The neutron energy range covered was ~ 0.04 to 4000 eV, and the lowest temperature ~ 0.1°K. Separate background and unoriented nuclei measurements were also made.

The data have not yet been analysed in detail, but the fission anisotropies are expected to follow a relation of the form $W(\theta) = 1 + A_2 f_2 P_2 (\cos \theta)$ + higher terms, where A_2 is a nuclear parameter depending essentially on J, the total angular momentum, and K, its projection on the symmetry axis, and f_2 is an orientation parameter depending on the electric quadrupole coupling constant and the absolute temperature. Preliminary surveys of the data indicate (a) that the effect tends to saturation as the temperature is reduced, so that little is to be gained by cooling below ~0.08°K (see Fig. 2); (b) in the low energy region significant changes in the anisotropy occur in a small energy range (see Fig. 3). The variation with energy is in qualitative agreement with the experimental results of Dabbs et al.(1). The same value for the coupling constant as used by Dabbs et al. ($P/k = 0.0154$ K) was also used to derive A_2 in Fig. 3.

Similar measurements on ^{233}U are about to start. In this case it will be more difficult to achieve such low temperatures, because the α-particle heating of the sample is of the order of 100 erg.sec^{-1}.

(1) Dabbs J. W. T., Walter F. J. and Parker G. W. Proceedings of the Physics and Chemistry of Fission Conference, Salzburg, Vol. 1, 39 (1965).

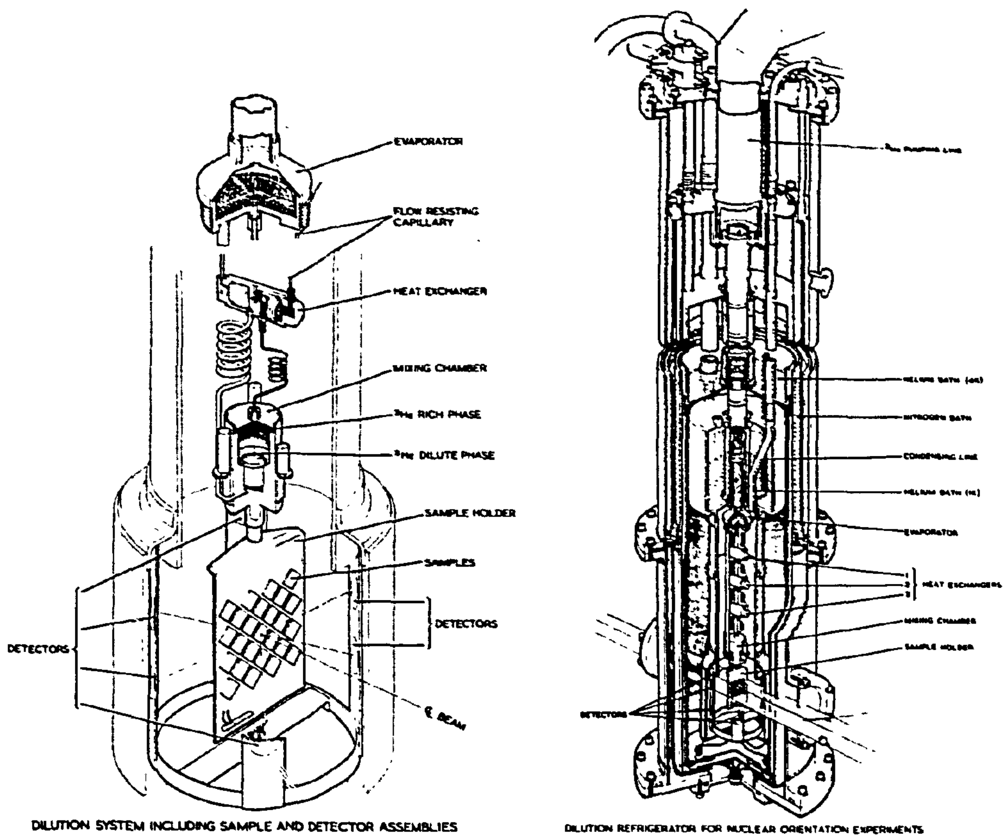

Fig. 1. Layout of refrigerator, sample and detector assemblies.

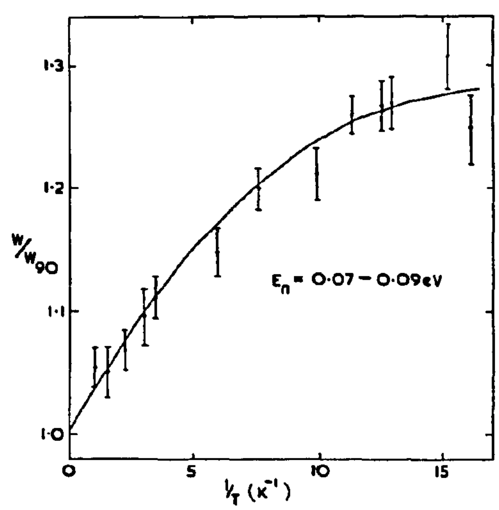

Fig. 2. Variation of ^{235}U fission anisotropy with temperature.

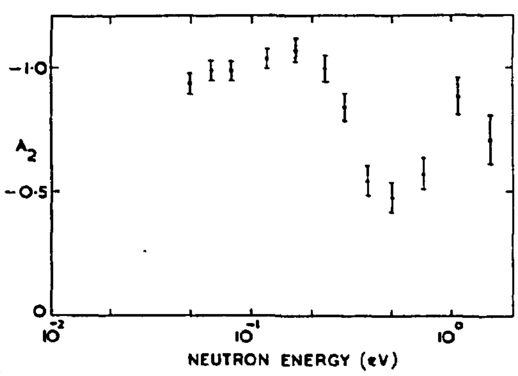

Fig. 3. Variation of ^{235}U fission anisotropy with incident energy.

Scattering of 9.72 MeV neutrons from ^{10}B and ^{11}B. (J. A. Cookson)

The analysis of this measurement, for which the experimental work was performed with the time of flight system of the A.W.R.E. tandem, is now almost complete. Elastic and inelastic neutron groups were measured at nine angles and Fig. 1 shows results for the elastic scattering. Geometrical and multiple scattering corrections have been applied and are also shown, together with a theoretical curve using the Wilmore and Hodgson optical potential with U and W chosen for the best fits. At 9.72 MeV the elastic cross sections for ^{10}B and ^{11}B are found to be 933 ± 68 mb (including the 0.717 MeV excited state), and 895 ± 63 mb respectively.

The best optical potentials are being used in a Hauser Feshbach calculation for comparison with the inelastic angular distributions.

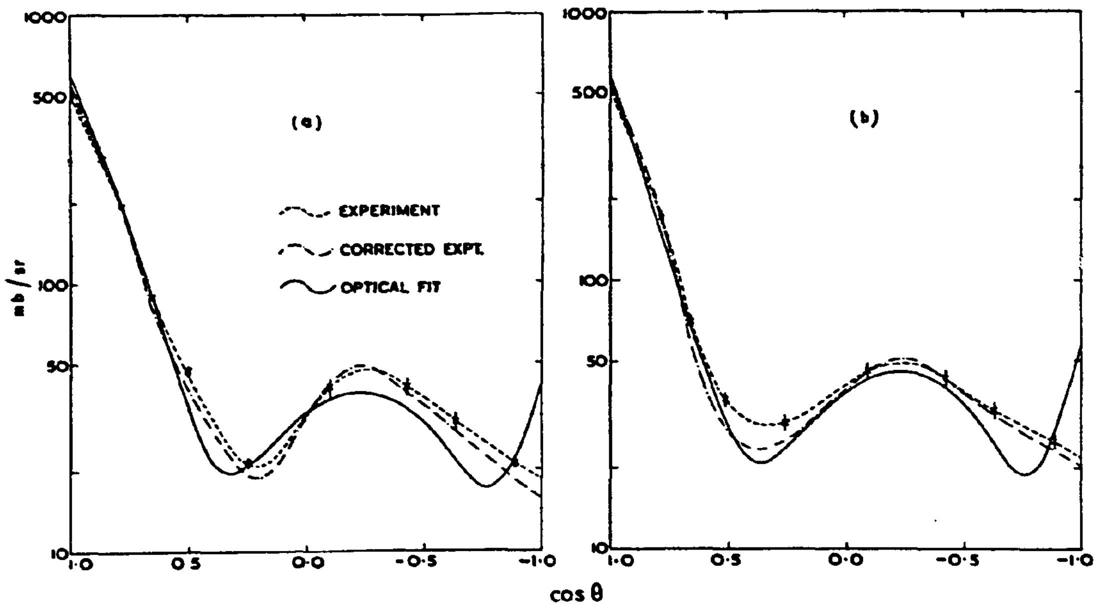

Fig. 1. Angular distribution of neutron elastic scattering from (a) ^{10}B and (b) ^{11}B.

Search for isomeric states in the region Z>50, N>82 produced by (C^{12}, Xn) reactions. (T. W. Conlon and A. J. Elwyn).

Calculations[1] indicate the existence of nuclei with stable oblate equilibrium deformation in the region Z<50, N>82 (see also PR/NP 15, p. 25). For some of these nuclei stable prolate shapes with very similar deformation energies are expected, so that low-lying excited states that have equilibrium deformations opposite in sign to the ground state may exist. It is expected that gamma-ray transitions between such states and the ground state should be hindered because of the associated change in nuclear shape.

We are searching for examples of shape-hindered gamma-ray transitions produced following reactions of the type (C^{12}, Xn) on separated isotopes of Sn, Cd, and Sb. Our technique involves the use of pulsed beams of 88 MeV C^{12} ions from the Harwell Variable Energy Cyclotron, and permits total half-lives of greater than 5 μs to be measured.

---

(1) Arseniev, D. A., Sobiczewshi, A. and Soloviev, V. G. Nucl. Phys. A126, 15 (1965).

Several short lived isomers in the region $Z>50$, $N<82$ have been observed. The targets, reactions and final nuclei together with the measured half-lives of the isomeric states are tabulated below. No isomers with half-lives in the range accessible to us have been observed in even-even nuclei. Analysis of the gamma-ray spectra from the isomers listed in Table I is in progress to determine the level schemes and probable nature of the isomeric and ground states of the final nuclei.

TABLE I

Target Final Nucleus	$T_{1/2}$ (secs)
$Sn^{118}(C^{12},5n)Ba^{125}$	73×10^{-5}
$Cd^{116}(C^{12},5n)Xe^{123}$	67×10^{-6}
$Cd^{113}(C^{12},4n)Xe^{121}$	12×10^{-5}
$Sb^{123}(C^{12},[4,5]\,n)La^{131,130}$	17×10^{-5}
$Sb^{121}(C^{12},[4,5]\,n)La^{129,128}$	56×10^{-2}
$In^{NAT}(C^{12},[4,5]\,n)$	51×10^{-2}

High precision n-p total cross section in the energy range 0.5 to 7.0 MeV. (A. Langsford and P. J. Clements (Oxford University))

The neutron-proton total cross section has been determined from a series of measurements of the relative transmission of a neutron beam through carbon and hydrocarbon samples, in which both the mass of material in the beam and the ratio of hydrogen to carbon in the sample was varied. The accuracy sought was that both statistical errors and systematic uncertainties should each be approximately 0.1% of the cross section. With this accuracy it was expected that a check could be made on charge independence in low energy n-p and p-p scattering by comparing values for the singlet effective range calculated from n-p and p-p cross section measurements. In comparing our measurements with the effective range expansion for the cross section, we have used the following values of the scattering lengths and effective range, recommended by Houk and Wilson(1):

$$a_s = -23.714 \text{ fm}, \quad a_t = 5.425 \text{ fm}, \quad r_{ot} = 1.763 \text{ fm}.$$

The values of shape parameters $P_s = 0.050$ and $P_t = 0.025$ have been given by Noyes(2) who has also calculated the value of $r_{os} = 2.73 \pm 0.03$ fm from the results of p-p scattering experiments, assuming charge independence(3).

The cross sections have been evaluated in 10 contiguous energy bands and the statistical errors in the five points below 2.2 MeV are about 0.12% of the cross section. Above this energy they increase to 0.2% at 5.9 MeV. In addition there is a systematic uncertainty in the magnitude of the background correction. While this is reasonably well determined at low energies, being approximately 0.03%, at higher energies it becomes equal to the statistical errors. This background is thought to arise from delayed emission of γ-rays from the target and from the production of γ-rays in the collimation. However, the most significant contribution to systematic uncertainties arises from the uncertainty in the resolving time of the coincidence system used in the detection of neutrons. This leads to an uncertainty of ~ ± 7 mb in the absolute cross section values.

The results of the present measurements and the predicted cross section values are shown in Table I. In Fig. 1 the present results (solid circles) are expressed as percentage deviations from the theoretical values. Only the statistical errors are shown on these points. Also presented in a similar manner are results by Engelke et al.[4] (open squares) and the lowest energy point of the three measurements of Lebowitz[5] (solid square), which in statistical accuracy are comparable with the present data, and a selection of earlier data made by Hafner for Noyes[2] (open circles). It can been seen that the results of the present measurement and these of Engelke and Lebowitz lie above the charge independence prediction while those from earlier measurements lie below it. The value of singlet effective range favoured by our measurement is $r_{os} = 2.60 \pm 0.03$ fm, if statistical errors only are included. However, the uncertainty is increased to ± 0.01 when all the systematic effects are taken into consideration. The results of Engelke and Lebowitz give a value of $r_{os} = 2.62 \pm 0.06$ fm. This value and that derived from the present experiment are in agreement, but disagree with the earlier data, which gave a value of $r_{os} = 2.95 \pm 0.08$ fm. When comparing results with the charge independence prediction, 2.73 ± 0.03 fm, one must note that uncertainties in the values of the other parameters used on the effective range expression for the cross section introduce a further uncertainty of ± .08 fm into the value obtained for r_{os}. Thus the present data and those of Engelke and Lebowitz are consistent with the charge independence prediction, while the earlier data are not.

TABLE I

Energy MeV	Cross section b		Errors b	
	Experimental	Theoretical	Statistical	Systematic
0.841	4.691	4.677	± 0.005	± 0.008
1.161	3.947	3.936	± 0.004	± 0.007
1.453	3.493	3.486	± 0.004	± 0.008
1.750	3.155	3.146	± 0.003	± 0.007
2.045	2.893	2.881	± 0.004	± 0.008
2.346	2.674	2.661	± 0.004	± 0.007
2.719	2.439	2.437	± 0.003	± 0.007
3.324	2.163	2.152	± 0.003	± 0.007
4.375	1.796	1.795	± 0.003	± 0.005
5.858	1.455	1.456	± 0.003	± 0.004

A recent paper by Hrehuss and Czibok[6] suggested the presence of an oscillatory term in the energy dependence of n-p total cross section in the energy range we have investigated. Instead of combining our data into 10 energy bands, on the assumption that the cross section varied smoothly with energy, we analysed the data in 203 energy bands to see if the oscillation were present.

Hrehuss and Czibok used a function of the form

$$\sigma(E) = \sigma_{np}\ (\text{experimental}) - \sigma_{np}\ (\text{theoretical}) = K \sin^2 \left(\frac{\pi}{2}\cdot\frac{\alpha}{\sqrt{E}}\right) + a + bE + cE^2$$

Any oscillations produced by the term $K \sin^2 \left(\frac{\pi}{2}\cdot\frac{\alpha}{\sqrt{E}}\right)$ have a peak to peak amplitude K and a period determined by α. In thier analysis of the cross section, Hruhuss and Czibok found a best fit to the data when α had a value in the range 24 to 28 MeV$^{1/2}$ and a value of K about 40 ± 9 mb in the energy range 0.6

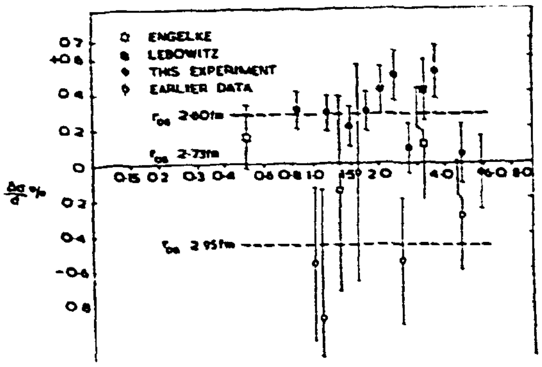

Fig. 1. The percentage deviation of the measured values of the n-p total cross section from that predicted by effective range theory and assuming chrage independence.

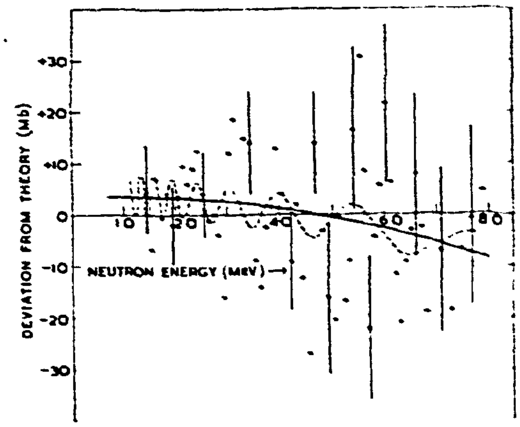

Fig. 2. The absolute deviation of the n-p total cross section from theory. The dashed oscillating curve shows the maximum value of any oscillating term in the cross section, the solid curve is a fit to the data assuming no oscillation. To help clarify the presentation original 203 points have been combined into about 50.

to 1.5 MeV and 145 ± 11 mb in the 2.58 to 5.34 MeV interval. The error on each of the 203 points used in the analysis of the present data is ~20 mb and fluctuations of the magnitude reported by Hrehuss and Czibok should be clearly visible. In order to reduce the confusion of data points Fig. 2 shows the present data divided into 50 energy bands, each band between 1.5 and 5.5 MeV encompassing about 4 bands used in the analysis. Allowing K, a, b and c to be freely variable the minimum value of χ^2 so obtained was found to be almost independent of the value of α over a wide range in α. The error on the value of K, for these value of α was almost constant and ~4 mb. Table II presents the results of the analysis of the present data for values of α ranging from 20 MeV$^{1/2}$ to 36 MeV$^{1/2}$. While a minimum of χ^2 was found for α = 28 MeV$^{1/2}$ giving a value of K ≈ -7.7 mb the value of χ^2 for the neighbouring point α = 27 MeV$^{1/2}$ is only 2 greater with K = + 6.0 mb. For the 198 degrees of freedom in the present analysis χ^2 would have to deviate from the most probable value of 198.5 by ± 29 for the change to be statistically significant.

TABLE II

α MeV$^{1/2}$	K mb	χ^2
20	+ 3.7	196
24	− 3.5	197
26	+ 4.7	195
27	+ 6.0	194
28	− 7.7	192
29	− 0.9	197
30	+ 2.5	197
32	− 2.8	197
36	+ 1.4	197

We therefore conclude that the present measurement affords no evidence for an oscillatory term in the n-p total cross section of the type reported by Hrehuss and Czibok greater than ~6 mb.

Indeed if the term is omitted from the analysis we obtain a χ^2 of 197 for 200 degrees of freedom showing that the data are indeed well fitted by an oscillation free variation of the total cross section with energy. The result of the analysis for $\alpha = 28$ MeV$^{1/2}$ and for $K = \alpha = 0$ are shown in Fig. 2 as the dashed and solid curves respectively.

---

(1) Houk T. and Wilson R. Rev. Mod. Phys. 40, 672 (1968).

(2) Noyes H. P. Phys. Rev. 130, 2025 (1963).

(3) Noyes H. P. Nuc. Phys. 74, 508 (1965).

(4) Engelke C. E. et al. Phys. Rev. 129, 324 (1963).

(5) Lebowitz J. M. Thesis, Faculty of Pure Science, Columbia (1965).

(6) Hrehuss G. and Czibok T. Phys. Lett. 28B, 585 (1968).

REPORTS, PUBLICATIONS AND CONFERENCE PAPERS

REPORTS

AERE - R 5980 The low energy scattering cross section of ^{10}B. A. Asami and M. C. Moxon.

PUBLICATIONS

ASAMI A., MOXON M. C. and STEIN W. E. A new technique for the partial wave assignment of a slow neutron resonance. Physics Letters 28B, No. 10, 656 (1969).

JAMES G. D. Fission components in ^{242}Pu resonances. Nuc. Phys. A123, 24 (1969).

PATRICK B. H. and JAMES G. D. A correlation analysis of the slow neutron induced fission cross section of ^{239}Pu. Physics Letters 28B, No. 4, 258 (1968).

IN COURSE OF PUBLICATION

ARMITAGE B. H., FERGUSON A. T. G., NEILSON G. C. and PRITCHARD W. D. N. Energy levels of ^{56}Fe: the $^{56}Fe(n,n'\gamma)^{56}Fe$ reaction and the γ-spectrum of ^{56}Co. Nuc. Phys.

CONLON T. W. and ELWYN A. J. On oblate nuclear shapes and shape isomers in the region $Z < 50$, $N < 82$. Physics Letters.

JAMES G. D. and SLAUGHTER G. G. The total cross section of ^{234}U and the parameters of its sub-threshold fission resonances. Nuc. Phys.

CHEMISTRY DIVISION, A.E.R.E.
(Division Head: Dr. W. Wild)

V.E.C. Studies

Fission of the Compound Nucleus ^{210}Po Formed with Varying Amounts of Angular Momentum.
(J. G. Cuninghame, I. F. Croall and J. P. Unik*)

The first stage of this experiment has now been completed. Fragment mass distributions are found to be unaffected by angular momentum, while broadening with increase of excitation energy. An increase of kinetic energy with increasing angular momentum and also with excitation energy is found. These results were reported at the I.A.E.A. Fission Conference, held in July in Vienna.

As soon as the V.E.C. again becomes available, further runs with ^{198}Pt and ^{206}Pb targets will be made and it is hoped that the results will enable a more rigorous testing of the theories of Nix to be made.

Fission Studies with the V.E.C. (Data Processing). (I. F. Croall)

During the past year G.C. Best (Elec. & A.P. Division) has developed a new display system which will be used with the PDP-8 in 'on-line' fission studies. During the long shut-down of the V.E.C., the opportunity has been taken to develop a new data collection system which will improve the resolution of the fission experiments. The earlier system allowed only 128 x 128 channel resolution, this has now been improved to 256 x 256 channels. The new system makes use of the disc backing store for the main data array, only a pointer list being held in core. This technique is made possible by the new display system which works on data break and requires very little processor time. Testing of the new system will be completed and it will be ready for use by the time the V.E.C. is again available to users.

Mass Spectrometry

Natural Isotopic Abundances of Molybdenum Isotopes. (E. A. C. Crouch, I. C. McKean and M. Brownsword)

Further consideration of the accuracy of mass-spectrometric measurements carried out in the past (Nature 202, 1282 (1964), Isotopic composition and atomic weight of naturally occurring Mo; etc.) has been prompted by some parallel work at Argonne National Laboratory, U.S.A. (C. Stevens, private communication). Inaccuracy is due to mass-discrimination occurring during measurement of the isotopic ratios. In the case of molybdenum this is very difficult to determine because it consists of seven isotopes of adjacent mass numbers and similar abundances. Theoretically double spiking with separated isotope mixtures should enable the determination of the mass discrimination (Dobson, J. Sci. Inst. (1969) 2, p. 490), but no experimental results have been published using this technique. We have made mixtures of separated ^{94}Mo and ^{98}Mo purified chemically by solvent extraction followed by sublimation of the oxide, and have determined the mass-discrimination on them and thus their absolute isotopic compositions. Work on the naturally occurring molybdenum isotope is continuing.

The double spiking technique is being applied to nuclear data measurements.

---

*Returned to Argonne National Laboratory in July 1969.

Multiple Neutron Capture in ^{239}Pu. (E. A. C. Crouch, I. C. McKean and M. Brownsword)

It was report in PR/Chem 16 that the calculated Pu isotopic ratios for long irradiations in DIDO could not be made to agree with the experimentally determined values (especially $^{238}Pu/^{239}Pu$ and $^{241}Pu/^{239}Pu$), if accepted nuclear data were used. The decay of ^{241}Pu is the first step of the ^{238}Pu production route and it had been assumed that the failure of the calculations was somehow connected with this relation. During the reporting of the work alternative possibilities were explored and it was realized that ^{238}Pu could be formed in the experimentally found quantities by the γ,n reaction on ^{239}Pu. There exists in the reactor a sufficient flux of γ-rays above the required energy threshold (5.6 MeV), being the n-caputure γ radiation in Al and other metals, and part of the fission prompt γ-radiation. Having explained the early production of ^{238}Pu in this way, it was found that ^{241}Pu production could be explained by the assumption of a high value (compared with existing data), for the n-absorption cross-section. This now appears consistent with work done by Scheitlin (O.R.N.L.), and Bockhoff at G.E.E.L. recently (private communication). This work has now been reported.

Mössbauer Studies on Fission Products

Chemical Applications of the Mössbauer Effect. (N. R. Large and R. J. Bullock)

In the case of measurements of the isomer shift of europic oxide relative to europic fluoride it was observed that different preparations of the oxide gave isomer shifts which showed a significant variation. In particular, a sample of enriched $^{151}Eu_2O_3$ obtained from the Electromagnetic Separator Group gave an isomer shift ~0.2 mm/sec lower than that obtained from most of the other samples examined. It seems probable that this variation is due to differences in crystal structure, and since europic oxide is commonly used as a reference standard this problem is being further investigated.

As part of the S.R.C. collaborative programme with Leeds University further experiments with samarium and gadolinium [EDTA]H^+ sources at both room temperature and liquid nitrogen temperature have been carried out. These have confirmed the preliminary findings that the spectra of the gadolinium complexes have a much lower intensity than those of the corresponding samarium complexes, and that there are no indications of short-lived products at either temperature.

Application of Mössbauer Effect to Corrosion Films. (N. R. Large, J. R. Haddon and G. N. Walton)

As part of a collaborative programme with Oxford University (Loan Agreement) work has been carried out on the Mössbauer spectrum of magnetite formed from ferrous hydroxide under high pressure conditions in static autoclaves. It has been shown that at near neutral pH (8.5) the product has an altogether different spectrum to that formed at high pH (10.5) with sodium hydroxide. The two spectra are attributed to the differences of the magnetic domain in the crystal structures formed under the different conditions. In the near neutral conditions the lattice structure is estimated to be only 100 Å in extent, i.e. the particles are extremely small, whereas in the alkaline conditions the full crystalline structure is obtained. These observations are relevant to the behaviour of magnetite in high pressure water systems at different pH's.

The work is in course of publication.

Publications

Isomer shift of the Mössbauer spectrum of $^{151}EuF_3$.
N. R. Large, R. J. Bullock, P. Glentworth and D. A. Newton, Phys. Letters 29A, 352 (1969).

The preparation of gadolinium-151 for Mössbauer spectrometry of europium-151.
R. J. Bullock, N. R. Large, I. L. Jenkins, A. G. Wain, P. Glentworth and D. A. Newton, J. Inorg. Nucl. Chem. 31, 1929 (1969).

Dependence of fission fragment total kinetic energy and mass distributions on the excitation energy and angular momentum distribution of the fissioning nucleus ^{210}Po. J. P. Unik, J. G. Cuninghame and I. F. Croall, Presented at the I.A.E.A. Second Symposium on the Physics and Chemistry of Fission, Vienna, Paper SM 122/58 (1969).

Techniques for on-line fission experiments with the V.E.C. I. F. Croall and J. G. Cuninghame. Presented at International Conference on the Use of Cyclotrons in Chemistry, Metallurgy and Biology, Oxford (September 1969).

The effects of Gd-151 electron-capture decay and Sm-151 beta-decay on the Mössbauer spectrum of Eu-151 in europium multidentate chelates. N. R. Large, R. J. Bullock, P. Glentworth and D. A. Newton, Presented at the International Symposium on Chemical Effects of Nuclear Transformation, Cambridge (July 1969).

Calculated independent yields in thermal neutron fission of ^{233}U, ^{235}U, ^{239}Pu, ^{241}Pu, and in fission of ^{232}Th, ^{238}U and ^{240}Pu. E. A. C. Crouch, AERE-R 6056 (1969).

Distribution

Distribution of this report is limited to the U.K.A.E.A. Libraries only.